AFRL-IF-RS-TR-2004-287
Final Technical Report
October 2004

PROGRAMMABLE SELF-ASSEMBLY OF DNA-DENDRIMER AND DNA-FULLERENE NANOSTRUCTURES

University of Wisconsin-Madison

Sponsored by
Defense Advanced Research Projects Agency
DARPA Order No. 290/01

AIR FORCE RESEARCH LABORATORY
INFORMATION DIRECTORATE
ROME RESEARCH SITE
ROME, NEW YORK

STINFO FINAL REPORT

This report has been reviewed by the Air Force Research Laboratory, Information Directorate, Public Affairs Office (IFOIPA) and is releasable to the National Technical Information Service (NTIS). At NTIS it will be releasable to the general public, including foreign nations.

AFRL-IF-RS-TR-2004-287 has been reviewed and is approved for publication

APPROVED: /s/
GEORGE O. RAMSEYER
Project Engineer

FOR THE DIRECTOR: /s/
JAMES A. COLLINS, Acting Chief
Information Technology Division
Information Directorate

REPORT DOCUMENTATION PAGE

Form Approved
OMB No. 074-0188

1. AGENCY USE ONLY (Leave blank)	2. REPORT DATE	3. REPORT TYPE AND DATES COVERED
	Oct 04	Final Jan 01 – Dec 03

4. TITLE AND SUBTITLE

PROGRAMMABLE SELF-ASSEMBLY OF DNA-DENDRIMER AND DNA-FULLERENE NANOSTRUCTURES

5. FUNDING NUMBERS

C - F30602-01-2-0555
PE - 60110E
PR - BIOC
TA - M2
WU - 90

6. AUTHOR(S)

Robert M. Corn

7. PERFORMING ORGANIZATION NAME(S) AND ADDRESS(ES)

University of Wisconsin-Madison
Dept of Chemistry
1101 University Ave.
Madison, WI 53706

8. PERFORMING ORGANIZATION REPORT NUMBER

9. SPONSORING / MONITORING AGENCY NAME(S) AND ADDRESS(ES)

Defense Advanced Research Projects Agency
3701 N. Fairfax Drive
Arlington, VA 22203

AFRL/IFTC
26 Electronic Pky
Rome, NY 13441-4514

10. SPONSORING / MONITORING AGENCY REPORT NUMBER

AFRL-IF-RS-TR-2004-287

11. SUPPLEMENTARY NOTES

AFRL Project Engineer: George Ramseyer, IFTC, 315-330-3492, ramseyeg@rl.af.mil

12a. DISTRIBUTION / AVAILABILITY STATEMENT

Approved for public release; distribution unlimited.

12b. DISTRIBUTION CODE

13. ABSTRACT ***(Maximum 200 Words)***

The scientific goal for this project was to fabricate nanostructures from deoxyribonucleic acid (DNA)-dendrimers, DNA-nanotubes and DNA-diamond adducts, and then to assemble these nanostructures into larger scale functional constructs. The five major areas of research were: 1) The creation and characterization of highly regular DNA-dendrimer and DNA-nanotube nanomaterials; 2) The development of the appropriate modification chemistry for both gold and silicon surfaces for the specific absorption by hybridization of DNA-dendrimer and DNA-carbon nanotube materials; 3) The use of DNA hybridization to control the assembly of nanotubes onto a surface by modifying that surface with one sequence of DNA and with the carbon nanotubes with the complementary sequence; 4) The design and testing of large, well-behaved sets of short DNA oligomers or "words" that will be used in the DNA-nanoparticles and surface attachment patterns; and 5) The development of various enzymatically amplified detection technologies for DNA and RNA biosensors. Well characterized, functional DNA-dendrimers, DNA-nanotubes and DNA-diamond adducts were created which have a specific number of one or more DNA sequences on the exterior of the dendrimer or nanotube and were capable of internally incorporating a variety of materials such as enzymes.

14. SUBJECT TERMS

Nanostructures, Deoxyribonucleic acid, Dendrimers, Nanotubes, DNA-hybridization, DNA-oliogomers, DNA-nanoparticles, DNA-computing, DNA-biosensors, RNA-biosensors, Programmable self-assembly

15. NUMBER OF PAGES

106

16. PRICE CODE

17. SECURITY CLASSIFICATION OF REPORT	18. SECURITY CLASSIFICATION OF THIS PAGE	19. SECURITY CLASSIFICATION OF ABSTRACT	20. LIMITATION OF ABSTRACT
UNCLASSIFIED	UNCLASSIFIED	UNCLASSIFIED	UL

TABLE OF CONTENTS

LIST OF FIGURES

LIST OF TABLES

1. EXECUTIVE SUMMARY

Currently several fields of research are converging towards the creation and use of nucleic acid nanostructures for both biological and non-biological applications. These areas are: (i) the miniaturization of biosensors and biochips into the nanometer scale regime, (ii) the fabrication of nanoscale objects that can be placed in intracellular locations for monitoring and modifying cell function, (iii) the replacement of silicon devices with nanoscale molecular-based computational systems, and (iv) the application of biopolymers in the formation of novel nanostructured materials with unique optical and selective transport properties. The highly predictable hybridization chemistry of deoxyribonucleic acid (DNA), the ability to completely control the length and content of oligonucleotides, and the wealth of enzymes available for modification of the DNA, make nucleic acids an attractive candidate for all of these applications. Additionally, all of these systems require the creation of well-characterized, functional DNA nanostructures.

The scientific goals of this project were to fabricate nanostructures from DNA-dendrimers and DNA-nanotubes, and then to assemble those nanostructures into larger scale functional constructs. An alternative method was to fabricate DNA-diamond adducts. The overall technological result of this work was the creation of a new class of programmable thin film materials that can be implemented in biosensor applications and bioactive optoelectronic devices. Initially the reaction chemistries were established for the preparation of dendrimer-DNA bioconjugates. Thiol-disulfide exchange reactions were exploited to prepare these conjugates. Protocols to characterize the products of these reactions have been developed utilizing gel electrophoresis and matrix-assisted laser desorption/ionization-time-of-flight (MALDI-TOF) mass spectrometry. The attachment strategy commenced with a discrete dendritic architecture, and yielded a mixture of products that was identified and separated by high pressure liquid chromatography (HPLC). The resulting material was analytically pure (99%) and monodisperse. Hybridization studies confirmed that these constructs amplify Surface Plasmon Resonance (SPR) signals. More complex dendrimers affording multi-site

attachment have also been prepared, and the elaboration of these structures into multivalent bioconjugates continues.

In addition to DNA-dendrimers, a photochemical modification scheme was developed to chemically modify clean, hydrogen- (H-) terminated nanocrystalline diamond surfaces grown on silicon substrates, producing a homogeneous layer of amine groups that serve as sites for DNA attachment. Comparison of DNA-modified ultra-nanocrystalline diamond films with other commonly used surfaces for biological modification, such as gold, silicon, glass and glassy carbon, showed that diamond is unique in its ability to achieve very high stability and sensitivity while also being compatible with microelectronics processing technologies. We have also conducted experiments on the synthesis and characterization of biologically modified adducts of C_{60} (C_{60} is a molecule that consists of 60 carbon atoms, arranged as 12 pentagons and 20 hexagons) and carbon nanotubes. Experiments on C_{60} demonstrated that the high strain of the nanostructures leads to rapid degradation, which resulted in the transfer of our efforts to carbon nanotubes. Consequently, several new methods that link biomolecules and single-wall carbon nanotubes have been developed, including a covalent linking chemistry as well as a modification of carbon nanotubes by the use of various combinations of electric fields and chemical interactions.

It was determined that DNA-modified carbon nanotubes exhibited a number of highly desirable properties, including being highly stable, biological accessible, and selective in hybridization with complementary vs. non-complementary sequences. The modification of DNA with biotin was demonstrated as a method to achieve biologically directed assembly. Additionally, a novel approach to covalently link nano-objects to gold surfaces in an addressed format has been developed using DNA words and enzymatic ligation. These ligation methods included template directed enzymatic ligation of large DNA molecules, fluorescent antibodies/antigens, and fluorescent nanoparticles and universal ligation with degenerate oligonucleotide templates. The major improvements in DNA word design resulted in a maximizing attachment specificity.

To facilitate the development of DNA based materials, new algorithms have been developed for DNA word design that incorporate thermodynamic data. These methods yielded thermodynamically better sets than more traditional, combinatorial word design methods. A major component of the DNA word design software is the PairFold tool, which predicts the minimum free energy secondary structure of a pair of Ribonucleic Acid (RNA) or DNA molecules. In addition, the RNA Designer algorithm was developed for the design of RNA strands that fold to a specific secondary structure. Both the PairFold and RNA Designer tools are available at www.rnasoft.ca.

Various enzymatically amplified detection methodologies were developed using RNA and DNA microarrays in the application of direct detection of genomic DNA and viral RNA. These novel methods of enzymatic signal amplification can be used with many different techniques (e.g., Surface Plasmon Resonance (SPR) imaging fluorescence quenching, nanoparticle labeling) and with other surfaces. The ability to detect genomic DNA and RNA should greatly accelerate their application in the areas of genetic testing, bacterial and viral recognition, and gene expression analysis.

These major accomplishments have been disseminated by various applications including 16 publications, 2 conference papers, 3 patent applications, 23 overview presentations in conferences and 7 project presentations at research institutes. DNA9, the 9th International Meeting on DNA Based Computers, was organized and held at Madison, Wisconsin, which focused on current theoretical and experimental results in the areas of biomolecular computation and DNA nanoscale self assembly.

2. INTRODUCTION

Dendrimers, and more generally dendritic molecules, may be used as sophisticated adapter units between an oligonucleotide for recognition and/or molecular computation. Also, dendrimers may be used as reporter groups. The use of DNA constructs in DNA-machines,[1] DNA-computing,[2] antisense therapy,[3] and biosensors[4] has fueled intense research into suitable methods for immobilizing DNA on surfaces[5] and preparing soluble DNA-nanoparticle assemblies.[3] Most of the latter applications rely on nanoparticle modification with multiple copies of ssDNA oligonucleotides of a particular sequence. For example, multiple ssDNA oligonucleotides have been attached to soluble organic polymers[6] and gold nanoparticles.[7] However, methods for the covalent attachment of individual ssDNA oligonucleotides to soluble nanoparticles are surprisingly rare.[3] Synthetic methods that provide a means for conjugating precise numbers of identical or different ssDNA oligonucleotides to particular locations on nanoparticles could allow for simultaneous probing of multiple target oligonucleotides or for constructing interesting, new recursive materials. If methods are developed to provide a means for attaching additional active components, such as fluorescent or electrochemical tags, the usefulness would be further increased.

Many of the most interesting and unique properties of nanoscale materials are realized only when integrated into more complex assemblies.[8] In biology, the highly selective binding between complementary sequences of DNA plays the central role in genetic replication. This selectivity can, in principle, be used to assemble a wider range of materials by forming adducts between DNA and the material of interest.[9] While biomolecules such as DNA can be linked to nanotubes via noncovalent interactions,[10] the use of covalent chemistry is expected to provide the best stability, accessibility, and selectivity during competitive hybridization. Here is reported a multistep route for covalently linking DNA to single-wall carbon nanotubes (SWNTs). The DNA molecules covalently linked to SWNTs are accessible to hybridization and strongly favor

hybridization with molecules having complementary sequences compared with noncomplementary sequences.

Recent advances in biotechnology and molecular electronics have fueled an interest in the fabrication of well-defined, highly stable interfaces between biomolecules and solid supports. Much attention has been given to the attachment of biomolecules to polymers[11] and glass substrates.[12] However, the desire to characterize the electrical properties of biomolecules for applications such as direct electronic biosensing systems is leading to increased interest in alternative substrates such as gold,[2] silicon,[13] and diamond.[14] Diamond is a particularly attractive substrate material because of its chemical stability and biocompatibility[14] and because it can be doped and deposited in very thin films on a variety of substrates even at comparatively low temperatures.[15] Diamond is used in applications such as internal-reflection elements for infrared spectroscopy because of its good optical properties and chemical stability,[16] but typical diamond surfaces do not have well-defined chemical or biochemical groups on the surface and therefore lack chemical specificity. Since diamond can be made conductive by doping, it is also of interest for a variety of electrically based chemical and biological sensing applications that would achieve improved performance by selective biological modification.[17]

The essence of programmable self-assembly is the complete control over the template for construction. The template, in this case, is a surface that is covered in an addressed format with localized patches of highly unique single-stranded DNAs. Assembly of objects on the surface is programmed by covalently attaching an oligonucleotide to that object such that the oligonucleotide is complementary to the surface immobilized DNA. The specificity of assembly is governed by the relative thermodynamic stability of the perfectly complementary oligos compared to other points of hybridization. The stability of the assembly depends on stability of the underlying self-assembled monolayer and on the completeness of the ligation reaction. The results in this proposal detail our achievements in all pertinent areas of “programmable self assembly”.

DNA-based nanostructures and their programmable self-assembly rely heavily on the hybridization of sets of short (< 30 bases) oligonucleotides. The highly predictable hybridization chemistry of DNA, the ability to completely control the length and content of oligonucleotides, and the wealth of enzymes available for modification of DNA, make the nucleic acids attractive for all types of applications. In some cases, it is required that ssDNA molecules in a set only interact with their perfect complements to form double-stranded DNA (dsDNA), and not bind to any other complementary oligonucleotides in the solution. Examples of applications for these well-behaved "DNA word" sets of oligonucleotides are the creation of non-interacting DNA tags that can be used in the formation of universal chips similar to the "zip-code arrays" of Affymetrix.[18] Intensive efforts have focused on designing non-interacting DNA words for DNA computing using combinatorial constraints on the composition of a set of DNA code words for specific applications.[19,20] During the whole granting periods, some new approaches to design well-behaved sets of short DNA words were developed to facilitate the attachment of nanoparticles to the surface and to connect nanoparticles to each other: (i) computer design of DNA strands, for use in linking dendrimer particles together, and (ii) designing DNA strands with specific structural properties.

The direct analysis of genomic DNA and RNA in an array format without labeling or Polymerase Chain Reaction (PCR) amplification would be extremely useful for the detection and identification of viral[21] and bacterial samples,[22] gene expression analysis[23-25] and a variety of other applications. While a number of strategies have been proposed, the label free refractive index technique of Surface Plasmon Resonance (SPR) imaging is an excellent candidate for this application, and has already been applied to the direct detection of DNA,[26] RNA,[27] and proteins[28] in a microarray format. To date, the application of SPR imaging to the detection of genomic DNA, with typical concentrations in the one to one hundred femtomolar (fM) range (0.002 - 0.2 μg/μl),[29] has not been possible due to a detection limit of approximately one nanomolar (16-20mer).[27] A nanoparticle amplification method that increased the sensitivity of SPR imaging to one picomolar has been reported,[30] but this technique requires a sandwich assay format similar to that used by fluorescence based methods.[31-33c] A modulated SPR

technique has recently been used to detect 54 fM of a 47mer oligonucleotide, but this method is a single channel measurement that does not use an array format.[34] Here several novel surface-based enzymatic processes are described that can be used with RNA or DNA microarrays to lower the detection limit for SPR imaging measurements of ssDNA to a concentration of 1 fM.

3. METHODS, ASSUMPTIONS AND PROCEDURES

This project has been classified into several research areas leading to DNA based nanomaterials for biosensor applications. Various detection techniques and attachment chemistry on different substrates along with the creation of DNA-dendrimer/or nanotube or diamonds have been developed/employed.

3.1. Synthesis of Dendron

Figure 1 shows a synthetic route of dendrons incorporate reactive thiopyridyl groups, which could subsequently undergo exchange with appropriately functionalized DNA oligonucleotides.

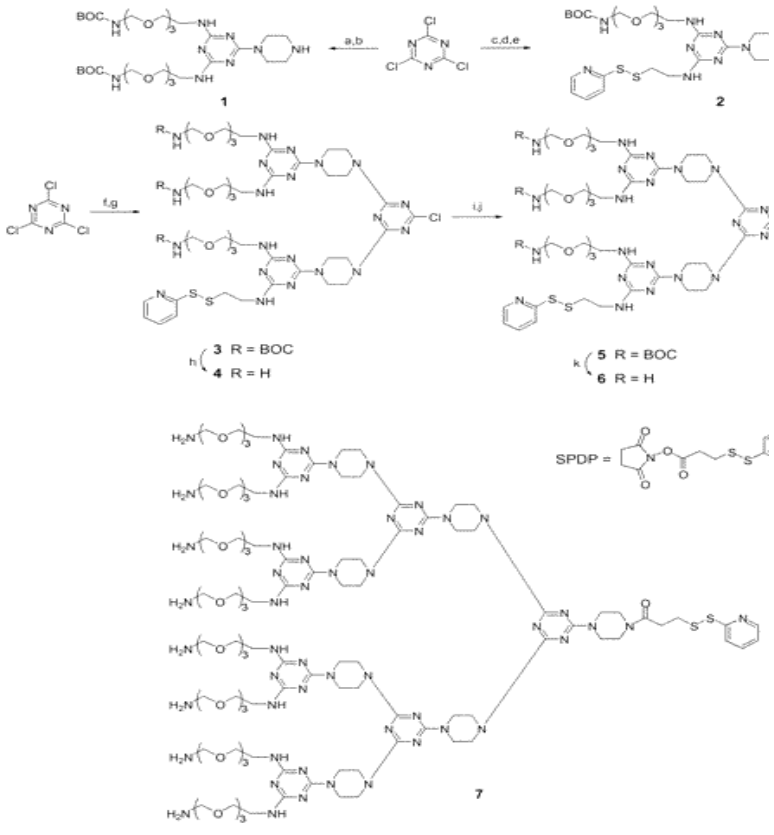

Figure 1. Synthesis scheme for dendrons incorporate reactive thiopyridyl groups.

3.1.1. Synthesis of 1

$BOCNHCH_2(CH_2OCH_2)_3CH_2NH_2$ (1.77g, 6.05 mmol) in THF (15 mL) was added drop wise to a cooled (-6 °C), stirred THF solution (30 mL) of cyanuric chloride (0.581 g, 3.17 mmol) and DIPEA (1.5 mL, 4.84mmol). After 2 hr the reaction mixture was warmed to room temperature, and more DIPEA (1.5 mL, 4.84 mmol) was added. Stirring for 14 hr at room-temperature resulted in a pale yellow solution with white precipitate, yielding a single TLC spot (*Rf*) 0.65.) Piperazine (1.64 g, 19.02 mmol) and DIPEA (1.5 mL, 4.84 mmol) were added, and the mixture was stirred for 14hr at room temperature. After removal of solvent, the residue was partitioned between CH_2Cl_2 and water. The organic phases were concentrated to yield a pale yellow oil, which was purified via silica gel column chromatography (100:3, CH_2Cl_2:MeOH eluent). A pale yellow oil was obtained (0.123 g, 82.3%). 1H NMR (300 MHz, CD_3OD) ‰ 3.72 (tr, 4H, NCH_2), 3.62 (m, 24H, CH_2OCH_2), 3.49 (tr, 4H,-C(O)$NHCH_2CH_2$), 3.20 (tr, 4H, $NHCH_2CH_2$), 2.79 (br, 4H, HNC*H*2), 1.42 (s, 18H, OC(C*H*3)3). 13C NMR (75 MHz, CD_3OD) ‰ 166.2, 165.0, 157.1, 78.9, 70.4, 53.9, 43.7, 43.0, 40.4, 27.8; MALDI-TOF (*m*/*z*): [M + H]+ calculated for $C_{33}H_{63}N_9O_{10}$, 746.5; found, 746.8.

3.1.2. Synthesis of 2

$BOC\text{-}NHCH_2(CH_2OCH_2)_3CH_2NH_2$ (1.39 g, 4.75 mmol) in THF (10 mL) was added drop wise to a cooled (-6 °C), stirred solution of cyanuric chloride (0.908g, 4.95 mmol) and DIPEA (3.3 mL, 9.82 mmol) in THF (30 mL). After 2 hr the reaction mixture was warmed to room temperature, and more DIPEA (1.5 mL, 4.84 mmol) was added, followed by a THF solution (15 mL) of neutralized pyridyl cysteamine hydrochloride (1.10 g, 4.95 mmol). Stirring for 14 hr at room-temperature resulted in a pale yellow solution with white precipitate, yielding a single TLC spot (*Rf*) 0.58. A 6-fold excess of piperazine (2.55 g, 29.7 mmol) and DIPEA (1.5 mL, 4.84 mmol) was added, and the mixture was stirred for 14 hr at room temperature. After removal of solvent, the residue was partitioned between CH_2Cl_2 and water. The organic phases were concentrated to yield a pale yellow oil which was purified via silica gel column chromatography (100:3, CH_2Cl_2:MeOH eluent). A pale yellow oil was obtained (1.56 g, 49%). 1H NMR (300

MHz, CD_3OD) ‰ 8.2 (tr, 1H, *o*-CH), 7.75 (m, 2H, *m*-C*H*), 7.2 (tr, 1H, *p*-C*H*), 3.75 (br, 4H, NCH_2) 3.63 (m, 12H, C*H*$_2$OCH_2), 3.50 (tr, 4H, C(O)NHC*H*$_2$$CH_2$ and NC*H*$_2$$CH_2$S), 3.21 (tr, 2H, NHC*H*$_2$$CH_2$), 3.02 (tr, 2H, NCH_2C*H*$_2$S), 2.82 (br, 4H, NHC*H*$_2$), 1.43 (s, 9H, OC(C*H*$_3$)$_3$). 13C NMR (75 MHz, CD_3OD) ‰ 167.6, 166.1, 161.2, 150.1, 139.2, 122.6, 121.2, 80.2, 71.4, 49.9, 46.3, 44.5, 41.4, 40.8, 39.6, 28.9; MALDITOF (*m*/*z*): [M + H]+ calculated for $C_{27}H_{45}N_9O_5S_2$, 640.3;found, 640.4.

3.1.3. Synthesis of 3

Dendron **1** (0.601 g, 0.807 mmol) was dissolved in 15 mL of THF and added drop wise to a cooled (-6 °C), stirred solution THF solution (30 mL) of cyanuric chloride (0.148 g, 0.807 mmol) and DIPEA (1.5 mL, 4.84 mmol). After 2 hr the reaction mixture was warmed to room temperature, and more DIPEA (1.5 mL, 4.84 mmol) was added, followed by a THF solution (15 mL) of **2** (0.505 g, 0.807 mmol). Stirring for 14 hr at room-temperature resulted in a pale yellow solution with white precipitate. After removal of solvent, the residue was partitioned between CH_2Cl_2 and water. The organic phases were concentrated to yield a pale yellow oil, which was purified via silica gel column chromatography (100:3, CH_2Cl_2: MeOH eluent). A white, sticky solid was obtained (0.86 g, 71.2% yield). 1H NMR (300 MHz, CD3OD) ‰ 8.2 (m, 1H, *o*-C*H*), 7.78 (m, 2H, *m*-C*H*), 7.19 (tr, 1H, *p*-C*H*), 3.75 (br, 16H, NC*H*$_2$), 3.62 (m, 36H, CH_2OC*H*$_2$), 3.50 (br, 8H, C(O)NHC*H*$_2$$CH_2$ and NC*H*$_2$$CH_2$S), 3.22 (m, 6H, NC*H*$_2$) 3.04 (tr, 2H, NCH_2C*H*$_2$S), 1.43 (s, 27H, OC(C*H*$_3$)$_3$); 13C NMR (75 MHz, CD_3OD) ‰ 169.5, 166.1, 165.0, 164.4, 160.0 157.0, 150.0, 137.8, 121.1, 119.8, 78.9, 71.2, 70.2, 43.5, 42.9, 40.3, 27.9. MALDI-TOF (*m*/*z*): [M + H]+ calculated for $C_{63}H_{10}N_{21}O_9S_2$, 1495.5; found, 1495.8.

3.1.4. Synthesis of 4

Dendron **3** (0.86 g, 0.57 mmol) was reacted with 85% trifluoroacetic acid (TFA, 3 mL) for 14 hr (1:1 TFA:CH_2Cl_2). A pale yellow oil was obtained after solvent evaporation (0.81 g, 94.2%). 1H NMR (300 MHz, CD_3OD) ‰ 8.12 (m, 1H, *o*-C*H*), 7.82 (m, 2H, *m*-C*H*), 7.45 (tr, 1H, *p*-C*H*), 3.84 (br, 14H, NC*H*$_2$), 3.78 (br, 6H, NH_2C*H*$_2$$CH_2$), 3.65 (m, 36H, CH_2OC*H*$_2$), 3.22 (m, 6H, N-C*H*2), 3.04 (tr, 2H, NHCH_2C*H*$_2$S); 13C NMR (75

MHz, CD_3OD) ‰ 166.1, 165.0, 164.4, 157.0, 150.0, 137.8, 121.1, 119.8, 71.2, 70.2, 43.5, 42.9, 40.3. MALDI-TOF (*m*/*z*): [M + H]+ calculated for $C_{48}H_{82}ClN_{21}O_9S_2$, 1196.6; found, 1196.6.

3.1.5. Synthesis of 5

Dendron **3** (0.100 g, 0.17 mmol), piperazine (0.072 g, 1.40 mmol), DIPEA (0.160 mL, 1.4 mmol), and THF (15 mL) were heated at 70 °C for 14 hr in a sealed, thick-walled reaction vessel. After removal of solvent, the residue was partitioned between CH_2Cl_2 and water. The organic phases were concentrated to yield a pale yellow oil which was purified via silica gel column chromatography (20:1, CH_2Cl_2:MeOH eluent). A pale yellow oil was obtained (42 mg, 35.3%). The oil was stirred at room temperature with THF (10 mL), DIPEA (0.25 mL, 0.807 mmol), and SPDP (9.0 mg, 0.029 mmol). After removal of solvent, the residue was partitioned between CH_2Cl_2 and water. The organic phases were concentrated to yield a pale, yellow oil which was purified via column chromatography (100:5, CH_2Cl_2:MeOH eluent) yielded an off-white viscous oil. 1H NMR (300 MHz, CD_3OD) ‰ 8.37 (m, 2H, *o*-C*H*), 7.77 (m, 4H, *meta*-C*H*), 7.16 (tr, 2H, *p*-C*H*), 3.68 (br, 24H, NCH_2), 3.59 (m, 48H, CH_2OCH_2), 3.48 (tr, 2H,C(O)NHCH_2CH_2S), 3.21 (tr, 10H, NHCH_2), 3.04 (tr, 2H, C(O)NHCH_2CH_2S), 1.41 (s, 27H, OC(CH_3)$_3$). 13C NMR (75 MHz, CD_3OD) ‰ 171.2, 166.2, 165.9, 161.6, 158.0, 149.8, 122.1, 120.9, 119.2, 80.1, 71.5, 71.2, 71.1 44.2, 41.3, 36.2, 33.8, 31.9, 28.9. MALDI-TOF (*m*/*z*): [M + H]+ calculated for $C_{75}H_{122}N_{24}O_{16}S_4$, 1743.7; found, 1743.7.

3.1.6. Synthesis of 6

Dendron **5** (100 mg, 0.069 mmol) was deprotected with TFA (1:1 TFA:CH_2Cl_2), yielding a sticky yellow oil (32 mg, 75.6%). 1H NMR (300 MHz, CD_3OD) ‰ 8.48 (d, 1H, *o*-C*Ha*), 8.40 (d, 1H, *o*-C*Hb*), 7.98 (m, 2H, *m*-C*Ha*), 7.88 (m, 2H, *m*-C*Hb*), 7.39 (tr, 1H, *p*-C*Ha*), 7.25 (tr, 1H, *p*-C*Hb*), 3.85 (br, 24H, N-C*H*2), 3.67 (m, 48H, CH_2OCH_2), 3.56 (tr, 2H, C(O)NHCH_2CH_2), 3.13 (tr, 10H, NHCH_2), 2.92 (tr, 2H, C(O)CH_2CH_2S); 13C NMR (75 MHz CD_3OD) ‰ 170.5, 165.5, 162.4, 158.0, 149.4, 138.0, 121.1, 120.0, 119.9, 115.1, 70.3, 70.2, 70.0, 68.7, 66.7, 43.9, 42.8, 40.4, 39.4, 34.1, 32.2. MALDI-TOF (*m*/*z*):

[M + H]+ calculated for $C_{60}H_{98}N_{24}O_{10}S_4$, 1443.5; found, 1443.7.

3.1.7. DNA Conjugation

All solvents and reagents used in DNA reactions were spectroscopic grade. Water, methanol, and acetonitrile were further purified by filtration through a 0.22 μm filter. Disulfide-modified oligonucleotides were purchased from Trilink Biotechnologies (San Diego, CA). The lyophilized powders were dissolved in UV/UF purified (Barnstead) water [0.1 OD/μl]. The fluorescently labeled oligo 5'-(Oregon Green 514)-TAGGACTTACGC-(C3-thiol), and nonlabeled 12mer 5'-TAGGACTTACGC-(C3-thiol) (referred to as DNAa), were deprotected on immobilized TCEP (2-carboxyethylphosphine) for 15 min at room temperature and eluted with two volumes of TBE (45 mM Tris-borate, 1 mM EDTA) pH 8.3 buffer. The use of other buffers, including tris(hydroxymethyl) aminomethane buffer at pH 6.0 and 7.4, did not elute the DNA from the resin. In a typical conjugation, deprotected Oregon-Green labeled 12-mer [2.5 OD, 25 μL H2O] was incubated with thiopyridyl containing dendron **7** (41.8 nmol, 0.05 mg). After 12hrat room temperature the reaction was stopped, yielding the corresponding disulfide conjugated DNA-dendrimer. MALDI-TOF (*m*/*z*): [M + H]+ calculated for DNA-dendron, **7-D**, 7227.4; found, 7227.6.

3.1.8. MALDI-TOF

An overlayer preparation was used with a 2,4,6-trihydroxyacetophenone (THAP) matrix. A 1:1:1 mixture of 1 *m*M aqueous reaction mixture, 10 mg/mL THAP matrix in methanol, and 15 mg/mL aqueous ammonium citrate was spotted in 1 μL aliquots on a bed of THAP matrix. The analyte-doped matrix crystals were washed repeatedly (5-15 times) with 5 μL of cold water to remove alkali metals. MALDI-TOF mass spectra were acquired in positive- and negative-ion mode on a Voyager-DE STR mass spectrometer (Applied Biosystems, Framingham, MA) equipped with a pulsed nitrogen laser emitting at 337 nm. Samples were analyzed in linear mode using a delayed extraction time of 550 ns and an accelerating voltage of 20 kV. The laser light intensity was adjusted to provide the optimal signal-to-noise ratio. All spectra were the result of signal averaging 50-100

laser shots. Positive-ion mass calibrations were performed internally with the $[M + 2H]^{2+}$, $[M + H]^{+}$, and $[2M + H]^{+}$ ions of insulin (bovine). Negative-ion calibrations were performed externally with the $[M - H]^{-}$ and the $[2M - H]^{-}$ ions of DNA.

3.1.9. Gel Electrophoresis

Polyacrylamide gels (20%) were prepared according to a standard protocol (*23*). Gels were run between 70 and 80 V for 2-3 hr. The sample buffer was 0.25% bromophenol blue and 40% (w/v) sucrose in water. Samples were prepared by adding 0.1 volume of running buffer to each dendron and conjugate solution. The running buffer was TBE (90 mM Tris-Borate, 2 mM EDTA). Ethidium bromide and Coomassie Brilliant Blue R250 were used for staining and visualization.

3.2. Synthesis of DNA- Single-Wall Carbon Nanotubes Adducts

Figure 2 shows an overview of the covalent attachment process. Purified single-wall carbon nanotubes (SWNTs) were oxidized to form carboxylic acid groups at the ends and

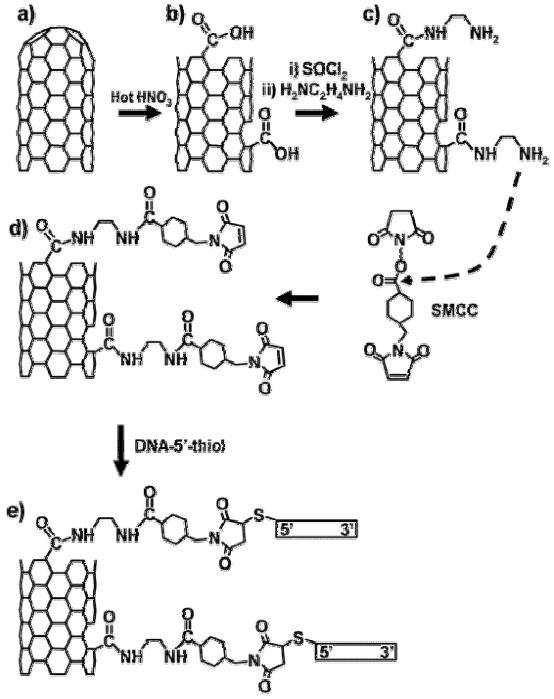

Figure 2. Overall scheme for fabrication of covalently linked DNA-nanotube adducts.

sidewalls (Figure 2b). These were reacted with thionyl chloride and then ethylenediamine to produce amine-terminated sites (Figure 2c). The amines were then reacted with the heterobifunctional cross-linker succinimidyl-(4-*N*-maleimidomethyl)cyclohexane-1-carboxylate, (SMCC), leaving the surface terminated with maleimide groups (Figure 2d). Finally, thiol-terminated DNA was reacted with these groups to produce DNA-modified SWNTs (Figure 2e).

Single-wall nanotubes (Carbolex, Lexington, KY) were first purified[35] by refluxing nanotubes in 3 M nitric acid for 24 hr and then washing the SWNTs with water using a 0.6 micron polycarbonate membrane filter (Millipore). Elemental analysis (Desert Analytics) showed that this procedure reduces the Ni contamination from 19% to 4.0 wt %, and the Yttrium contamination from 4.8% to 0.75%. Previous studies have shown that this procedure results in partial oxidation of the nanotubes, leaving carboxylic acid groups at the nanotube ends and at sidewall defect sites.

3.3. Synthesis of DNA-Modified Nanocrystalline Diamond Thin-Films

Two types of thin-film diamond samples were investigated. Before growth, both types of samples were treated with nanocrystalline diamond powder in an ultrasonic bath to achieve very high nucleation densities.[36] Ultra-nanocrystalline diamond (UNCD) films,[37] 0.75 microns thick, were grown on n-type Si (100) substrates at Argonne National Laboratory in a 2.45 GHz microwave plasma reactor using 1% CH_4 and 99% Ar at 150 torr pressure and 800 °C for approximately two hours. Nanocrystalline diamond (NCD) films (0.5 0.2 m thick) were grown on n-type Si (100) substrates at the Naval Research Laboratories in a 2.45 GHz microwave plasma reactor (Astex Model PDS-17) using purified hydrogen (900 s.c.c.m.) and methane (99.999%, 3 s.c.c.m.) at a total pressure of 15 torr. The samples were cleaned in a series of acid baths and then, immediately before each experiment, were exposed to a 13.56 MHz inductively coupled hydrogen plasma (15 torr) for 20 minutes at 800 °C, as described previously.[38] This procedure preferentially etches any graphitic carbon and leaves the diamond surface terminated with C-H bonds.[38] The DNA attachment sequence is summarized in Figure 3. The H-terminated samples are

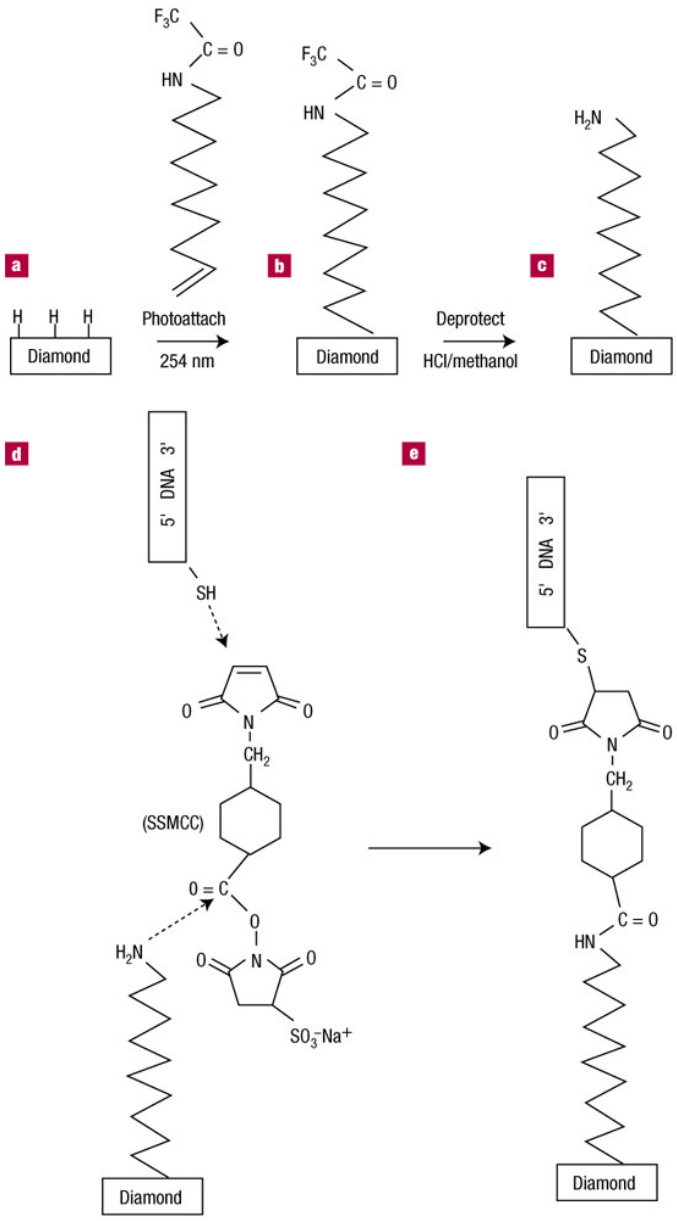

Figure 3. Sequential steps in DNA attachment to diamond thin films.

photochemically reacted with a long-chain unsaturated amine, 10-aminodec-1-ene, that was protected with the trifluoroacetamide functional group.[39] We refer to this protected amine as TFAAD. The protected amine is then deprotected, leaving behind a primary amine (Figure 3c). The primary amine is reacted with a heterobifunctional cross linker sulfosuccinimidyl-4-(*N*-maleimidomethyl)cyclohexane-1-carboxylate (SSMCC) and finally reacted with thiol-modified DNA (Figure 3d) to produce the DNA-modified

diamond surface (Figure 3e).

3.4. SPR Imaging Measurements

All SPR imaging experiments were performed on an SPR imager apparatus using excitation from an incoherent light source. Figure 4 shows a schematic diagram of the SPR imaging apparatus used to detect the adsorption of biopolymers (e.g. DNA) in solution to surface-immobilized biomolecules, such as DNA and RNA. SPR imaging measures the change in percent reflectivity at a fixed angle caused by the adsorption or desorption of biomolecules onto the surface. Briefly, p-polarized collimated white light incident on a prism/Au/thin film/buffer flow cell assembly was set at a fixed angle. Reflected light from this assembly was passed through a band pass filter centered at 830 nm and collected with a CCD camera.

3.5. Surface Attachment Chemistry

The development of well-characterized surface chemistries for the attachment of biological molecules onto gold thin films in an array format is necessary for SPR imaging measurements of biomolecular binding affinity. In this section, we will discuss some specific attachment chemistry employed for creating DNA and peptide on gold surface using two different cross-linkers. Noble metal thin films are required for the propagation of surface plasmons. As a consequence, commercially available DNA arrays made on glass substrates, such as those produced by Affymetrix,[40] or peptide arrays, prepared by the SPOT synthesis technique on cellulose membranes,[41] are not viable options for SPR

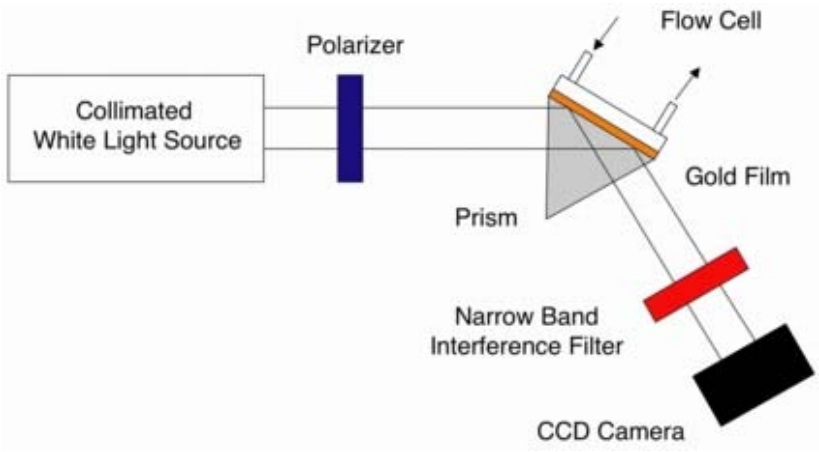

Figure 4. Schematic representation of the SPR imaging apparatus.

imaging investigations. Instead, we have employed self-assembled monolayers of long chain alkanethiols that are ω-terminated with an amine functional group as the foundation of the array.[26] Chemical modification of the self-assembled monolayers is used to tether biological molecules to the surface. Two methods using the bifunctional linkers A) SSMCC (sulfosuccinimidyl 4-(*N*-maleimidomethyl) cyclohexane-1-carboxylate) and B) SATP (*N*-Succinimidyl *S*-acetylthiopropionate) are described below for the covalent attachment of thiol-containing DNA, peptide, carbohydrate and capture probe molecules.

3.5.1. SSMCC Attachment Chemistry

In the first reaction scheme, the heterobifunctional linker SSMCC, which contains both an *N*-hydroxysulfosuccinimide (NHSS) ester and a maleimide functionality, is used to covalently link the amine terminated self-assembled monolayer to a thiol modified probe molecule (Figure 5a);[26] (i) The NHSS ester moiety of SSMCC is reacted with the free amines of the alkanethiol monolayer to form amide bonds terminating with maleimide groups. (ii) Thiol modified DNA or cysteine containing peptides are introduced to the thiol reactive maleimide monolayer and attached by the creation of a thioether bond.

DNA molecules attached by this method have a surface coverage of 1.0 x 10^{12} molecules/cm^2.[27]

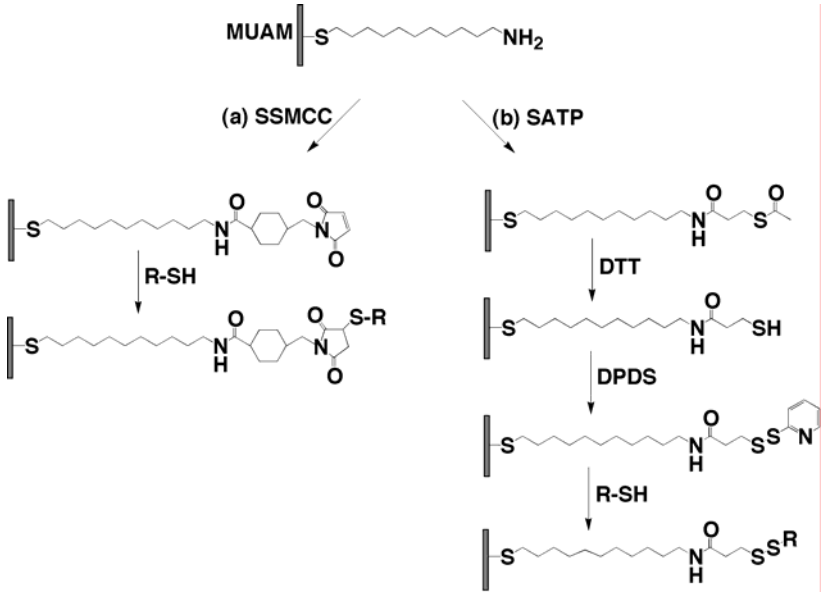

Figure 5. Surface attachment chemistry for the immobilization of thiol-modified DNA and cysteine containing peptides.
(a) the linker SSMCC and (b) SATP

3.5.2. SATP Attachment Chemistry

The second reaction scheme, more amenable for generating peptide arrays, involves the attachment of thiol containing biomolecules onto gold surfaces through a disulfide linkage.[5] The reaction scheme for this surface modification process is shown in Figure 5b. (i) A self-assembled monolayer of 11-mercapto-undecylamine (MUAM) is reacted with the molecule SATP, a bifunctional linker containing an NHS ester and a protected sulfhydryl. The NHS ester reacts with the amines present on the surface to form a stable amide bond resulting in a protected sulfhydryl surface. (ii) Exposure of the surface to an alkaline solution containing DTT removes the protecting acetyl group revealing an active sulfhydryl surface. (iii) The sulfhydryl surface is reacted with 2,2′–dipyridyl disulfide to form a pyridyl disulfide surface. Thiol-disulfide exchange reactions are then performed in order to attach thiol-modified DNA or cysteine containing peptides to the substrate, with a surface coverage of 10^{13} molecules/cm^2. This surface attachment chemistry has the advantage of being reversible; the disulfide bond can be cleaved in the presence of DTT to regenerate the sulfhydryl-terminated surface.

3.6. Array fabrication by Photo-Patterning

Arrays used for SPR imaging experiments contain multiple individually addressable components and are prepared by a combination of self-assembly, surface attachment chemistry, and array patterning using either photopatterning or PDMS microfluidic channels. This section will explore the first array fabrication methodology developed within our laboratories for the creation of robust DNA and peptide arrays using chemical protection and deprotection and photopatterning. This multi-step fabrication procedure is outlined in Figure 6.[26,42] The first step of the fabrication method is the creation of a temporary hydrophobic background using the bulky amine protecting group, 9-fluorenylmethoxycarbonyl (Fmoc), frequently used in solid phase peptide synthesis. The *N*-hydroxysuccinimide ester of Fmoc (Fmoc-NHS) is reacted with the terminal amines of a packed self-assembled alkanethiol monolayer to form a stable carbamate linkage. The surface is then exposed to UV light through a patterned quartz mask to create arrays

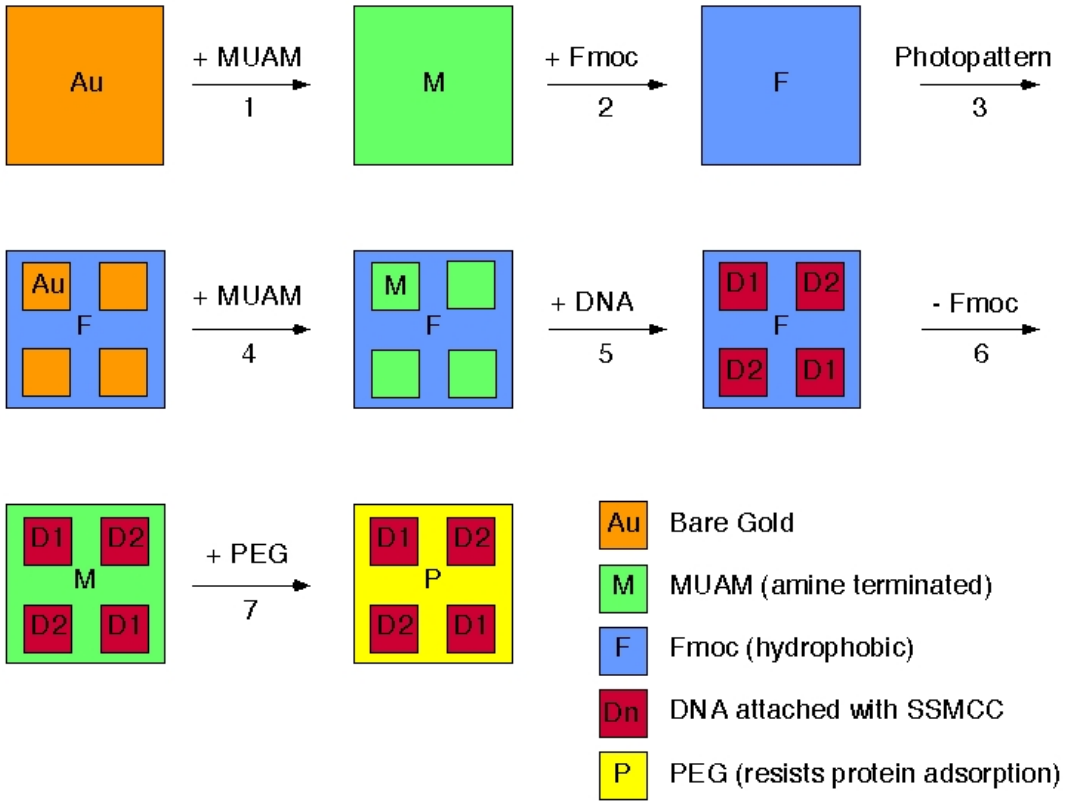

Figure 6. Multi-step procedure for creating DNA arrays with a protein adsorption resistant background on a thin gold film surface.

composed of 500 μm by 500 μm square elements with 500 μm spacing between the elements. The gold-thiol bond is cleaved in the regions where the light shines through the mask resulting in a patterned gold surface that consists of bare gold pads surrounded by Fmoc. Next, the surface is immersed in an ethanolic solution of 11-mercapto-undecylamine (MUAM). The amine-terminated alkanethiols self-assemble in the bare gold pads producing a surface containing reactive hydrophilic MUAM pads surrounded by the hydrophobic Fmoc background. The lower left hand corner of Figure 6 contains an image of an array showing the individually addressable hydrophilic spots surrounded by a hydrophobic background. Chemical protection allows droplets of hydrophilic DNA or peptides to be "pinned" without contaminating other sequences contained on neighboring pads on the array and covalently attached using the linkers SSMCC or SATP. These arrays can be easily used with a mechanical array spotter to introduce multiple peptide or DNA elements onto one chip for high-throughput studies. For example, arrays composed of more than 300 elements can be produced using square elements with 250 μm widths.

The array fabrication is then completed by removing the hydrophobic Fmoc background and replacing it with polyethylene glycol (PEG) to reduce the non-specific adsorption of biopolymers. Since Fmoc is a base-labile protecting group, the original amine-terminated surface can be easily regenerated by the use of a basic secondary amine. An NHS derivative of polyethylene glycol (PEG) can react with the terminal amines of the SAM to form a stable amide linkage. The formation of the temporary Fmoc surface is necessary, since PEG is too hydrophilic to prevent contamination between DNA or peptide droplets. The DNA arrays can then be analyzed by SPR imaging using a 500 μL flow cell to introduce biopolymer analytes to the array surface. DNA arrays fabricated using SSMCC attachment chemistry can be used for more than 25 hybridization cycles[43] while the SATP chemistry can be used for more than 30 cycles without degradation of the array.[5]

3.7. Array Fabrication with Microfluidics

A fabrication and detection approach based on the coupling of microfluidic networks was used with the specific aim of lowering detection limits, speeding up analysis time and reducing chemical consumption and sample volume. This approach relies on the creation of microfluidic networks within the polymer polydimethylsiloxane (PDMS), which are physically sealed to chemically modified gold surfaces.[44] We have used these PDMS microchannels to (i) fabricate "1-D" single-stranded DNA (ssDNA) line arrays that were used in SPR imaging experiments of oligonucleotide hybridization adsorption, and (ii) create "2-D" DNA hybridization arrays in which a second set of PDMS microchannels were placed perpendicular to a 1-D line array in order to deliver target samples.

The 1-D line arrays are an alternative to the multi-step fabrication procedure involving reversible protection/deprotection attachment chemistry and UV-photopatterning techniques described in section 3.6[42] and offer reduced fabrication time and chemical consumption. The fabrication process is as follows (see also Figure 7): 1-D line DNA microarrays were constructed by first flowing the heterobifunctional linker SSMCC through a set of parallel microchannels onto a self assembled MUAM monolayer on the

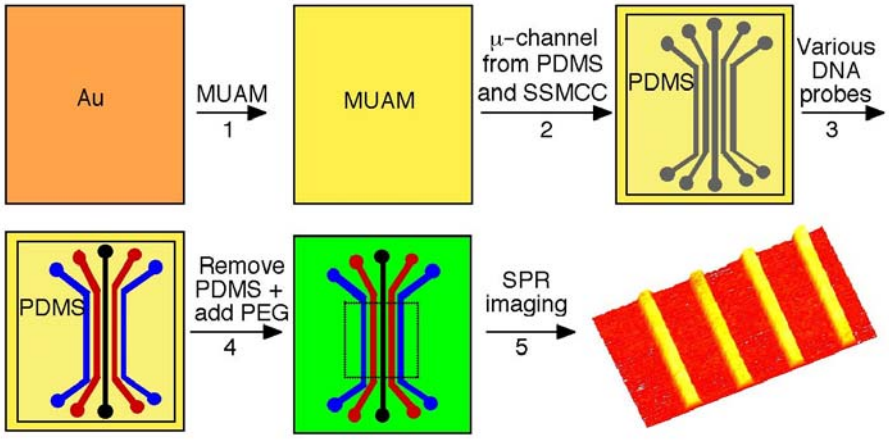

Figure 7. Schematic representation of the fabrication methodology used for creating 1-D DNA line and 2-D DNA hybridization microarrays.
The region enclosed by the dotted box in step 4 represents a SPR difference image (in step 5) obtained for the hybridization of target DNA onto an array of multiple surface bound DNA probes. The dimension of the microchannels used were 300 μm wide, 35 μm deep with a spacing of 1400 μm between channels.

gold surface. Single-stranded thiol DNA was then flowed into the microchannels to react with the SSMCC, tethering the ssDNA to the surface. In these 1-D line arrays, biomolecules were attached to the surface in a series of lines instead of squares. By implementing surface patterns as narrow as 50 μm, arrays containing 100 species can be fabricated on one chip.

For biological applications such as gene expression and the detection of microbial species, it would be preferable to use a significantly smaller sample volume. For this purpose, we have developed a novel approach, called 2-D hybridization arrays that use a second microfluidic network placed perpendicular to the 1-D line array for solution delivery. 2-D hybridization arrays were created in a two-step process: (i) a 1-D line array of ssDNA probe molecules was created on the gold surface and (ii) a second set of PDMS microchannels was attached to the surface perpendicular to the 1-D DNA line array in order to deliver target molecules to the surface. The intersection of the line arrays with the microchannels created a 2-D hybridization array of dsDNA probe spots. This resulted in reducing the sample volume from 500 μL to 1 μL and lowering the detection limit to

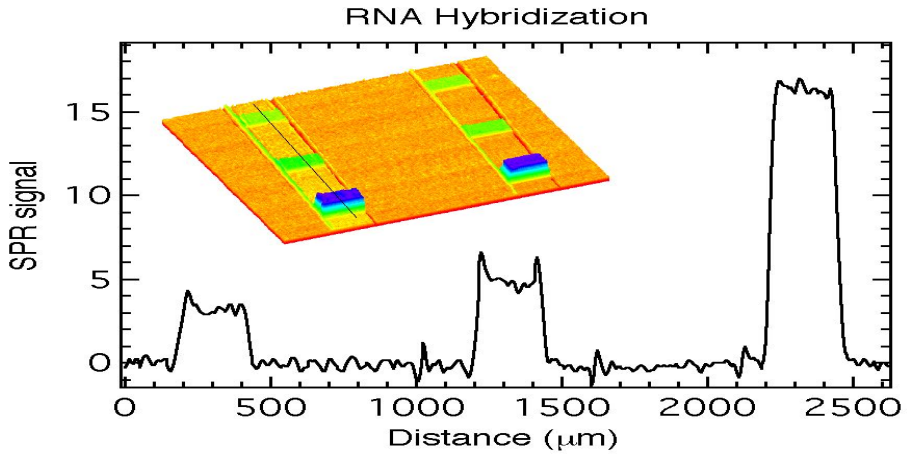

Figure 8. SPR difference image showing hybridization of the GUS gene RNA onto a 2-D hybridization array of surface bound probe DNA.

10 femtomoles.[44] Figure 8 shows some promising results for the detection of a 20 femtomole sample of *in vitro* transcribed RNA from a partial clone of the *uidA* gene using a 2-D hybridization array. This level of sensitivity would be sufficient for the direct detection of highly expressed mRNA, such as those found in transgenic plants and also for the detection of proteins using a small volume of target molecules.

3.8. PCR Product

PCR primers were commercially obtained from IDT and purified using reverse-phase binary gradient elution HPLC. These primers were selected to amplify the TSPY gene of the human Y chromosome taken from the sequence in genbank with accession # AF106331. The 24mer primers (E_L and E_R) are located at positions 1206 and 1749 of the TSPY gene, and their binding specificity was confirmed using the BLAST-programs (http://www.ncbi.nl.nih.gov/blast/), against the Human Genome Sequence Database. These sequences are as follows: E_L=5´ GCA AGC CCC ACC AG ACC GCA GAG, and E_R=5´ TCG CCT CCC CGT CCC CGT AAA CTA. Male and female genomic DNA isolated from whole blood samples was obtained commercially from Promega. PCR was performed with 250 ng of genomic DNA, 0.2 mM of dNTP, 50 pmol of each TSPY gene primer, one Hot Start Polymerase TaqBead (Promega), 5 mM $MgCl_2$ and 1X thermophilic DNA Polymerase reaction buffer (Promega) in a 50 µL reaction volume. The amplification reaction consisted of a 5 minute cycle at 95 °C followed by 30 cycles of 1 minute at 95 °C, 1 minute annealing at 58 °C, 1 minute at 72 °C and a final extension cycle at 72 °C for 5 minutes was performed on a thermal cycler (MJ Research, Model PTC-100).

3.9. Rolling Circle Amplification (RCA)

A template-assisted enzymatic ligation strategy was used to synthesize the single-stranded circular DNA. Hybridization of the 64bp linear precursor to the 20bp guide sequences brought the 5' and 3' end of the linear precursor in a juxtaposition which were then linked by a T4 DNA ligase to form a closed circular DNA. Non-circular molecules were subsequently removed by T7 gene 6 exonuclease and exonuclease I digestion. The DNA circles were further purified by QiAeuick Nucleotide Removal Kit (QIAGEN Inc.).

The purity of the circular DNA was assessed by gel electrophoresis on a 15% denaturing PAGE gel. After the circular DNA was made, RCA was then used to amplify the surface bound probe and the amplification fold was analyzed by labeling the amplified product with fluorescence reporters. Two different DNA oligonucleotides of 1μM that contain 5' thiol modification were immobilized on gold thin film described previously. One is designed as RCA primer, which can hybridize to the circular DNA and initiate the RCA reaction, while the other as a control probe can not hybridize to the circular DNA, thus no amplification would be expected to the control probe. After the circular DNA was annealed to the surface bound primer, the RCA reaction was performed at 37°C for 60 min with the addition of Sequenase 2.0 DNA polymerase, dNTP and *E. coli* single-strand-binding (SSB) protein. Through hybridization of fluorescently labeled complementary short oligonucleotides, the fluorescence result showed the signal amplification of the RCA primer is around 100 fold. Whereas, no amplification was observed for the control probe as expected. The lack of amplification of the control probe indicated the high specificity of the RCA reaction. Phi29 DNA polymerase was used as another alternative enzyme for RCA and the results showed higher amplification fold comparing to the case of Sequenase DNA polymerase.

4. RESULTS AND DISCUSSIONS

Four different research groups participated in this project to accomplish our goal towards the development of DNA based nanostructures and biosensors. These contributions are divided into (1) Development of chemistries for DNA-dendrimer, DNA-dendron bioconjugates from Dr. Richard Crooks' research group at U. Texas A&M and Dr. Robert Corn's research group at UW-Madison, (2) Development of ultra-sensitive DNA biosensors based on surface engineered enzymatic amplification from Dr. Robert Corn's research group at UW-Madison, (3) Development of biologically-modified single-walled carbon nanotubes and high-stability DNA assemblies on diamond thin films from Dr. Robert Hamers' research group at UW-Madison and (4) Design and testing of large and well-behaved sets of short DNA oligomers or words from Dr. Anne Condon's research group at U. British Columbia, Dr. Robert Corn and Dr. Lloyd Smith at UW-Madison.

4.1. Synthesis of New Dendrons and DNA-Dendron Conjugates

Dendrimers or dendritic molecules offer the potential as sophisticated adapter units between an oligonucleotide, which can be used for recognition and/or molecular computation and reporter groups. The synthesis of dendrimer-DNA conjugates commenced using dendrimers comprising triazine groups was first investigated. Triazine chemistry is straightforward and targets that display a range of functional groups can be prepared.

We have recently synthesized several new dendrons containing fluorophores at the periphery, namely pyrene (**1**, **2**), and are currently completing the synthesis of dansyl (**3**) functionalized dendrons (Figure 9). The attachment of fluorophores will aid our characterization of DNA-dendron conjugates, and also our ability to visualize

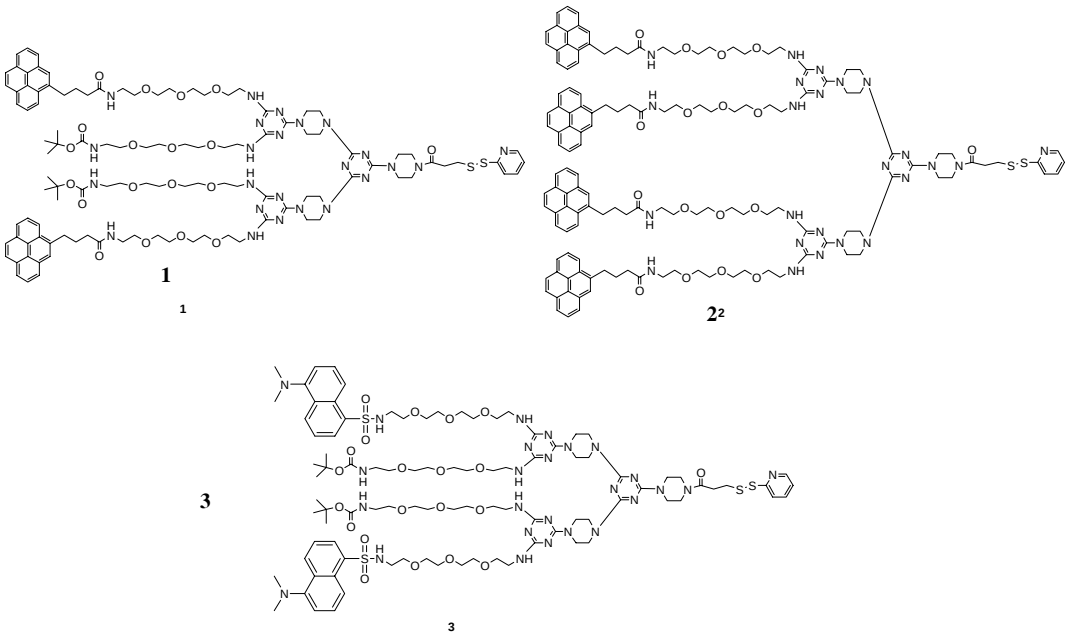

Figure 9. Fluorophore dendrons.

hybridization to surface bound DNA probes. Additionally, attachment of multiple fluorophores could allow an improved spectroscopic sensitivity, compared with DNA that typically contains only a single fluorophore. We are currently completing studies of DNA conjugation to these fluorophore-dendrons. In particular, we had trouble with the hydrophobic nature of the pyrene dendrons, which prevents successful conjugation by aqueous based methods previously utilized. Dansyl functionalized dendrons should allow us to overcome this issue.

In addition to the synthesis of novel DNA-dendron conjugates, we have been focusing on the purification of DNA-conjugates that have already been characterized, and whose structure has been confirmed. Our current efforts on purification had revolved around separation by polyacrylamide gel electrophoresis. Recently, however, we have found HPLC to be a more effective technique for DNA-dendron conjugate isolation and purification. Several DNA-dendron conjugates are currently being analyzed and purified by HPLC using the method described below, which can be used for DNA, dendron, and DNA-dendron conjugates. Four products can be produced by TCEP promoted disulfide

reduction of DNA starting material (Scheme 1). A molecular weight spin filter eliminated HS-C6-ODM, whose molecular weight is under 3000.

12mer-S-S-C6-ODMT + TCEP → 12mer-SH + HS-C6-ODMT
+ 12mer-S-S-C6-ODMT + 12mer-S-S-12mer

Scheme 1 – Thiol-terminated DNA produced by TCEP reduction of DNA disulfide.

The three other products, thiol terminated 12mer, the 12mer-C6 disulfide, and the 12mer-12mer disulfide were observed at retention times 6.6, 8.0, 10.0 minutes respectively by HPLC on a Waters model 600 HPLC using a Waters XTerra MS C18, 2.5 μm, 4.6 X 50 mm column. The peaks were collected, and after several injections like peaks were pooled, concentrated, and analyzed by MALDI-TOF.

Previous work revealed difficulties conjugating DNA to dendrons functionalized with pyrene fluorophores (**1**). We postulated that this was due to a lack of hydrophilicity of these pyrene-dendron entities. Consequently, we have completed the synthesis of dendrons containing dansyl fluorophores (**2**) (Figure 10). As expected, these dansyl groups have improved the water solubility of the dendrons of interest. Subsequent reaction of thiol-terminated oligonucleotides has allowed us to synthesize DNA conjugates of these fluorophore-functionalized dendrons (**3**). We are currently undertaking hybridization of these conjugates to surface-bound complementary oligonucleotides as well as undertaking fluorescence spectroscopy of these DNA-dendron conjugates.

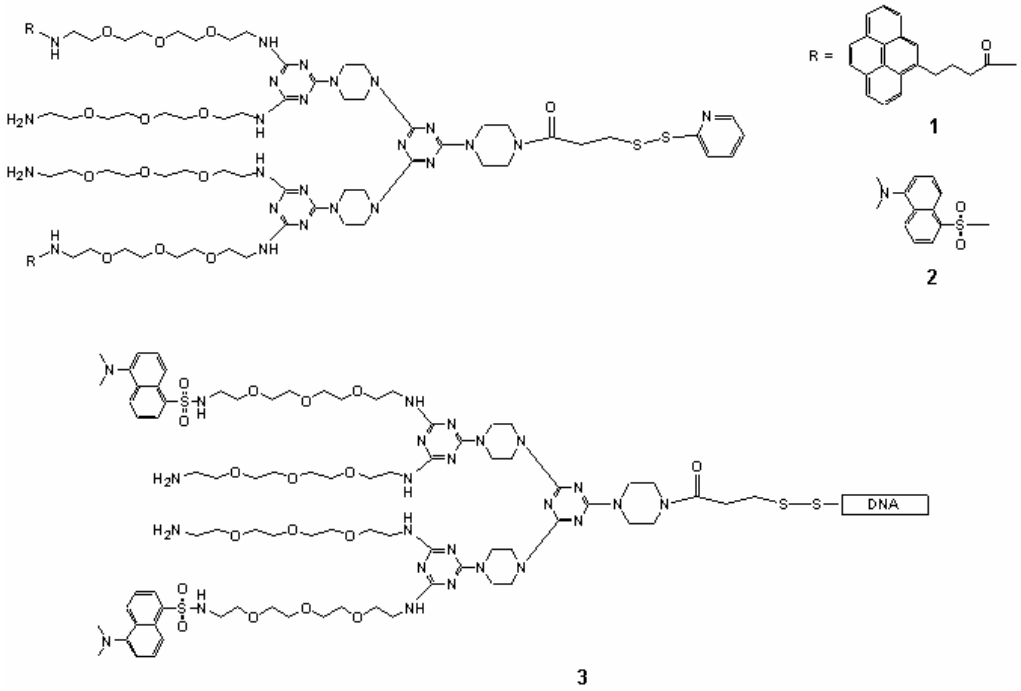

Figure 10. Improvement made on the synthesis of fluorophore dendrons.

We are also undertaking synthetic strategies to produce dendrons having two different oligonucleotides attached. Our current strategy revolves around producing dendrons that contain chemical moieties that react specifically with amine- and thiol- terminated DNA (Figure 11). This will allow the synthesis of novel DNA architectures both in solutions and on surfaces.

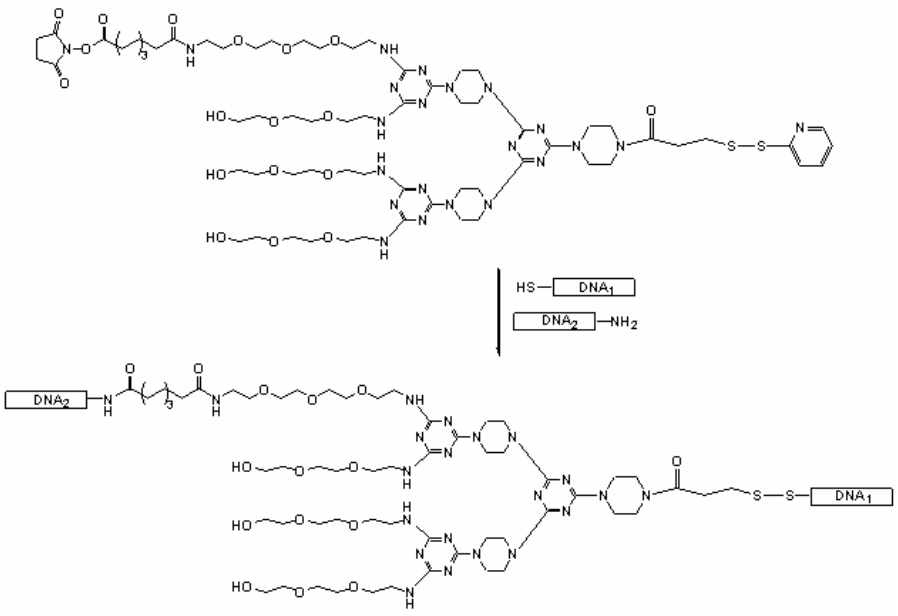

Figure 11. Asymmetric DNA conjugation.

To demonstrate control of DNA-dendrons in solution, restriction digests of double-stranded DNA-dendron dimers are currently being performed. Since most endonuclease buffers must contain DTT or a similar reductant, a non-disulfide linkage method was necessary and we developed substrates for this work. First, the linker activated dendron was prepared by adding heterobifunctional linker *N*-*e*-maleimidocaproxyloxy succinimide ester (ECMS) to piperazine functionalized dendron in methanol, and reacting overnight at room temperature, as shown in Figure 12.

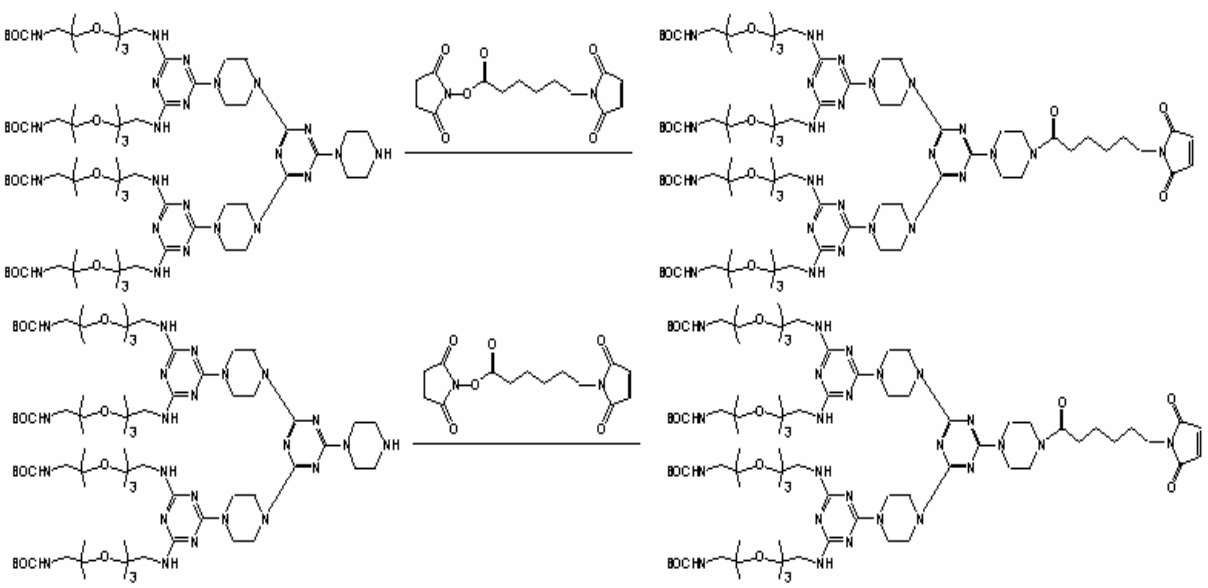

Figure 12. Dendron without disulfide linker.

4.2. Synthesis of DNA-Dendron Conjugates

Our ability to synthesize, characterize, purify, and utilize DNA-dendrimer conjugates continues to advance. Initial technical challenges to purification and characterization have been surmounted with the development of improved mass spectrometry techniques and HPLC protocols. Current efforts focus on the more efficient preparation of these conjugates, the incorporation of "function", and the study of these constructs on patterned surfaces. An example of our state-of-art is represented by the preparation of the conjugate shown; a generation two dendron (G2p) that undergoes thiol-disulfide exchange to produce a bioconjugate (see Figure 13).

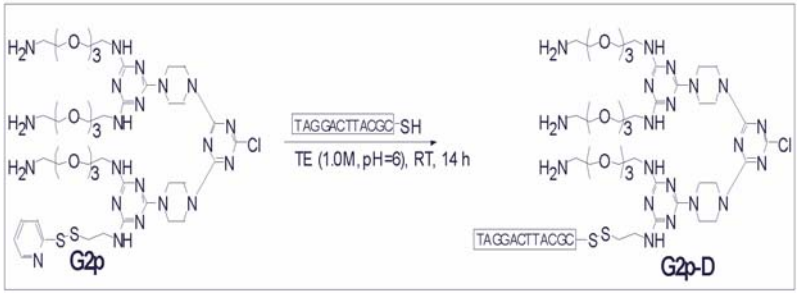

Figure 13. Dendron-DNA conjugates synthesized via a thiol-disulfide exchange reaction.

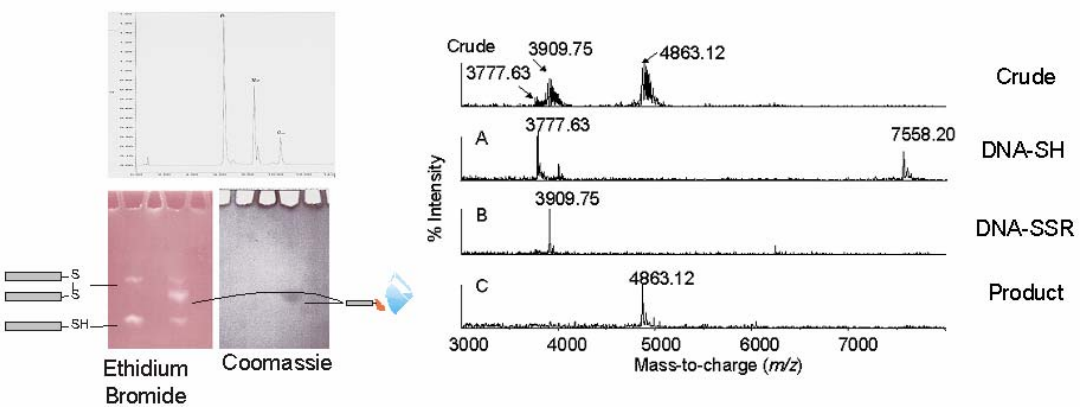

Figure 14. MALDI-TOF mass spectrum of crude, SH-DNA, DNA-SSR and products and PAGE gels.
They are visualized by differential staining with ethidium bromide and Coomassie Brilliant Blue R-250.

As shown in Figure 14, the crude reaction mixture has been evaluated with mass spectrometry and gel electrophoresis. Furthermore, HPLC can provide pure material (C) for subsequent application.

Currently, fluorescent labels have been incorporated into the dendrimers and their use on surfaces is being explored. Groups appropriate for solid-phase oligonucleotide synthesis have been incorporated into dendrimers, and used in the solid-phase synthesis of DNA-dendrimer conjugates. Proof-of-concept has been obtained for maleimide-thiol conjugation protocols. This linking strategy is stable to the reducing environment required for many enzymes. Utilizing PAGE and ethidium bromide stain, we can observe these three products, along with the final DNA-dendron conjugate. Additionally, we have developed a technique that uses Coomassie Blue stain to independently prove the presence of dendron in PAGE bands. We have developed strategies for the attachment of DNA oligonucleotides to dendrimers based on melamine. The attachment is afforded through thiol-disulfide exchange reactions. Protocols to characterize the products including gel electrophoresis and MALDI-TOF mass spectrometry have been developed.

The attachment strategy commences with a discrete dendritic architecture, and yields a mixture of products that can be identified and separated by HPLC. The resulting material is analytically pure (99%) and monodisperse. Hybridization studies confirm that these constructs can be used to amplify SPR signals. (See section 4.4).

The preparation of more complex conjugates (dye-labeled constructs) is inherently limited by the need to establish design early. Accordingly, testing hypotheses puts a significant burden on synthesis if a particular design fails. While this strategy was successfully used to prepare fluorescently labeled species **1-3** (see Figure 15), a more general solution to the problem was required.

Our next strategy relied on initial synthetic investment to prepare an orthogonally-protected dendrimer that could be selectively manipulated after the burden of synthesis was overcome. These targets have 5 and 6 orthogonally reactive groups that can be selectively exposed for post-synthetic manipulation. One of these sites already is present as a pyridyldisulfide group to facilitate our established thiol-disulfide exchange chemistry. Other sites can be unmasked to provide handles for labels or additional oligonucleotides.

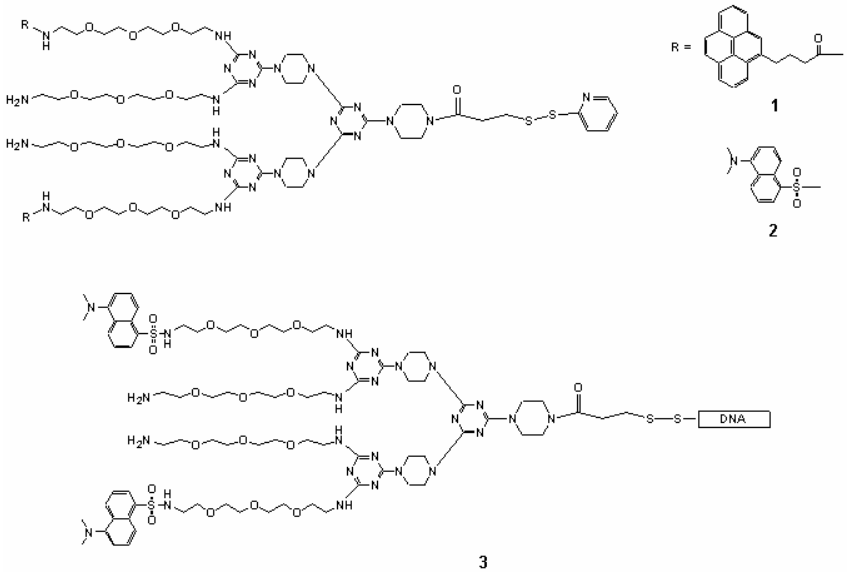

Figure 15. Synthetic scheme for more complex conjugates.

The synthesis of this elaborate dendrimer has been completed on the multi-gram scale and its manipulation has been established using model substrates. Further studies are required to determine whether it is useful for bioconjugate synthesis.

4.3. Synthesis of Photo-Reactive Psoralen-Containing Dendrimers

We report the synthesis and characterization of photo-reactive psoralen-containing dendrimers in order to develop a novel labeling method for the detection of DNA. Psoralens are unique in their ability to detect hybridized DNA: planar psoralen molecules intercalate into a double-stranded DNA, and covalent addition of the psoralen molecules to DNA is achieved by irradiation with long-wave length UV light. The psoralen-dendrimer conjugates were synthesized by the reaction of fourth-generation amine-terminated poly(amidoamine) dendrimers with NHS-ester-containing psoralen derivatives. 1H NMR analysis revealed that ~5 of the 64 terminal amine groups are modified with psoralen groups. Subsequently, the remaining amine groups were modified with hydroxyl groups to prevent the nonspecific interactions between DNA and amine groups in the course of DNA detection. We are currently investigating the DNA intercalating ability of psoralen-dendrimer conjugates on double-stranded DNA-modified solid surfaces.

We discovered a novel method for the sensitive detection of DNA hybridization using dendrimer-encapsulated Pd nanoparticles (Pd DENs) that contain photo-active, DNA-intercalating psoralen groups on the dendrimer periphery. To achieve amplified optical DNA detection, we chose a hybridization signaling reaction based on the one-electron reduction of viologen, which is catalyzed by Pd particles in the presence of hydrogen gas and leads to the formation of intensively colored viologen radical cations. In this approach, the use of Pd DENs provides a means not only to detect double-stranded DNA via the intercalating ability of psoralen groups, but also to amplify the detection signal via the catalytic reaction with Pd nanoparticles. Pd nanoparticles were encapsulated within the fourth-generation psoralen-modified poly(amidoamine)dendrimers by extraction of the metal ions into their interior, followed by chemical reduction. To investigate catalytic capability of the resulting Pd DENs, optical signal changes of a mixture of Pd DENs and

methyl viologen in a hydrogen-saturated aqueous solution were monitored by UV-vis absorption. The result showed that the lower detection limit was ~2 nM (6 pmol) of Pd DENs without appreciable effort to optimize the system. We are currently investigating the intercalating ability of Pd DENs into double-strained DNA immobilized on polystyrene beads, and their signal amplification ability for sensitive DNA detection.

4.4. DNA-Dendrimers and DNA-Dendron Conjugates on Surfaces

For signal amplification with programmable nanoscale DNA biosensors, the use of DNA molecules attached to either gold nanoparticles or dendrimers has been recently exploited. To do so, we synthesized DNA-dendrimer adducts using a hetero-bifunctional cross-linking agent to react amine-terminated dendrimers with thiol-modified DNA words (16 bases). To determine the feasibility of using these DNA-dendrimer adducts in future applications, it will be necessary for the attached DNA sequences to retain their ability to hybridize to complementary DNA sequences. Preliminary SPR data shows that

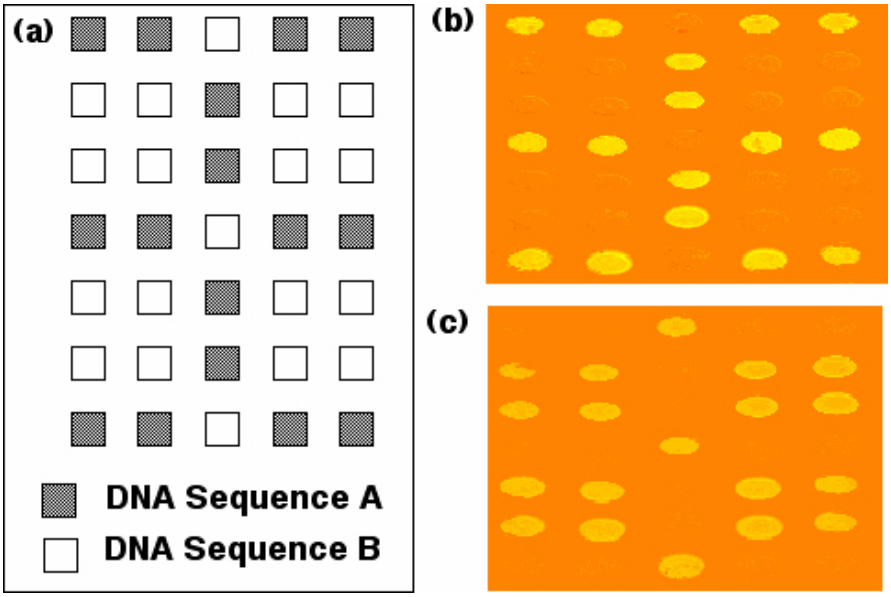

Figure 16. SPR difference images showing the hybridization adsorption of two different sequences of DNA conjugated to the periphery of dendron onto a DNA array.
(a) The pattern used for immobilization of single-stranded DNA probes. Hybridization of (b) DNA A sequence conjugated to a dendron and (c) DNA B sequence conjugated to a dendron onto the DNA array.

the DNA from the DNA-dendrimer adducts hybridized to its complementary sequence. In addition, the SPR signal corresponding to hybridization adsorption was increased by a factor of 5 for the adducts due to the additional mass of the dendrimer. This work will be further employed to enhance the readout signal of the programmable DNA biosensors fabricated using the technique of nanosphere lithography to create periodic nanometer sized gold particles immobilized on glass substrates.

We have also investigated the feasibility of applying DNA-dendron conjugates synthesized and purified from Prof. Crooks' group in TAMU for use in programmable biosensors. One of the advantages of using a dendron is that the modification of dendrons can be easily controlled since it contains only 2 different types of reactive functional groups. In a first test, a DNA-dendron conjugate was composed of a single DNA sequence (16 bases) covalently attached to the periphery of dendron. We first demonstrated the feasibility of using these DNA-dendron conjugates by measuring the hybridization of the conjugates to complementary DNA sequences immobilized on surfaces using the SPR imaging technique. Figure 16 shows two SPR difference images demonstrating the hybridization specificity of the DNA-dendron conjugates for their perfect matched DNA probes on the surface. We have also shown enhancement of SPR signal by the use of DNA-dendron conjugates that will be used for signal amplification with programmable nanoscale DNA biosensors. However, we have realized that the separation and purification of DNA-dendrimer conjugates from unreacted dendrimer and DNA are critical steps for our SPR assay to provide high quality and reliable data as well as to prevent non-specific binding of free DNA or dendrimer to the surface.

Next, we have focused on both the qualitative and quantitative characterization of DNA-dendrimer attachment chemistry and purification of the adducts. Our attachment approach involves three steps: 1) the attachment of amine-terminal groups on dendrimer with a hetero-bifunctional cross-linker, SSMCC and 2) the consequent reaction of maleimide-terminated dendrimer with thiol-DNA to form DNA-Dendrimer conjugates and 3) the separation of DNA-dendrimer conjugate. We used Ninhydrin test and NMR to see how many amino groups of the dendrimer were modified during the first step.

Ellman's reagent was then used to determine the number of DNA attached to the dendrimer. After the completion of the dendrimer-DNA adduct production, polyacrylamide gel electrophoresis was employed to separate different DNA-dendrimer conjugates.

It has been shown that the SPR signal of target DNA can be greatly enhanced by the use of DNA-amine-terminated dendrimer adducts that will be used in the future for signal amplification with programmable nanoscale DNA biosensors. However, we found that amine-terminated dendrimer causes non-specific adsorption on the wrong DNA array elements due to electrostatic interaction of positively charged dendrimer and negatively charged DNA in the buffer condition used. Our alternative approach is to attach DNA to dendrimers that has a carboxylic acid terminal group. Because carboxylic acid terminated dendrimers are normally negatively charged under neutral pH condition, it is expected that it will significantly reduce the electrostatic interaction. Our synthetic strategy is as follows: 1) the carboxylic acid group of the dendrimer is activated by using thionyl chloride ($SOCl_2$) and 2) amine terminated DNA is introduced to react with the activated dendrimer. We found that the SPR signal is significantly enhanced by the use of DNA-carboxylic acid terminated dendrimer conjugates, while little non-specific adsorption is occurred at the other spots. We are currently working on the separation and purification of these DNA-dendrimers from unreacted dendrimer and DNA using ion-exchange chromatography and some other techniques.

In conjunction with dendrimer work, an alternative approach to enhance the SPR signal when the complementary DNA hybridizes to the DNA array was investigated using a direct amplification of free target DNA sequences based on the biotin-streptavidin interaction. The amplification principle is to introduce i) a biotin-labeled target DNA to hybridize to the DNA array, ii) streptavidin to bind to the biotin-DNA, iii) biotin-labeled anti-streptavidin to bind to the streptavidin complex based on either the biotin-streptavidin interaction or the antibody-antigen interaction and iv) repetition of processes ii) through iii). To test the efficiency of the current amplification method, 1 nM solution of biotin-labeled DNA was employed. Our preliminary data revealed that after a mere

three cycles of flowing streptavidin and anti-streptavidin solution, the SPR signal was increased to three times higher than the one for a 31mer DNA with a starting concentration of 100nM. This indicates that this methodology can be used for very low concentration of target DNA detection, possibly femtomole detection. We are currently working on creating three-dimensional DNA-based networks using streptavidin-biotinylated DNA that possessing at least two DNA sequences attached to each streptavidin molecule. This utilizes noncovalent and covalent linking schemes based on the fact that covalently modified streptavidin can retain its binding affinity toward biotin molecules. The next step will be to employ DNA-dendron conjugates that posses different and non-interacting DNA sequences to the periphery and core sites of dendron to fabricate a programmable self-assembly of DNA-dendron nanostructures on the surface for biosensor applications.

4.5. Biologically-Modified Single-Walled Carbon Nanotubes

The unique mechanical and electrical properties of carbon nanotubes make them attractive candidates for forming biological-nano hybrids. While previous studies of biologically-modified adducts of DNA with carbon nanotubes had relied on non-specific binding of the biomolecules, we investigated the *covalent* functionalization of single-walled carbon nanotubes with DNA and with biotin, and the biologically-directed assembly of these adducts on surfaces.

4.5.1. Creation of DNA-Modified Single-Walled Carbon Nanotubes

Our initial efforts in single-wall carbon nanotubes (SWNT) were aimed at understanding the chemistry of the tubes and exploring the biological accessibility and selectivity of DNA-SWNT adducts. Oxidation of carbon nanotubes produces carboxylic acid groups that can serve as the basis for covalent modification with biomolecules such as DNA. While nanotubes possess a small number of these in their nascent state, the number of sites can be increased by oxidation using oxidizers such as nitric acid. We have developed a covalent linking chemistry between DNA oligonucleotides and single-wall carbon nanotubes and have investigated the hybridization of the DNA-modified

nanotubes with complementary and non-complementary oligonucleotides. X-ray photoelectron spectroscopy was used to characterize the initial chemical modification to form amine-terminated SWNTs, which were then covalently linked to DNA. The net result of this modification scheme is a completely covalent link between the DNA molecules and the SWNTs. These DNA-modified single-walled carbon nanotubes (SWNTs) showed that they are stable, exhibiting high selectivity, reversibility, and accessibility.

X-ray photoelectron spectroscopy analysis of the carbon and oxygen core-level shifts showed that under the conditions used here, approximately 6% of the carbon atoms are oxidized and are then converted to amine groups; this suggest that the density of DNA molecules attached to the nanotube is quite high. It should be possible to control this density by controlling the extent of the initial oxidation.

To confirm the stability of the DNA-SWNT adducts, measurements were made of the fluorescence intensity after fluorescein-labeled DNA oligonucleotides were directly bonded to the SWNTs. These studies showed that the DNA-SWNT adducts exhibited high fluorescence intensity, indicating a high degree of functionalization (estimated at 1 DNA molecule per ~6 carbon sites, based upon the XPS data). Exposure of the DNA-SWNT adduct to hot buffer/surfactant solution produced virtually no change in the fluorescence intensity. This is strong confirming evidence that the DNA-SWNT adducts are indeed covalently linked, since DNA that might be non-specifically adsorbed would be expected to be removed completely by this process.

To investigate the DNA hybridization process, DNA-SWNT adducts were divided into two samples that were then exposed to solutions containing fluorescently-labeled oligonucleotides with complementary and non-complementary (4-base mismatch) sequences. These results show that the complementary sequences hybridize efficiently, while there is only very little hybridization with the mismatched sequences under identical conditions. Thus, the hybridization is specific. These adducts were then denatured to remove the hybridized DNA, and were then hybridized again with the

alternate sequence (i.e., the nanotubes that were previously hybridized with a perfect match were now exposed to a mismatch, and vice versa). The results again show that DNA-SWNT adducts hybridize *reversibly* and exhibit a strong preference for binding to complementary sequences with only minimal interaction with non-complementary sequences.

We also note that the covalent DNA modification greatly increases the affinity of the nanotubes for water and other aqueous solutions. This is significant because one of the practical difficulties in working with nanotubes has been their low solubility. The addition of negative charges contained on the DNA backbone apparently increases the solubility of the nanotubes.

Studies of biological modification of nanotubes described above have all relied on non-covalent interactions to bind the biomolecules to the nanotubes. The use of non-covalent interactions is disadvantageous because SWNTs modified in that way do not have the *stability* that is required for complex nanoassembly. We used entirely covalent chemistry to first produce amine-terminated SWNTs, and then used a heterobifunctional linker to attach thiol-modified DNA to the tubes, forming covalent DNA-SWNT adducts. These DNA-SWNT adducts have quite interesting physical properties, including a much higher solubility in aqueous solvents than non-modified SWNTs. We then investigated the hybridization of these DNA-SWNT adducts with complementary and non-complementary DNA oligonucleotides in solution. These results showed that the DNA-SWNT adducts exhibit very high selectivity, strongly favoring hybridization to complementary vs. non-complementary sequences. The DNA-SWNT adducts are also very stable, able to withstand repeated washings with hot buffer and other conditions that would rapidly degrade non-covalent adducts. This stability is important because it means that DNA-SWNTs can be used as reversible elements for nanoscale assembly. Overall, this work showed that the DNA-SWNT adducts exhibit the selectivity, stability, and reversibility needed for use in nanoscale assembly.

More recently, we have also extended this to the preparation of biotin-modified SWNTs. Much of the same chemistry can be used. While DNA hybridization is quite delicate, the biotin-avidin interaction is extremely strong and essentially irreversible. We successfully prepared covalently-bound biotin-SWNT adducts and showed that these will bind successfully to avidin. Because of the high strength and irreversible nature of the biotin-avidin interaction, biotinylated nanotubes can be used for strong, irreversible attachment to avidin. Avidin, in turn, has 4 accessible binding sites; while one or possibly two of them might be used in binding to biotinylated nanotubes, the remaining avidin sites should remain accessible, able to bind to other biotin-modified molecules. The use of avidin as a kind of "glue" for linking biotinylated structures has been known to be quite general.

While much of our initial work has focused on nanoscale assembly in solution, we have also taken steps to use biomolecular interactions as the starting point for assembly on surfaces. We successfully produced biotinylated glass and silicon surfaces and showed that after addition of avidin (thereby producing an avidin-modified surface), biotinylated SWNTs will selectively bind to these biotinylated regions. Thus, we formed a surface-biotin-avidin-biotin-nanotubes construct. Those experiments were successful demonstrating the ability to achieve biologically-directed assembly of carbon nanotubes with the biotin-avidin system. Moreover, biotin-modified SWNTs would bind strongly to the avidin-functionalized surfaces, but not to biotin-modified surfaces. Consequently, avidin can be used as a kind of "molecular glue" to bind biotin-modified carbon nanotubes to avidin-modified surfaces. However, the reversibility of DNA hybridization makes it a more attractive means for fabricating hybrid structures. Consequently, we have been revisiting this problem. In a series of experiments, we found that the assembly process could be improved by using a smaller concentration of DNA for the initial functionalization of the nanotubes, and by performing the experiment at a higher temperature. By operating near the melting point of the DNA duplexes, we found that the DNA-modified nanotubes still hybridized with the surface, while "free" DNA duplexes tended to denature. We believe that this is a simple collective effect in which SWNTs that

are bonded to the surface via multiple DNA-DNA interactions have a higher effective melting temperature than a single DNA-DNA duplex.

4.5.2. Alternate Approach to Attach Biological Molecules to Nanotubes

Our attention is now turning toward the use of electric fields to direct biologically-modified carbon nanotubes onto a surface. Our goal is to be able to modify the carbon nanotubes with biomolecules of interest, and then to use various combinations of electric fields and chemical interactions to control their assembly onto a surface. Using optical microscopy to follow the migration of nanotubes in a fluid, we have observed the field-directed motion and are now conducting experiments to better control the motion and to align the tubes parallel to an electric field. In addition to the covalent linkage of DNA to nanotube, we have developed several new methods for modifying carbon nanotubes. These new methods are much more gentle than those used previously and are therefore more amenable to use with nanotubes that are grown by chemical vapor deposition methods.

We have recently been working on using AC electric fields to pull biologically-modified nanotubes into micron-scale junctions between contact pads. The essential idea here is to use biologically-modified carbon nanotubes as a kind of molecular "fuse", in which biochemical interactions (such as DNA hybridization) would link nanotubes across electrical contact pads; because nanotubes are highly conductive, the directly assembly of nanotubes across contact pads would result in a kind of "digital biosensor" in which a small number of molecules would produce a very large change in current flow. As of this date we have not yet successfully completed this experiment, but we are working on this and hope to have some positive results within the next several months.

4.6. Fabrication of High-Stability DNA Assemblies on Diamond Thin Films

We have interacted with personnel at the Naval Research Laboratories (John Russell and James Butler) on the modification of diamond thin films for biological studies. They have grown diamond thin films for us, and we have sent a student to work at NRL for ~3

weeks. Because we have found that diamond thin films exhibit selectivity and stability that is superior to that of other DNA-modified planar surfaces, we have been conducting studies of the hybridization of DNA-modified SWNTs with DNA-modified diamond thin films.

Because fabrication of nanoscale assemblies on surfaces requires surfaces with very high stability, we have investigated the use of diamond thick films and diamond thin films (< 0.5 micron thickness) as substrates for biological modification. This work is an extension of several external collaborations with Dr. John Russell and Dr. James Butler at the Naval Research Laboratory and with Dr. Dieter Gruen and Dr. John Carlisle at Argonne National Laboratories. The external groups have great expertise in preparation of diamond thin films, and the Hamers and Smith groups have provided expertise in surface and biological modification chemistry. The most important result from this work is our recent demonstration that DNA-modified diamond surfaces show extraordinary stability. In repeated hybridization-denaturation experiments, thin-film diamond (only 0.5 micron on Si substrate) showed no change in efficiency or selectivity even after 30 repeated cycles. Comparison with a number of other substrate materials (glass, glassy carbon, etc.) showed that all other materials degrade under these conditions. Initial work by Knickerbocker showed that "free-standing" diamonds (i.e., thick films) are stable; however, these are too expensive to use in a practical sense. More recent results by Yang show that one can get essentially all the benefits of diamond in a practical way using very thin (<500 nanometer) diamond films on Si (and other) substrates, with suitable modifications to deprotection chemistry and other procedures.

The significance of this result is that DNA computing and DNA-based architectures would benefit greatly from very stable substrates. Diamond provides such a platform. The ability to use thin diamond films on silicon substrates also provides a pathway for integration with microelectronics technology. (thin-film diamond can be grown under conditions compatible with CMOS technology... see more below). This work was reported fairly widely in the press, including articles in *Chemical and Engineering News*

(Dec. 2, 2002), *Technology Research News* (Dec. 11/18, 2002), *New Scientist* (Dec. 2002).

We have recently shown that the electrochemical properties of biologically-modified diamond surface change in response to biological binding. This provides a label-free, real-time, low-power method for detecting biological binding processes. While most diamond thick films are highly resistive, thin films can be made conductive (p-type). By integrating thin-film diamond with silicon and using electronic detection, we should be able to get unprecedented stability and all the advantages of electronic detection for completely integrated biological detection systems.

4.7. DNA Biosensors Engineered by Various Surface Based Enzymatic Reactions

4.7.1 Rolling Circle Amplification Process on Surfaces

We have investigated an enzymatic amplification approach that enables the detection of immobilized DNA probe molecules with low concentrations on gold surfaces. Our approach was to use rolling circle DNA amplification that employs DNA polymerase to construct a long DNA molecule containing hundreds of copies of the circular DNA sequence. The RCA process is known to posses several unusual features including efficient synthesis, isothermal reaction process and a dramatic increase in the numbers of copies of circular template produced. The RCA process for our surface bound DNA involves three steps: i) synthesis of a 64mer circular DNA template obtained through a template assisted ligation, ii) purification and characterization of circular DNA by gel electrophoresis, iii) RCA amplification on the surface to produce a long DNA product that remains linked to the DNA primer. The RCA reaction efficiency and specificity was first investigated by means of hybridization of fluorescence labeled complements onto the RCA amplified DNA attached to the gold surface. From the fluorescence imaging data, it was observed that the fluorescence signal was enhanced 10 times when using RCA amplification than the signal obtained in the absence of RCA.

We have then employed this RCA of DNA probes on the gold surface for SPR detection of unlabeled target DNA molecules. In order to lower the amount of circular template and enzyme used in this experiment, we have employed micro-fluidic channels from PDMS to deliver small volumes (1 to 5 μL) of reactants and target molecules onto gold surfaces. The relationship between the degree of amplification and the concentration of DNA probes has been investigated. Our approach was to use mixed DNA sequences containing a 16mer DNA sequence and a single-base spacer with varying ratio from 0% to 100% (=10 μM) that can also be beneficial to the control of surface density of the immobilized DNA. A set of parallel microfluidic channels from PDMS was first used to immobilize a series of DNA probes with different concentrations on the gold surface. This creates lines of DNA patterns on the surface. The key point is that the initial surface immobilized DNA concentration was 10 μM, which is 100 times lower than what we usually use (1 mM). After immobilization, the microfluidic channels were removed and a second set of microfluidic channel in a wrap around configuration was physically attached on the surface perpendicular to the line array. The background was replaced with polyethylene glycol (PEG) through the second channel to prevent non-specific adsorption. After PEGlation, the synthesized circular template was delivered to hybridize to the surface bound probes through the microfluidic channel. Subsequently, RCA reaction was carried out with Sequenase 2.0 polymerase at 37°C for 30 min. After the reaction was completed, SPR imaging was used to monitor the hybridization of complementary DNA sequences to the amplified surface bound DNA probes.

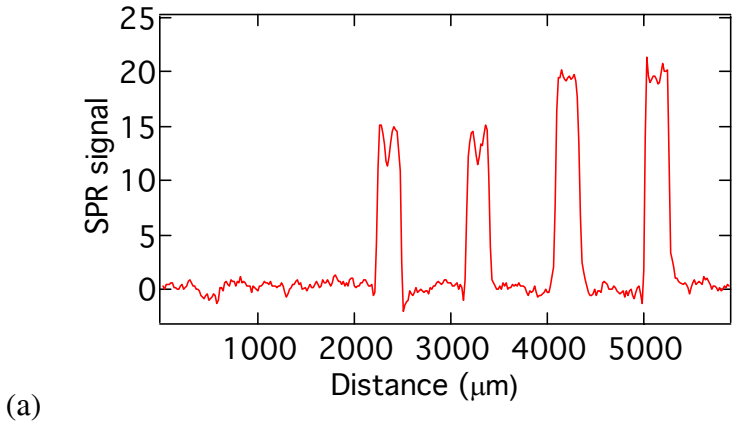

(a)

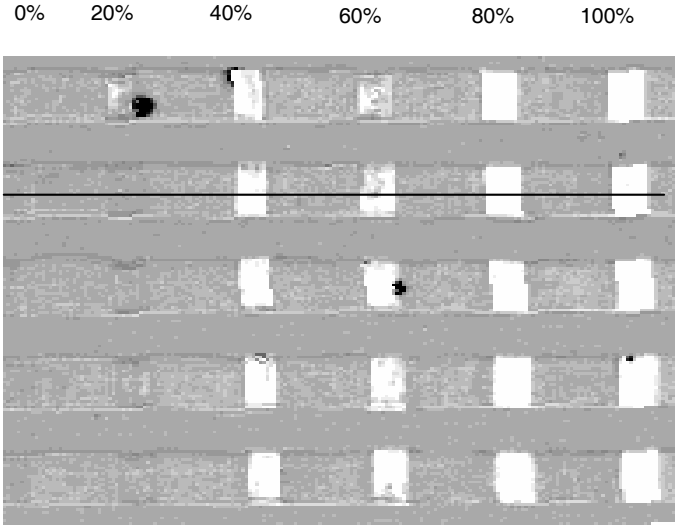

(b)

Figure 17. (a) SPR difference image. (b) Line profile of difference image.

Figure 17 shows the SPR difference image and corresponding line profile before and after the surface is exposed to the complementary sequences. It can be clearly seen that the SPR signal for the RCA amplified 10 μM initial DNA probe is even higher than that from 1mM surface bound probes in the absence of RCA. This demonstrates the RCA of surface bound DNA has been successfully achieved. Non- linear relationship between the degree of amplification and the initial concentration of DNA probes was next investigated. We have tested 5 different probe concentrations together with a control sequence immobilized on the surface with different geometry shapes as shown in Figure 17(a). After the RCA reaction for 30 min with Sequenase 2.0 polymerase, the amplification of probe concentrations higher than10 μM was observed, while no obvious amplification was observed below 1μM probes (see Figure 17 (b). At 100 μM probe

concentration, the degree of RCA reaches the maximum (data are not shown). Further studies to characterize the surface density of the amplified probes are in progress using fluorescence wash-off experiments. In addition, the relationship between the number of DNA hybridizing to the surface and various probe concentrations is still under investigation.

The second set of experiment we carried out was to study the concentration dependence of target complementary DNA hybridizing to the RCA amplified surface probe (initial probe concentration of 100 μM) using SPR imaging. As low as 10 pM of complementary DNA can be detected when using RCA probe, while the complementary DNA lower than 10nM cannot be detected for the non-RCA probe. This indicates that RCA of the probe can lower the detection limit to 3 magnitudes. Figure 18 shows the surface coverage (θ) as a function of logarithmic concentration of complementary DNA using a Langmuir adsorption isotherm. The adsorption coefficient, K_{ads} was found to be 1.4 x 10^6 M^{-1}, which was lower than that for DNA-DNA hybridization in the absence of RCA ($K_{ads} \cong 10^7$ M^{-1}).

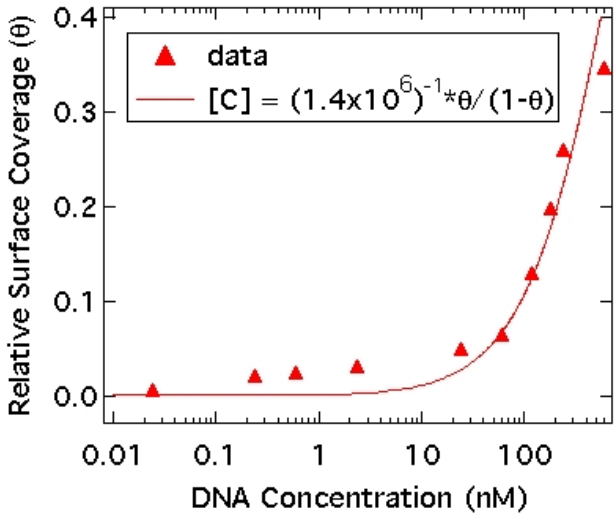

Figure 18. Langmuir isotherm fits for the adsorption of complementary DNA hybridizing to the RCA amplified surface probe.

4.7.2 Development of a New Class of DNA-Based Materials

The highly predictable hybridization reaction of DNA, the ability to completely control the length and content of oligonucleotides, and the wealth of enzymes available for modification of DNA make the nucleic acids attractive for both biological and nonbiological applications. In order to realize these applications, the essential challenge is to design sets of non-interacting short oligonucleotides, or "DNA words". These DNA words should hold the following properties:

i) Each DNA word W_i should bind strongly to its complement Ci and no significant binding between W_i and C_j for $i \neq j$ (the complement problem).

ii) No significant binding between W_i and W_j or C_i and C_j for $i \neq j$ (the reverse complement problem).

iii) No significant binding between W_i and itself (the inverted repeat problem).

Our group has previously used the template-map strategy to create a set of non-interacting oligonucleotides. In this case, the reverse complement and the inverted repeat problems were not considered. To overcome these problems, we have developed a new strategy to design DNA words based on *De Bruijn* sequences. *De Bruijn* sequences are part of a mathematical theory of strings, codes, and information that provides a foundation for addressing this computational biology question. By definition, a k-ary *De Bruijn* sequence of order n is a circular k-ary string containing every k-ary string of length n as a substring exactly once. Thus a *De Bruijn* sequence has a length of k^n. For n=3 and k=2, the lexicographically smallest *De Bruijn* sequence is 00010111. The number of k-ary *De Bruijn* sequences of order n is given by (k!)^{k^{n-1}}k^{-n}. For example, for the case of n=3, k=4, 1.89×10^{20} *De Bruijn* sequences are available. The complement problem was then addressed by restricting repeated substrings with maximum length 3 or n=3. For n=3 and k=4 (4 alphabets, A, T, C and G), each sequence has a length of 64. We provided an algorithm for generating these sequences uniformly at random from the 1.89×10^{20} total possibilities and analyzing their performances. Among those sequences, we first eliminated sets of sequences that possess secondary structures. We then chose two 64mer *De Bruijn* sequences to verify if these are interacting with each

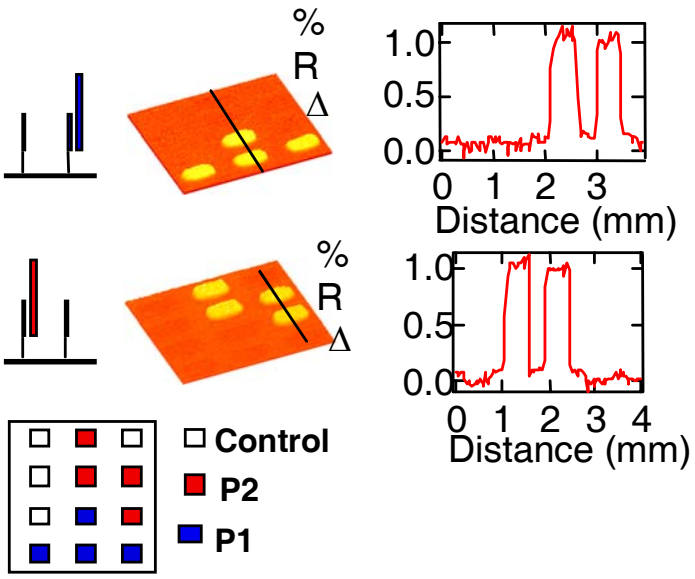

Figure 19. SPR difference images showing two complementary De Bruijn sequences binding to their perfectly matched probes immobilized on gold surfaces.

other on surfaces. Figure 19 shows SPR difference images obtained for two non-interacting *De Bruijn* sequences. Each *De Bruijn* sequence only binds specifically to its own complementary DNA strand on the gold surface. No binding was observed for unmatched ssDNA probes and control probes. In the near future, we will work on creating a set of non-interacting *De Bruijn* sequences with user defined set size. The fundamental difficulty lies in finding good algorithms to construct a large set of non-interacting sequences from numerous *De Bruijn* sequences that can satisfy the reverse complement and inverted repeat problems.

Next, we have focused on the creation of DNA based materials using these *De Bruijn* sequences for the application of nanoscale networks and bridges and many other interesting nano engineering. Our strategy was first to use rolling circle amplification (RCA) process as described in section 4.7.1 to control the length of selected *De Bruijn* sequences. We have studied the RCA process both in solutions and on the surface using *De Bruijn* sequences. First, a template-assisted enzymatic ligation strategy was used to synthesize the single-stranded circular DNA. After the circular DNA was made, RCA was then used to amplify the *De Bruijn* sequence in the solution. Figure 20 shows the gel

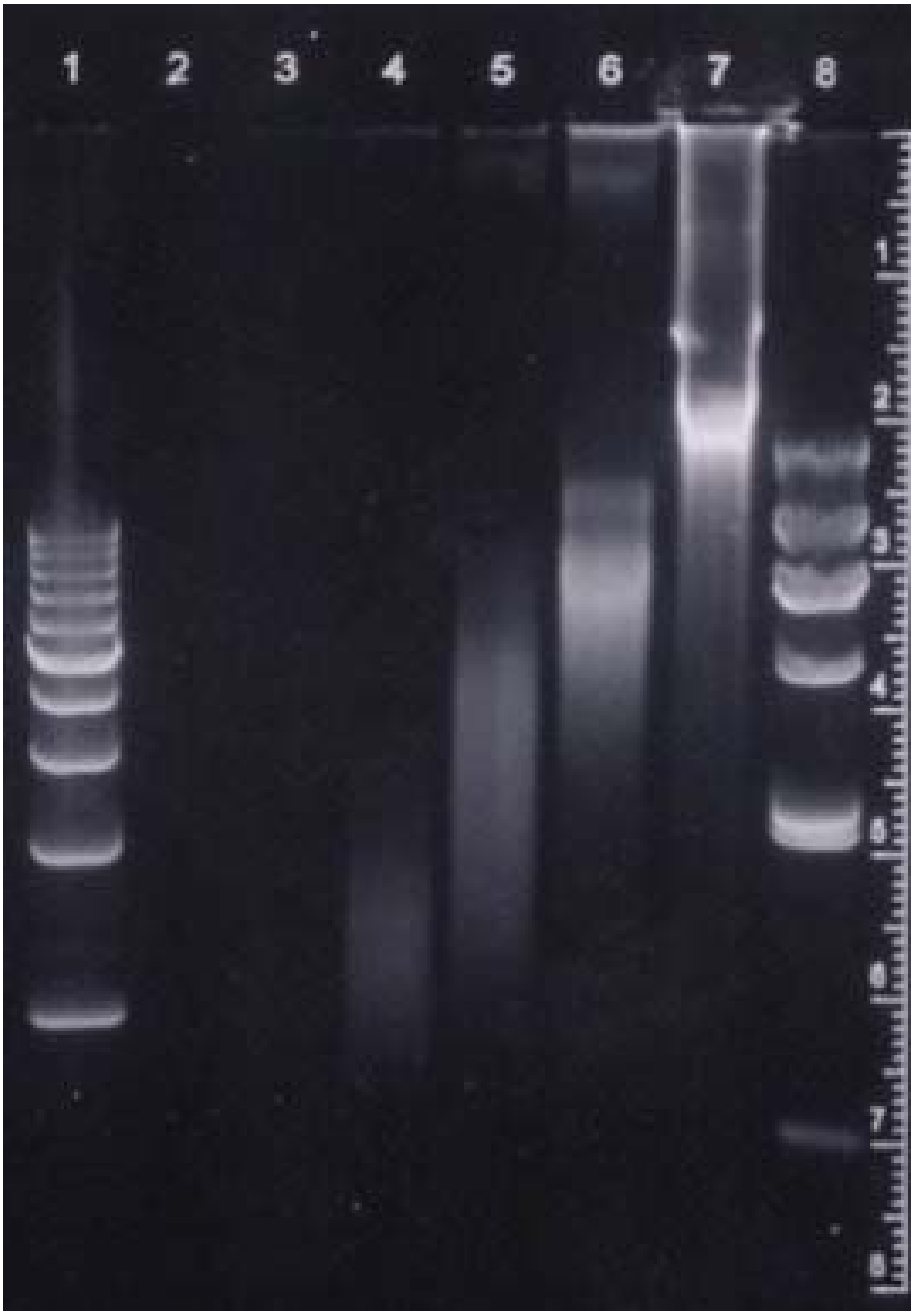

Figure 20. Gel electrophoresis result of RCA product as a function of reaction time on 0.8% agarose gel.

Lane 1: 1kb DNA marker
Lane 2: no DNA circles
Lane 3: 5 min RCA
Lane 4: 20 min RCA
Lane 5: 35 min RCA
Lane 6: 1hr RCA
Lane 7: overnight RCA
Lane 8: Lamda marker

electrophoresis result of RCA as a function of time. The RCA product grows as the reaction time increases and can exceed 25kb after 1hour reaction. RCA products can not be seen if DNA circles are not present in the reaction. To verify the sequence of the RCA product, a band around 5kb from lane 6 was cut from the gel and purified with gel extraction kit. The DNA sequencing results confirm the RCA product as a long strand containing multiple copies of the DNA circles.

To investigate the time dependence of the rolling circle reaction, most researchers used either gel electrophoresis or labeled decorator probes through hybridization. In both cases, the reactions need to be stopped and signals must be periodically recorded. These processes are laborious and time consuming. In contrast, SPR imaging is a surface sensitive and label-free technique used to study the adsorption of molecules onto chemically modified thin gold films by monitoring changes in the reflectivity that occur as a result of adsorption onto the surface. The kinetic study of RCA reaction on surface by *in-situ* monitoring the RCA reaction in real time is investigated using SPR imaging. After the circular DNA was made, RCA was then used to amplify the surface bound probes on the gold surface. One control probe and two other RCA primers diluted to different concentrations with cysteine were immobilized on the surface. After the circular DNA was annealed to the surface bound primers, the RCA reaction was performed at 30°C with the addition of phi29 DNA polymerase and dNTP. Figure 21 shows the growth of RCA primers over reaction time monitored using SPR imaging. The result of this experiment shows that the RCA primers grow over a period of 90 min. RCA occurs with a fast rate in the first 30 min and gradually slow down and then reach the steady-state. No amplification effect was observed for the control probe as expected. This indicates the high specificity of the RCA reaction.

In the future, we are going to use RCA- *De Bruijn* products as bridges to assemble building blocks, such as DNA modified gold nanoparticles to form interesting nanostructures or networks.

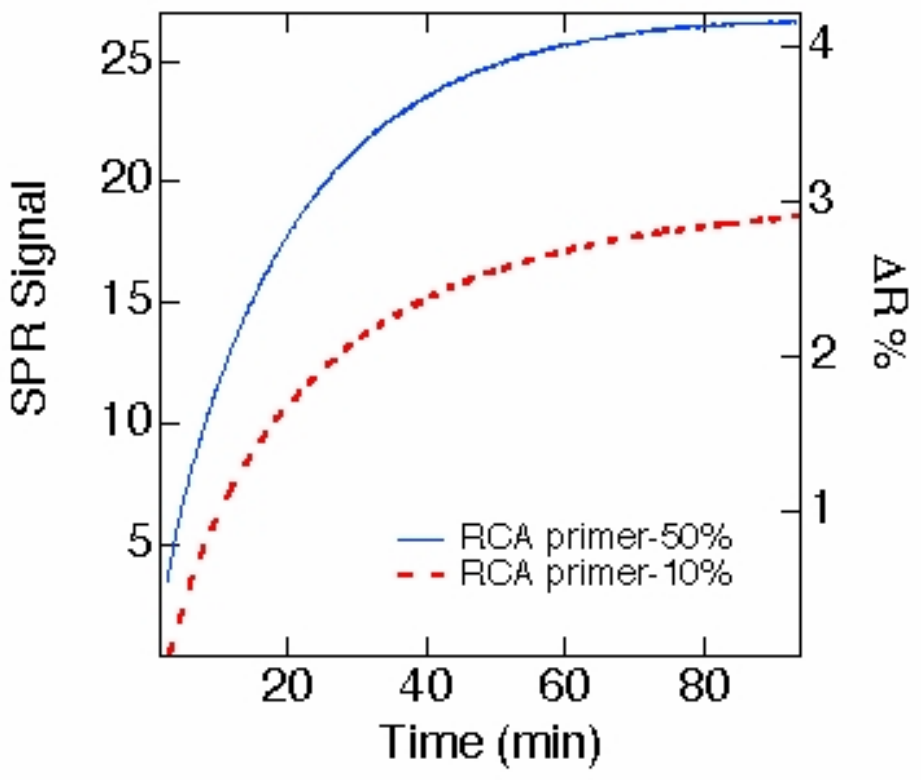

Figure 21. Plot showing the growth of rolling circle products on the gold surface as a function of time.
The RCA primers were diluted with cysteine before the immobilization.

4.8. Control of Surface Immobilized DNA Molecules on Gold Surfaces

To optimize our SPR detection signal from DNA hybridization, we have studied hybridization efficiency of complementary DNA to the surface immobilized DNA. There are many factors contributing to hybridization efficiency such as surface density, buffer stringency and temperature. Our efforts made during the granting periods can be classified into: i) influence of surface density of immobilized DNA probes and ii) differential binding efficiency between DNA sequences with different number of base mismatches.

4.8.1. Influence of Surface Density of Immobilized DNA Probes

The study of hybridization efficiency as a function of surface coverage of immobilized DNA molecules can be classified into two approaches: (i) Modulating the surface by a mixture of two non-interacting DNA sequences (16 mers and denoted as DNA A and

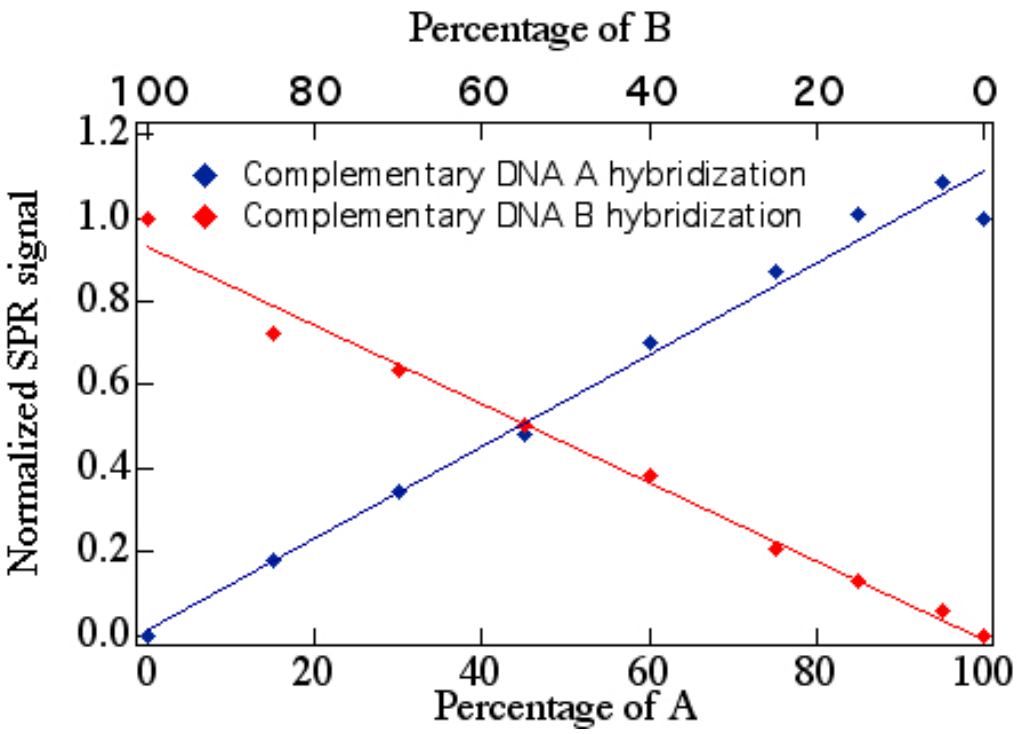

Figure 22. Plots showing the normalized hybridization SPR signal of complementary DNA A and B versus percentage of A or B DNA sequences immobilized onto the surface.

DNA B) that posses the same length on surfaces and (ii) Modulating the surface using a mixture of a mixture of a 16-mer DNA sequence (denoted as W3) and a spacer molecule. The non-interacting DNA sequences were generated using DNA word design strategies that we have previously published. The sequences of DNA A, DNA B and W3 are as follows: DNA A:5'-GTGTATCCGACATGTG -3', DNA B: 5'-ATGCTTCGATGCAACG -3', W3: 5'-GTGTTAGCCTCAAGTG-3'.

For the former case (i), the SPR signal for hybridization of each complementary DNA sequence to its perfectly matched probe DNA molecule on surface is linearly proportional to the percent concentration of its perfectly matched DNA probe molecules (**A** or **B**) immobilized on the surface (see Figure 22). This result indicates that the interaction between the two immobilized DNA probes is constant in the hybridization process and the hybridization efficiency (around 30% for a full monolayer of DNA probe) remains the same in both cases for fixed total surface density because the electrostatic repulsion between the two DNA probe molecules is always constant.

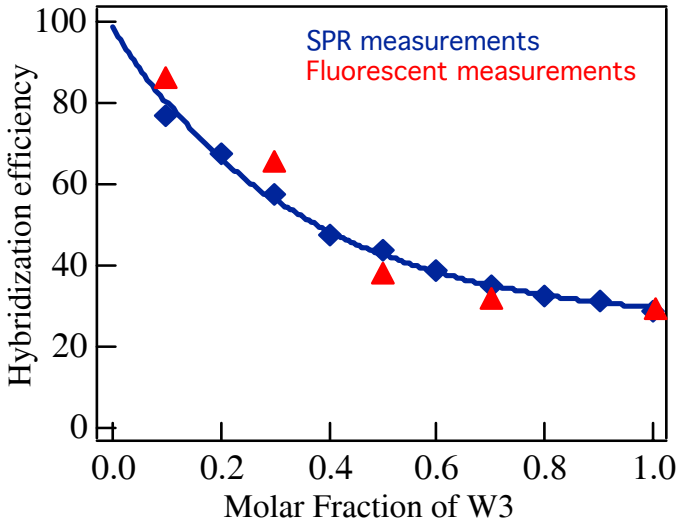

Figure 23. Plots showing the hybridization efficiency of complementary DNA W3 versus molar fraction of W3 immobilized onto the surface.

For the latter case (ii), we used cysteine as a spacer to dilute the surface density of the 16mer DNA and tested hybridization efficiency using SPR imaging. Figure 23 shows the relative hybridization efficiency converted from the SPR data versus molar fraction of W3. It can be clearly seen that the behavior of hybridization is certainly different from the mixture of the two 16-mers case. Surface density of 100% 16-mer is on the order of 10^{13}molecules/cm^2, and for such a high surface density due to the steric hindrance, it might be difficult for target DNA in the solution to get in and hybridize to the DNA probe. Our data supports this hypothesis and shows the highest hybridization efficiency for the lowest surface density. By using the hybridization efficiency value of 30% for a full probe monolayer, the SPR signals were converted into hybridization efficiency. As can be seen from Figure 23, when the surface density is reduced to 10%, hybridization efficiency is dramatically increased to about 80%, as compared with the original value of 30% for 100% surface density. The result from fluorescence wash off experiments is in good agreement with the SPR data.

4.8.2 Differential Binding Efficiency between DNA Sequences

We have studied the effect of base mismatches on the binding efficiency. We have first designed several sets of combinatorial DNA mixtures with different number of base

mismatches, as shown in Table I. Here W stands for either A or T. For example, in the 6-base mismatch combinatorial mixture, positions indicated by W are allowed to go through all possible combinations of A and T, which gives a total of 2^6 different sequences in the mixture. Among them, the majority of sequences contains 3-base mismatch. Similarly, the majority in the 8-base mismatch combinatorial mixture is a 4-base mismatch. Therefore we can obtain the relative binding efficiency of different sequences by employing these combinatorial mixtures without considering problems such as slide mismatches and hairpin formation which are usual when using single sequences. Further study of differential binding effect using SPR imaging can be applied to optimize the signal from DNA-based nanoscale biosensors.

Table I: Combinatorial DNA sequences

probe sequence	5'-GGCC TATA AAAT CCGG-3'
4-base mismatch	5'-CCGG ATTT WWWW GGCC-3'
6-base mismatch	5'-CCGG ATWW WWWW GGCC-3'
8-base mismatch	5'-CCGG WWWW WWWW GGCC-3'

4.9. Creation of High Fidelity Double-Stranded DNA on Gold

The DNA arrays have been characterized in terms of chemical stability, surface density and surface hybridization to complementary oligonucleotides from solution. The long-term stability of the DNA microarrays was observed by subjecting a single gold chip to over 40 cycles of hybridization-denaturation. The percentage of the single-stranded DNA (ssDNA) monolayer involved in surface hybridization, defined as the hybridization efficiency, was found to vary with ssDNA surface density and ionic strength in hybridization buffer. The hybridization efficiency was enhanced from 30% for a full ssDNA monolayer (surface density = 9×10^{12} molecules/cm^2) to 86% for a ssDNA monolayer with a reduced surface density of 9×10^{11} molecules/cm^2. Based on the characterization of DNA arrays, we have demonstrated that enzymatic processing can be used on these ssDNA arrays to produce high fidelity double-stranded DNA arrays for SPR imaging measurements of protein-DNA interactions.

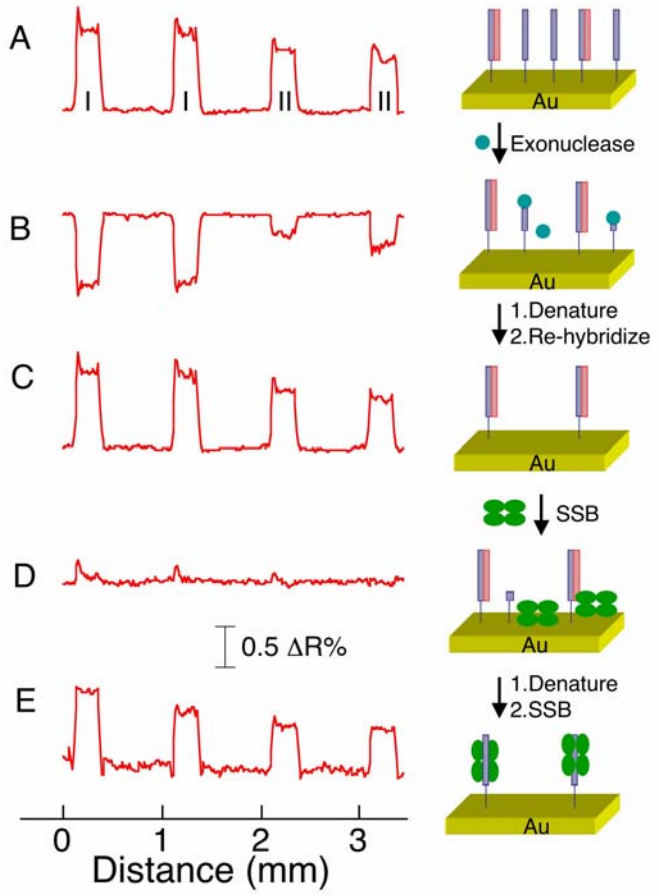

Figure 24. SPR data showing a series of enzymatic processing of a two-component DNA array with W3 and cysteine mixtures.
The array elements labeled as I on the left side are 100% W3, and the ones labeled as II on the right side are 50% W3-50% cysteine mixtures.

Figure 24 shows a series of SPR imaging results on a DNA array (two array elements of 100% W3 (16mer) and 50% W3-50% cysteine) during the processing with the enzyme, Exonuclease I from *E. coli* that selectively destroys single-stranded DNA in a 3' to 5' direction. Frame A shows the hybridization adsorption of C3, perfect complementary sequence of W3 to the ssDNA array. In Frame B, the surface was reacted with exonuclease for 3 hours to cleave the remaining ssDNA. A negative SPR imaging signal was observed due to the removal of ssDNA from the surface. As expected, more ssDNA was removed from the 100% W3 array elements than the 50% W3-50% cysteine array

elements because there is more ssDNA on the surfaces with higher DNA surface density. Frame C in Figure 24 shows a subsequent hybridization of C3 to this array after denaturing the surface with 8 M urea. The hybridization signal after the exonuclease processing was almost identical to the original hybridization signal. This dsDNA array was then exposed to 20 nM of single-stranded DNA binding protein (SSB), which binds exclusively to ssDNA, to verify the presence or absence of residual ssDNA. Prior to processing this array with exonuclease, some SSB binding was observed (not shown). After processing, as Frame D illustrates, virtually no SSB binding was seen for either dsDNA elements. After the array was denatured again with urea, exposure to SSB clearly resulted in binding to the array elements as shown in Frame E.

This clearly shows that Exonclease I from *Escherichia coli* to DNA microarrays after hybridization can remove remaining single-stranded DNA residues to produce dsDNA arrays. We have also demonstrated that the double-stranded DNA created with this method has no binding at all upon introduction of the single-stranded binding protein, demonstrating the fidelity of these dsDNA arrays.

In the future, we will explore this system to create high fidelity dsDNA array for the study of *Eco*RI methyltransferase and endonuclease restriction-modification system from the bacteria *E. coli*. Methylation plays an important role in living organisms. The mismatch repair system in *E. coli* uses difference in methylation pattern to distinguish the template and nascent strand for mismatch correction. Regulation of gene expression also involves methylation. Mutant cells deficient in methylase are not viable. Because of the essential function of methylation, studies of methylation related proteins will lead to the elucidation of their binding activity or enzymatic mechanisms. *Eco*RI endonuclease can introduce two staggered, single-strand scissions into the symmetric recognition sequence, 5'- GAATTC -3'. However, activity of *Eco*RI endonuclease is blocked once the second A on the restriction site is methylated by *Eco*RI methyltransferase. Therefore, at the presence of both enzymes the overall reaction will be a competition between methylation and endonuclease cleavage. Previously researchers have used radiolabeled substrates to study the enzymatic activity of *Eco*RI methyltransferase. We propose to study the

catalytic efficiency of *Eco*RI methyltransferase in a competition assay with *Eco*RI endonuclease using SPR imaging measurements. First the catalytic efficiency of *Eco*RI endonuclease can be obtained with SPR imaging by monitoring the decrease of SPR signal upon enzyme cleavage. Steady-state study of the initial velocity of enzymatic cleavage at different DNA surface densities should give information about the catalytic efficiency of endonuclease. Similarly, the cleavage rate of endonuclease can be measured at the presence of methyltransferase. Because methylation will block the endonuclease activity, the cleavage rate is expected to be slower than in the absence of methyltransferase. By comparing the difference in cleavage rate, methyltransferase activity can be obtained indirectly. This competition assay can be extended to other methylases that have corresponding endonuclease in nature such as *Hpa*II methyltransferase and endonuclease which recognizes the sequence 5'-CCGG-3'. Because in natural environment methylation by methylases always occurs at the presence of restriction endonuclease, information from competition assay is more relevant to the *in vivo* catalytic efficiency of methylases. An understanding of the recognition and catalytic mechanisms of these enzymes may facilitate the design of biocatalysts with novel specificities and chemical mechanism.

Since methylation of DNA sequences also controls gene expression, another interest of our future research is to characterize the affinity of some methylation specific proteins toward the methylated sites. In this case, endonuclease can be used to destroy the unmethylated DNA sequences after methylation by methyltransferase, forming uniformly methylated DNA arrays. This provides us the ability to control *in situ* surface DNA array modification. For all these purposes, the high fidelity dsDNA arrays created by Exonuclease I serves as a basic characterization tool. The absolute absence of ssDNA residues on our dsDNA arrays guarantees that no non-specific binding of proteins to ssDNA happens on the DNA array, thus eliminating the arising of potential false signal.

4.10. Development of Enzymatically Amplified SPR Imaging

The direct detection of DNA and RNA is important for diagnosing viral and bacterial infections, gene expression analysis, and forensic identification purposes. While a

number of strategies have been proposed, most are based on fluorescent or radioisotope labeling to detect target DNA. A label-free technique such as SPR imaging would be extremely useful for this purpose. During the last granting period, we have developed a novel scheme that utilizes two different enzymatic approaches to amplify the SPR detection signal of DNA microarrays to the binding of target DNA for the direct detection of genomic DNA: (i) Exonuclease III and RNase H.

4.10.1. Exonuclease III

By controlling the orientation of immobilized DNA and the structure of DNA duplex, the enzyme Exonuclease III is able to specifically and repeatedly hydrolyze the immobilized DNA strand from duplex DNA, resulting in an enhanced loss of SPR signal. The amplification mechanism of Exonuclease III on surfaces is overviewed in Figure 25. 5'-thiol modified ssDNA is first immobilized on chemically modified gold surfaces. When the DNA array is exposed to a solution containing both target DNA sequences and Exonuclease III, the target DNA will first bind to its DNA complement on the surface to

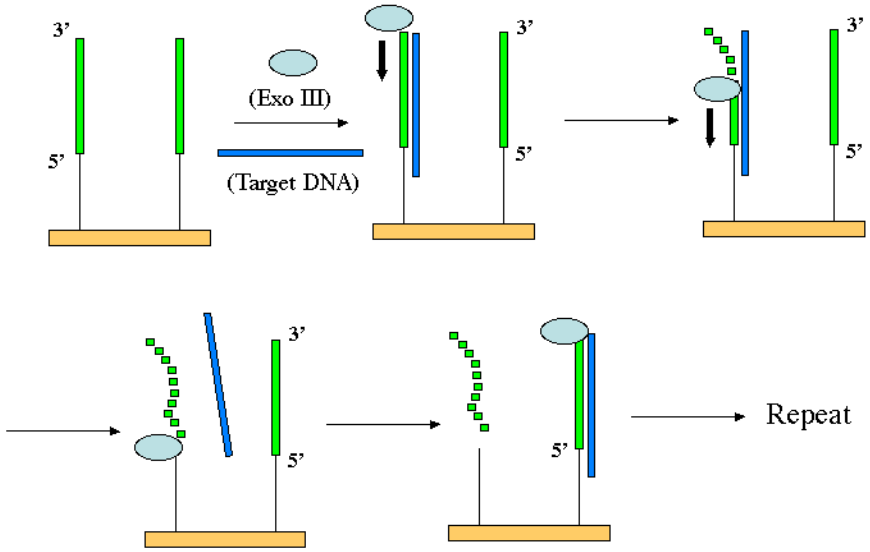

Figure 25. Schematic presentation of a surface enzymatic reaction for the amplification of SPR signal by selectively removing immobilized DNA probes.

form the duplex. It should be pointed out that an overhung at the 3'-end of the target DNA sequence is required in order to resist the cleavage of target DNA by the enzyme. Since Exonuclease III can catalyze the stepwise removal of mononucleotides from 3'-hydroxyl termini of duplex DNA, the immobilized DNA strand from the duplex will be gradually hydrolyzed from the 3'-end by the enzyme, while the target strand is protected, releasing the target DNA strand back to the solution. The released target DNA will then bind to another immobilized DNA molecule on the surface, resulting in the second hydrolysis of immobilized DNA by Exonuclease III. This cyclic hybridization and hydrolysis process will lead to an amplification effect so that a very small amount of target DNA can be detected by SPR imaging.

Figure 26 (a) shows the SPR difference image for 500 nM target DNA hybridized to the perfectly matched probe DNA immobilized on the surface. A positive SPR signal is observed corresponding to this hybridization adsorption in the line profile shown in the upper left portion of the figure. After the surface was denatured, a solution of 100 pM target DNA and 30 units of Exonuclease was injected to the surface. Figure 26 (b) shows

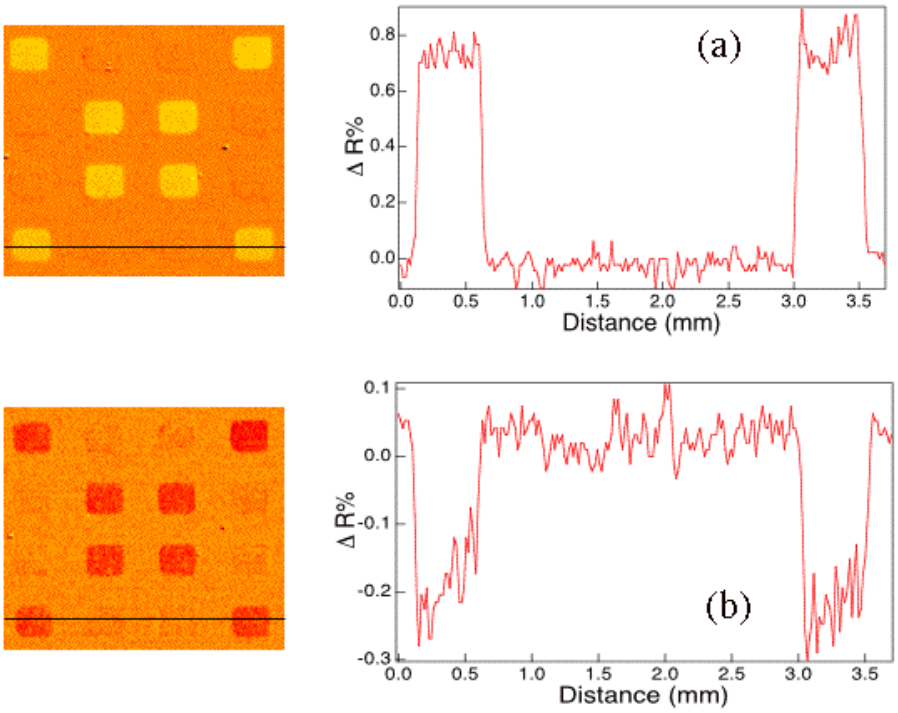

Figure 26. SPR difference images of (a) DNA-DNA hybridization and (b) Exonuclease III process on surfaces..

the SPR imaging result of the Exonuclease process. A negative signal was observed corresponding to the removal of immobilized DNA from the surface. It was demonstrated that Exonuclease III specifically and repeatedly hydrolyzed the immobilized DNA strand from duplex DNA, resulting in the loss of SPR response. By this approach, we can detect 10 pM solution of target DNA (18 bases long oligonucleotides) within 10 minutes. This is 10^3 improvement compared to the previous SPR imaging detection limit of 10 nM, solely based on hybridization adsorption. By optimizing the experimental condition and the reaction time of Exonuclease III, it will be possible to detect below 1 pM target DNA. We plan to use this amplification approach to directly detect genomic DNA and virus RNA without any PCR amplification.

4.10.2. Ribonuclease H

To achieve the direct detection of genomic DNA with SPR imaging, a novel scheme that utilizes RNase H to enzymatically amplify the response of RNA microarrays to the binding of complementary DNA is employed. This novel surface enzymatic amplification process that utilizes RNase H and RNA microarrays can enhance the sensitivity of SPR imaging measurements for the detection of 1 fM complementary DNA. This enzyme was shown to selectively hydrolyze the RNA in an RNA-DNA duplex, but not digest ssDNA, dsDNA, ssRNA or dsRNA. An overview of this amplification process is shown in Figure 27. A single-stranded RNA microarray is exposed to a solution that contains a complementary ssDNA sequence and the enzyme RNase H. The DNA will bind to its RNA complement on the surface, forming an RNA-DNA heteroduplex (step 1). The enzyme RNase H will then specifically hydrolyze only the RNA strand in this heteroduplex, releasing the DNA molecule back into solution. This DNA molecule can then bind to another RNA molecule on the surface, initiating the hydrolysis of a second RNA probe. This cyclic process results in an amplification effect whereby a small number of DNA molecules can cause the destruction of many RNA molecules from the surface. This irreversible loss of RNA probes from the surface causes a significant negative change in percent reflectivity. The decrease in percent reflectivity will become larger with time until all of the available RNA probes on the surface are hydrolyzed.

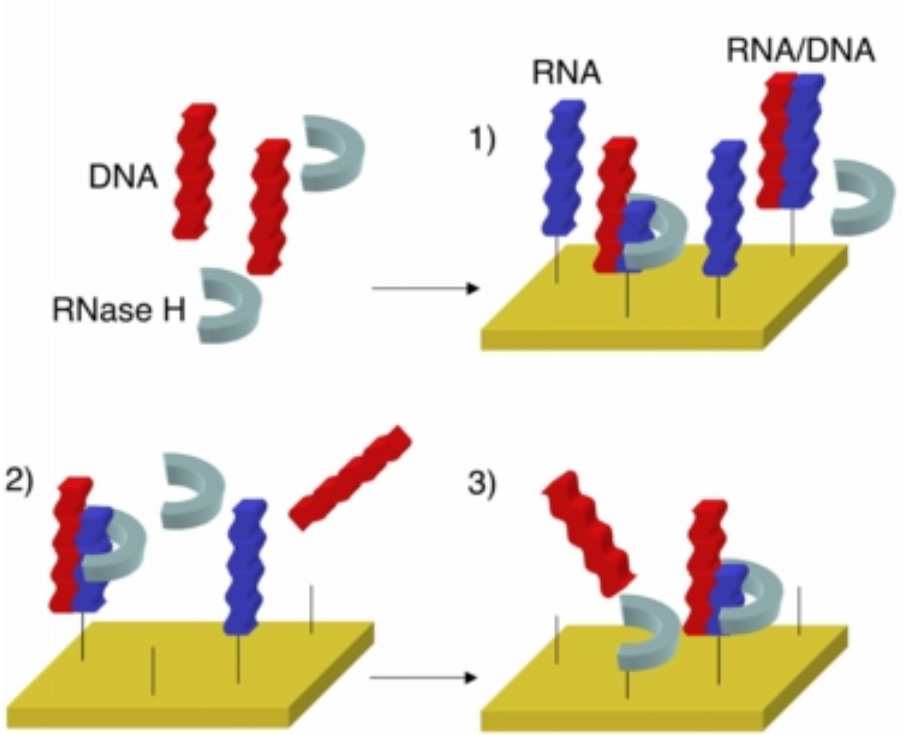

Figure 27. Schematic presentation of a surface enzymatic reaction for the amplification of SPR signal by selective RNA probe removal

To demonstrate the sensitivity that this enzymatic process for detecting low concentrations of DNA, a 1 fM solution of DNA oligonucleotides, complementary to RNA sequence R2, was detected by SPR imaging of an RNA microarray (see Figure 28a). The detection of a 1 fM solution of target DNA with this enzymatically amplified SPR imaging technique is a great improvement on the previous SPR imaging detection limit of 1nM for oligonucleotides based solely on hybridization adsorption.

In addition to single-stranded oligonucleotides, this enzymatically amplified SPR imaging method can be used to detect longer strands of dsDNA such as those created by the PCR amplification of a genomic DNA sample. A 544bp segment of the TSPY gene that contained sequences complementary to RNA probes R1 and R2 was obtained from human genomic DNA (Promega) by PCR amplification. Figure 28b shows the SPR reflectance difference obtained for this experiment. A decrease in percent reflectivity can be seen for the two RNA probes R1 and R2 which were designed to specifically bind to

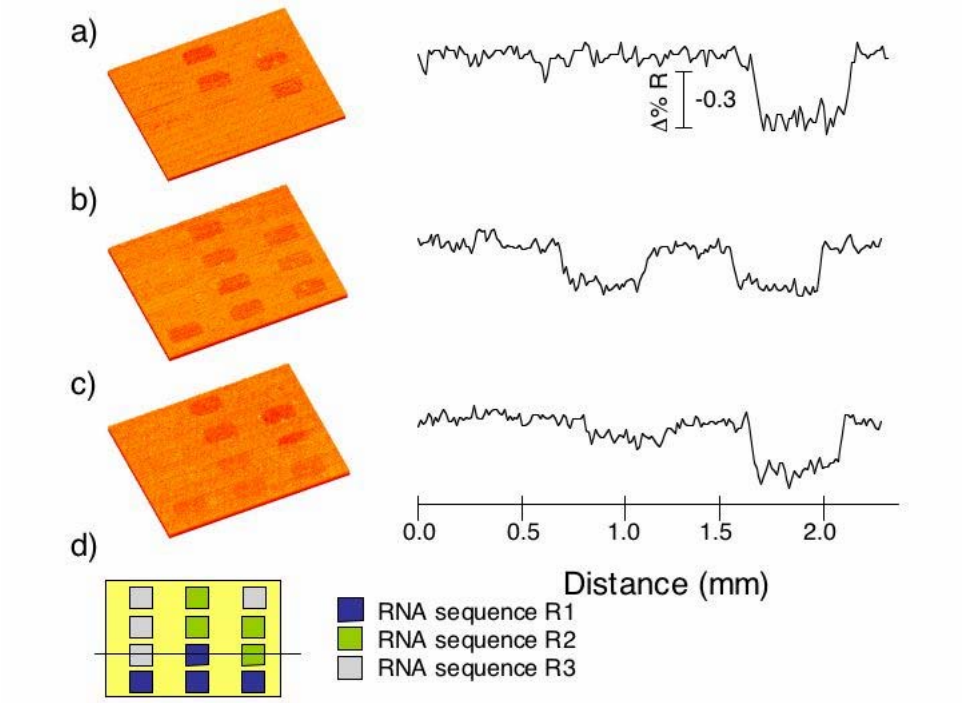

Figure 28. SPR difference images obtained for the detection of 20mer oligonucleotide.

(a) 544bp PCR product of the TSPY gene (b), and male genomic DNA (c). The inset (d) shows the design of the three-component array created using thiol-modified RNA sequences; R1 and R2 were designed to selectively bind the TSPY gene on the Y chromosome, and R3 is a negative control.

this PCR product, while the R3 negative control array element showed no change. This experiment illustrates that this enzymatic process can be successfully used to detect longer dsDNA PCR products.

The direct detection of genomic DNA *without* PCR amplification was observed by enzymatically amplified SPR imaging measurements. A three-component RNA microarray was constructed with the same RNA sequences: R1 and R2, designed to bind to the TSPY gene, and a third negative control RNA sequence R3. Commercially obtained male and female genomic DNA samples (Promega) were diluted in buffer, heated to 95 °C for 5 min, and then mixed with RNase H. The SPR difference image (see Figure 28c) shows that there is a decrease in percent reflectivity for the two probes specific for the TSPY gene while negligible nonspecific adsorption is observed to the

negative control probe or background. No change in the percent reflectivity was seen for any of the array elements when exposed to female genomic DNA under the same conditions.

This use of this surface enzymatic process to improve the detection limit of SPR imaging was further studied by measuring the hydrolysis of RNA microarrays in real time. Figure 29 shows the kinetics curves obtained for the enzymatic hydrolysis of surface bound RNA probes by RNase H in the presence of 10 nM, 1 nM, 100 pM and 10 pM complementary DNA solutions. The DNA concentrations used are all at or below the current detection limit of SPR imaging based solely on hybridization adsorption, yet the signal is easily observable by this amplification method. In Figure 29, the curve corresponding to a DNA concentration of 10 nM begins to level off after only 500 seconds, corresponding to the removal of almost all of the RNA probes from the array surface. A final change in percent reflectivity of −1.5% was observed after a 1 hour

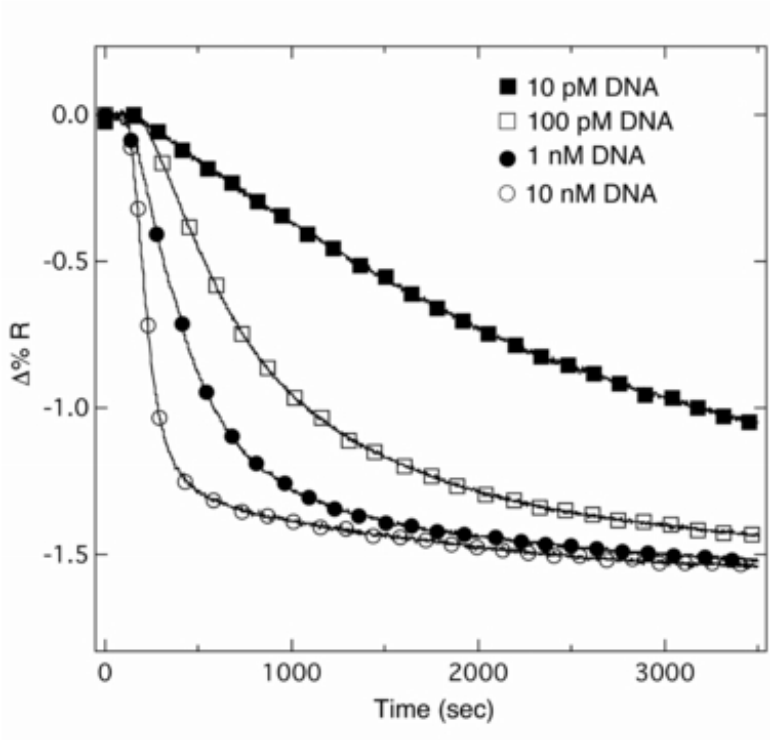

Figure 29. Kinetics curves measured for the hydrolysis of surface bound RNA probes by RNase H and complementary DNA molecules.

reaction time. This signal is considerably higher than detecting DNA based solely on hybridization adsorption, where the typical change in percent reflectivity for 10 nM DNA hybridization is about 0.1%. When the array was exposed to a 1 nM solution of complementary DNA and RNase H the time to reach the same change in percent reflectivity took approximately 1000 seconds longer at 1 nM than at a concentration of 10 nM. This was due to the extra hybridization/hydrolysis cycles needed to hydrolyze the same number of RNA probes on the surface. After a 1 hour time period the same change in percent reflectivity of –1.5% was obtained. A change in percent reflectivity of –1.4% was obtained for a 100 pM solution of complementary DNA after 1 hour, nearly the same as for the two higher concentrations. At a final concentration of 10 pM, the rate of reaction has slowed down considerably, and after the one hour time period a change in percent reflectivity of only –1.1% was observed, approximately 2/3 of the total signal obtained for the other concentrations. The slope of the kinetics curve suggest that the surface hydrolysis of RNA probe molecules would continue until a final change in percent reflectivity of –1.5% was reached.

From the kinetics curves taken for the hydrolysis of RNA arrays at different DNA concentrations, reaction rates were determined. The initial slopes of the kinetics curves were linearly fit to determine the rate of reaction at each concentration of complementary DNA. These rates of reaction were plotted as a function of the log of the DNA concentration and the resulting data was then fit to the Langmuir isotherm. A K_{ads} of 6.6 x 10^7 M^{-1} was obtained, which is in good agreement with other reported values.

Overall, this technique has lowered the detection limits of SPR imaging for ssDNA molecules from 1 nM down to 1 fM, corresponding to 10^6 enhancement in sensitivity. New methods involving a serial amplification step are being developed to improve upon this technique in both rate of reaction and ultimate detection level. It may also be useful to study 3' modifications to the RNA probes on the surface since some have been shown to increase the efficiency in RNase H recruitment and cleavage. This technique may find a wide variety of uses due to the fact that it is applicable to many other detection methods

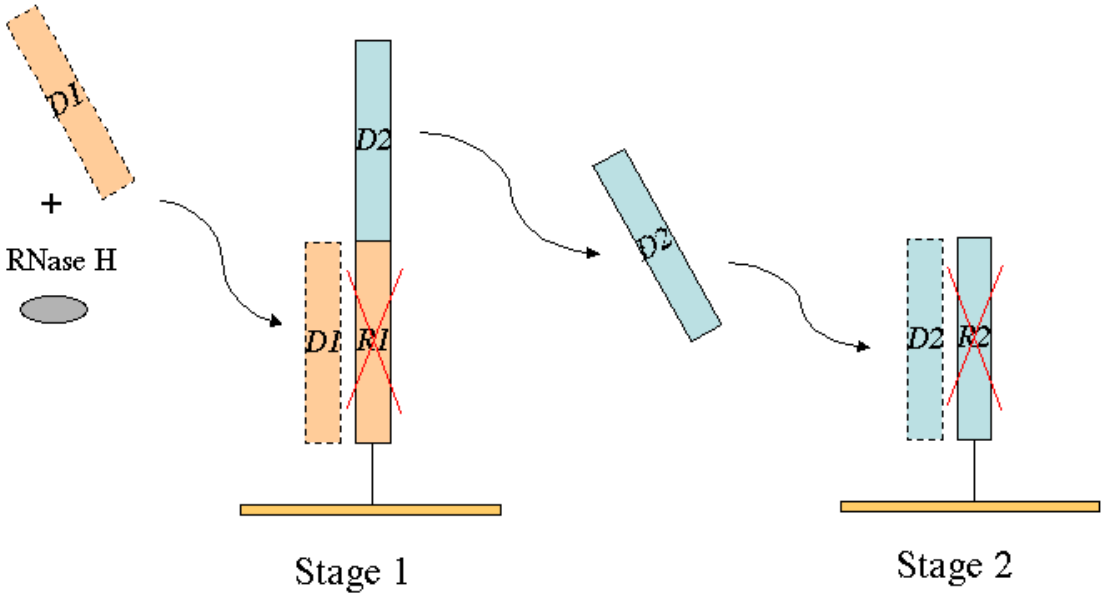

Figure 30. Serial Ribonuclease H signal amplification using chimeric RNA/DNA probes.

such as fluorescence quenching and nanoparticle labeling. This technique may be applied to DNA computing as a way to read out the results in replacement of PCR amplification or rolling circle amplification. We would also like to use this technique to study viral RNA, using a combination of reverse transcriptase and RNase H (RT-RNase H). This method would have the advantage over RT-PCR, in that not specialized equipment would be needed.

4.10.3. Toward future work: Direct Detection of Genomic DNA

The objective of our future work is to establish a general signal amplification scheme for the direct detection of genomic DNA and any other DNA targets based on serial RNase H signal amplification reaction. This represents a further improvement of our previously reported RNase H signal amplification method, which will result in lower detection limit down to a concentration of 1 fM (see section 4.5.2) and reduced measurement time in the analysis of any DNA samples. An overview of our serial RNase H signal amplification process is shown in Figure 30. The key point is to immobilize chimeric RNA/DNA probes at the first reaction step. Of the chimeric RNA/DNA probes immobilized on surfaces, the RNA part (R1) is designed to detect target DNAs (D1 here) based on DNA

hybridization. When a mixture of target DNA (D1) and RNase H is introduced, D1 will bind to the R1 part of the chimeric R1/D1 probe, forming a DNA/RNA heteroduplex. RNase H will then specifically hydrolyze R1 from R1-D1 duplex, while at the same time a DNA fragment, D2 will be released to the solution due to the cleavage of R1. Therefore, the hydrolysis of each R1 by RNase H will be accompanied by the release of one D2 fragment. At stage two, a new RNA probe (R2) is immobilized on different spots in the same system, where R2 is perfectly matched to the D2 fragment. It is clear that the released D2 at the first step will be the target of the second RNase H cleavage reaction. Each D2 can bind to R2, where R2 is then destroyed from R2-D2 heteroduplexes by the same enzyme RNase H. It is expected that these serial RNase H amplification scheme will give lower detection limit (< 0.1 fM) and shorter measurement time when detecting genomic DNA samples.

4.11. Kinetics Measurements of Peptide Microarrays

4.11.1. S Protein-S Peptide System

As a first application of real-time SPR imaging measurements, the adsorption and desorption of S protein to S peptide in array format was studied. The S peptide-S protein interaction was chosen as a model system because this interaction is completely reversible with very little S protein denaturation on the surface making these arrays amenable to the study of multiple association and dissociation cycles on one chip. The adaptation of SPR imaging for real-time measurements required the development of a new flow cell for rapid sample exchange as well as macros for data collection. To support this endeavor, a PDMS microfluidic handling system was designed to facilitate well-controlled and reproducible analyte delivery to each element on the array surface. Figure 31 shows a raw SPR image used as a mask for kinetics measurements. Regions of interest (ROI) including the background regions reacted with polyethylene glycol or immobilized peptides (labeled A, B, and C) were selected and the change in percent reflectivity at each ROI was collected as a function of time using a CCD camera.

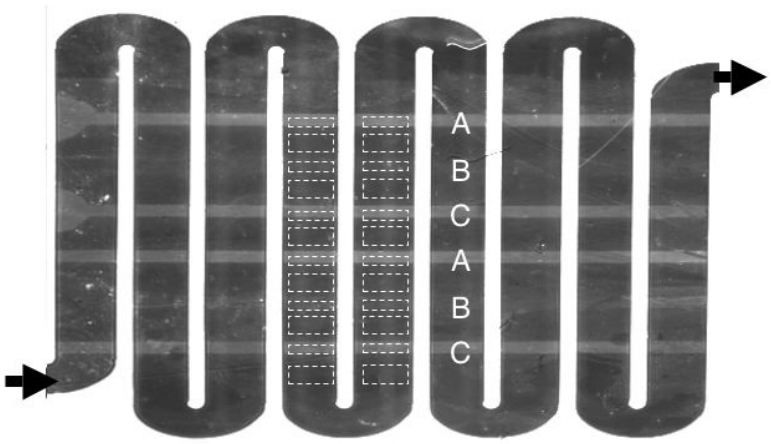

Figure 31. An SPR image of a peptide array composed of peptides A, B, and C is used as a mask for kinetics experiments.
The dotted lines indicate regions of interest (ROI) on the array, where the change in percent reflectivity is measured as a function of time using a CCD camera.

A representative curve binding is shown in Figure 32. This data was acquired by measuring the change in percent reflectivity as a 75 nM solution of S protein was introduced to the cell at a constant flow rate of 1 mL/min using a peristaltic pump. The plot was obtained by measuring the difference in percent reflectivity between the peptide array elements and the average of the PEG backgrounds on either side of each peptide

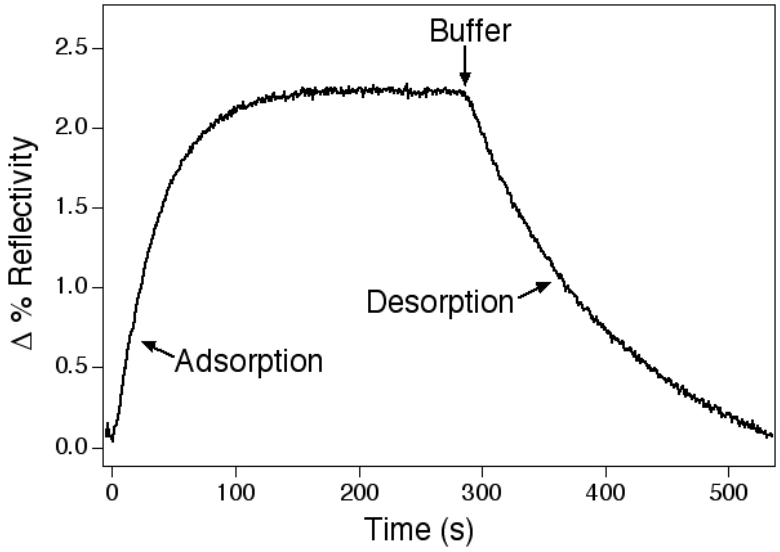

Figure 32. Plot showing the change in signal measured as a 75 nM solution of S protein was flown over an S peptide modified surface as a function of time.
Desorption kinetics were observed when the S protein solution was replaced with a constant flow of buffer. This curve was obtained by averaging the change in percent reflectivity measured at five S peptide array elements relative to the PEG background.

element while a solution of S protein was introduced. After the signal appears to level off, dissociation was measured by exposing the array to a constant flow of buffer and the bare peptide surface was regenerated. Additional experiments were performed to measure the association and dissociation constants (k_a and k_d) and calculating the adsorption constant (K_{ads}) for the interaction of S protein to immobilized S peptide and various S peptide analogs. In addition to S protein adsorption/desorption to S peptide, we have utilize this kinetic methodology to study RNase activity which is a particularly interesting feature of the S protein-S peptide complex system, while neither S protein, nor S peptide alone are enzymatically active.

4.11.2. Kinetics Study of Ribonuclease Activity

In this work, we describe a novel approach for the real-time investigation of the activity of Ribonuclease S formed by complexing of S protein to S peptide and its variants which are co-immobilized with RNA substrates on an array format. This method allows for the rapid determination of multiplexed kinetics of the ribonuclease activity in a homogeneous way.

Ribonuclease A (RNase A) represents one of the best studied of all enzymes, which efficiently catalyzes the cleavage of single-stranded RNA. A single peptide bond in native RNase A can be cleaved by the protease subtilisin. The product of this cleavage is called ribonuclease S (RNase S, where "S" refers to subtilisin), which consists of two tightly associated fragments. These fragments are S peptide, which derives from residues 1-20 of RNase A, and S protein, which derives from residues 21-124. It has been found that neither S peptide nor S protein alone has any enzymatic activity, whereas the two components together form active ribonuclease, with activity similar to the intact RNase A. The S peptide segment has been subject to continued synthetic studies by changing individual amino acids in its sequence to identify residues that play key roles in the interaction with S protein and in the activity of the complex. Most of the previous work however, is accomplished in a heterogeneous solution format, where only one peptide variant can be examined each time. In this work, we wish to report a novel scheme for the

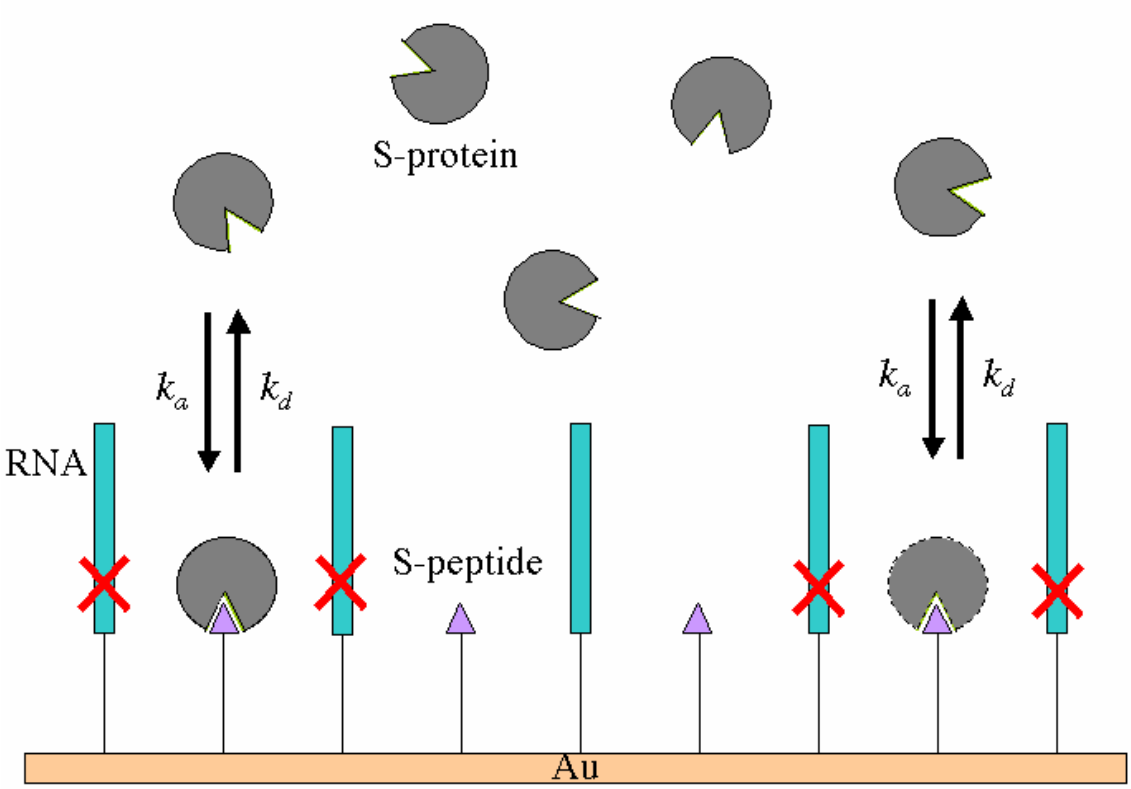

Figure 33. Cleavage of RNA substrates through multiple association/dissociation of S-protein/S-peptide complexes.

rapid and multiplexed study of the binding of S protein to S peptide and its variants on an array format using SPR imaging measurement. The activity of each RNase S complex is kinetically obtained by using a co-immobilized peptide and RNA microarray.

An overview of this process is shown in Figure 33. The key point is to immobilize a mixture of S peptides and RNA substrates (50%:50% at 1 mM each) on individual spot. When S protein solution is introduced to the surface, it will bind to the immobilized S peptide or its variants until an equilibrium is reached. We have determined the equilibrium binding constant (K_{Ads}) of 1.7×10^{7} M^{-1} based on both equilibrium measurements and kinetics measurements. Kinetics measurements of the S protein/S peptide interaction give a dissociation rate constant (k_d) of 1.1×10^{-2} s^{-1}, an association rate constant (k_a) of 1.9×10^{5} $M^{-1}s^{-1}$. Since we know neither S protein nor S peptide alone has enzymatic activity, each alone has no effect on immobilized RNA substrates. However, when a S protein molecule binds to a surface immobilized S peptide molecule,

they will form an active enzyme, which will cut all the RNA substrates around it upon association of the RNase S complex with RNA, as shown in Figure 33. Since there is an equilibrium maintained in the system, at each unit of time, the number of S protein molecules dissociated from the complex would be equal to that of S protein molecules associated to the surface, depending on the value of k_d. For example, for the native S protein/S peptide system, it means that about 1 percent of the complexes will decay per second. It is interesting to note that the newly associated S proteins have a chance to bind to S peptides at laterally different positions on the same spot, where fresh RNA probes around them are available for cleavage by the newly formed RNase S. It is clear that this multiple association/dissociation process causes a signal amplification whereby all of the available RNA substrates will be removed with time from the surface. The loss of RNA substrates from the surface results in a negative change in percent reflectivity, which will be detected in the SPR imaging measurement. By taking advantage of microarray techniques, which is capable of multiplexed determination of the RNase activity in a homogeneous way, we have utilized co-immobilized RNA and peptide arrays for the rapid profiling of different RNase S formed by associating of S proteins to S peptides and variants using real-time SPR imaging measurements (Figure 34). A four-component array was constructed consisting of cysteine-terminated S peptides and variants which were immobilized with RNA substrates (50%:50%) on each individual spot. Among them, N-cys S peptide and C-cys S peptide have the same sequence but with cysteine residues at different ends, so that each peptide will be annealed to the gold surface with opposite orientations. LB2 is a S peptide variant derived from phage display (LB2). FLAG is used here as a negative control. Inset of Figure 34 shows the kinetics result when the multiplexed peptide array was exposed to a 10 nM of S protein solution. Peptides with different sequences exhibited different kinetic behaviors, with both N-cys and C-cys S peptides showing fastest but similar activities when interacting with S proteins, indicating the orientation difference of immobilized S peptides has no significant effect on their binding and enzyme activities. A lower activity was observed in LB2 peptides. FLAG peptides have no binding with S-proteins, therefore no activity was observed. The kinetics data show that, as time elapsed, all of the available RNA substrates immobilized on each spot with N-cys, C-cys S peptides and LB2 were destroyed by regenerated

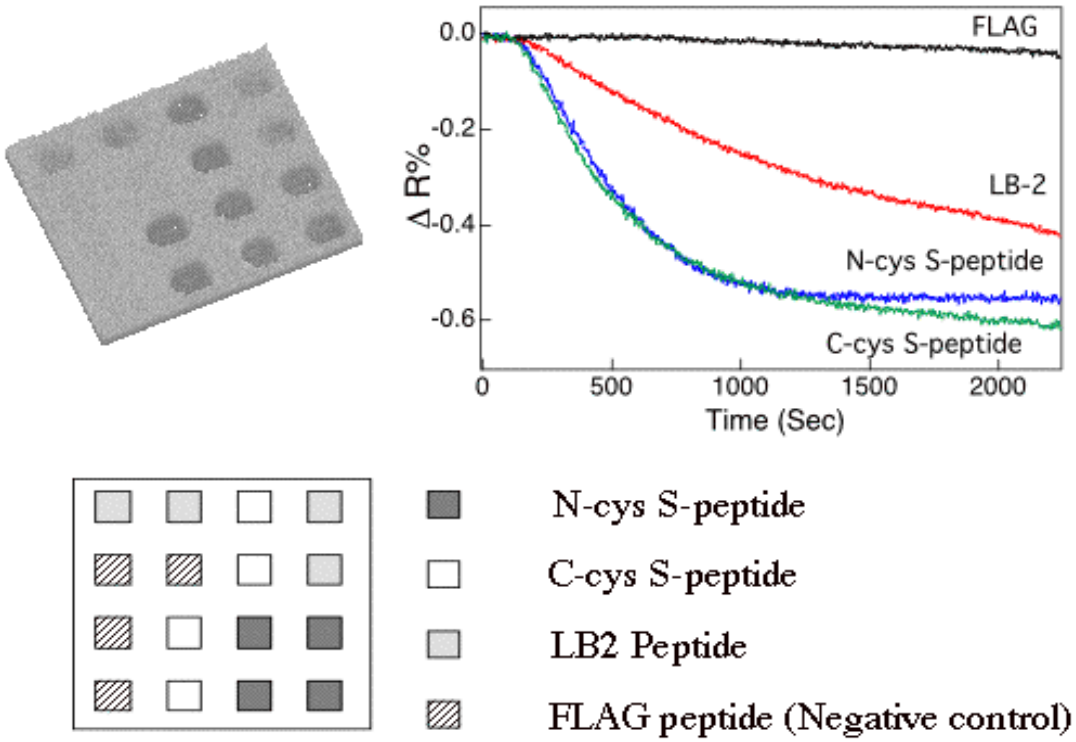

Figure 34. SPR imaging data showing the kinetic measurements of the activities of RNase S.
It was formed by complexing S protein (10 nM) to S peptides and their variants using co-immobilized RNA and peptide arrays.

RNase S through multiple association/dissociation processes (Figure 34). The above result clearly shows that our newly designed co-immobilized RNA and peptide microarrays provide a simple, rapid and efficient way for the real-time multiplexed investigation of enzyme complexes resulting from binding of S proteins to different S peptide its variants in a homogeneous format. It is expected that in the above experiment, the time to completion is dependent on the association rate constant (k_a), the dissociation rate constant (k_d), and the concentration of S proteins since at lower concentrations, more cycles of association/dissociation step is needed to remove all of the available RNA probes on each spot from the surface.

In the future work, efforts will be taken to examine several S peptide variants with individual amino acid residue varied which play key roles in the binding of S protein to S peptide and its enzymatic activity using multi-component peptide arrays, each of which is

immobilized with RNA probes on individual spot. We will also observe the effect of changing the molar ratio of RNA to peptides during immobilization on the surface cleavage of surface confined RNase S. Since RNase S would not digest RNA duplexes, complementary DNA or RNA sequences will be introduced to anneal RNA probes to see if they are protected from cleavage by regenerated RNase S on surfaces.

4.11.3. Surface Enzymatic Activity

In addition to RNase S activity measurements, real-time SPR imaging of peptide arrays was applied to study the surface enzymatic activities of the protease factor Xa. These measurements were used to determine how a single amino acid change in a peptide substrate diminished the rate of peptide cleavage. In vivo, factor Xa plays a crucial role in the regulation of the coagulation cascade. A three component peptide array was fabricated that contained array elements of a peptide substrate, a mutant substrate, and a control peptide. A decrease in percent reflectivity is observed as the immobilized peptides are removed from the surface by factor. Enzymatic cleavage of the substrate peptide was shown to follow first order kinetics and proceed at a rate ten times faster than that of the mutant peptide. These results demonstrated the utility of SPR imaging to quantitatively study enzymatic recognition sites using peptide arrays. Future measurements are being applied to study the reaction rates of peptide and DNA modifying enzymes using surface immobilized arrays.

The continued application of peptide arrays will be useful to the characterization of other proteins, such as calmodulin (CaM). CaM is a Ca^{2+} dependent protein that regulates a variety of structurally and functionally different enzymes, including the myosin light chain kinase (MLCK). CaM binds with high affinity to MLCK resulting in a conformational change that induces phosphorylation activity. Specifically, we are interested in studying the differential binding of CaM to peptides based on the MLCK binding site. Arrays based on this interaction will be applied as a calcium sensor, since CaM-MLCK binding is extremely sensitive to calcium concentration.

4.12. Other Surface Enzymatic Processes

In our approach toward the creation of design nanoparticle assemblies on surfaces, oligonucleotides play a central role. Oligonucleotides serve as the template and glue for specific attachment of nanoparticles to surfaces and to each other. Hybridization between oligonucleotides is the primary means for directed coupling. A unique sequence of bases functions as an address for attachment while the length of the sequence provides some crude measure of the attachment strength. Over the granting periods, we have made significant progress in achieving control over the strength and specificity of attachment through template directed enzymatic ligation. Ligation between oligonucleotides forms a permanent covalent linkage. In contrast, hybridization can be disrupted either by elevation of temperature or by addition of certain chemical agents (e.g. urea). We have also created a means for control of ligation specificity. We discovered that, in certain circumstances, it is advantageous to have universal ligation. A degenerate template as short as 4 bases is sufficient for ligation. Ligation occurs between all available sequences (those not specifically blocked at their terminus). Biotin, for instance, is an excellent blocking group. At the other end of the specificity scale, we can use long templates, elevated temperature and high fidelity ligases. In our work so far we have successfully ligated (A) large DNA molecules, (B) fluorescent antibodies/antigens, and (C) fluorescent nanoparticles to surfaces using our new enzymatic strategies (see Figure 35 A-C).

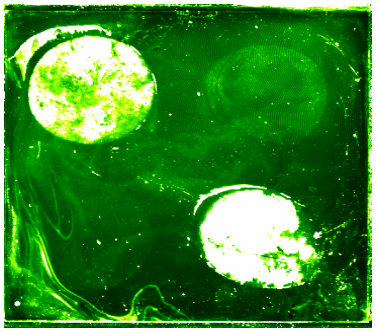

Figure 35. (A) Lambda DNA (48,502 bp) ligated to surface (bright spots) and control (dim spots).
DNA was visualized with fluorescent intercalating dye.

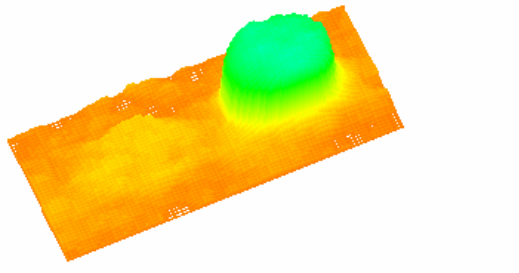

Figure 35. (B) A fluorescein modified oligonucleotide was attached to the surface with template specific ligation and then reacted with fluorescent antibody (anti-fluorescein rabbit IgG).
The control (dim spot) contained an oligo not recognized by the template.

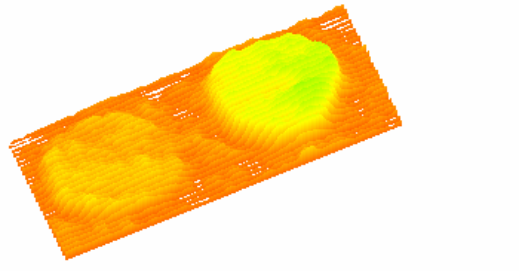

Figure 35. (C) Biotinylated oligos were bound to the surface with template directed ligation and reacted with streptavidin coated 40 nm fluorescent nanoparticles.
The control (dim spot) contained an oligo not recognized by the template.

One of the key parameters in performing successful enzymatic process at the surface is robust attachment chemistry. Because gold substrate was otherwise such an appealing substrate, we designed improvements to the former surface attachment chemistry. Performance was evaluated by measuring fluorescence from surface bound complement after repeated hybridization cycles. The foundation of the former system was a self-assembled monolayer (SAM) formed by a commercially available amine-terminated C_{11} alkanethiol. It is well-known that SAM stability increases with increasing chain length. Therefore, we devised and executed a simple synthetic scheme for an amine-terminated C_{18} alkanethiol. This new SAM material provided much added stability.

4.13. DNA Computing

Our DNA word design algorithm can generate DNA word sets that satisfy both thermodynamic and combinatorial constraints. Our first contribution was to find improved algorithms for DNA word design with combinatorial constraints. We developed a stochastic local search technique, which allows sophisticated search of the space of possible word sets in order to find a high quality design. For given combinatorial constraints, we showed that this method yields larger sets than previous methods.[45] The work at UBC has focused on the computer design of DNA strands which will be used to link dendrimer particles together. Earlier design approaches were based on the use of combinatorial constraints to ensure that strands interact only as intended. In order to incorporate thermodynamic constraints into the algorithm, we developed a new tool, Pairfold, which takes as input two distinct DNA or RNA strands and predicts the secondary structure formed by these strands. The underlying algorithm is based on the dynamic programming method of Zuker and Steigler (which, however, takes only a single strand as input), and thus it considers only pseudoknot free secondary structures. The tool will be useful in testing whether there is unwanted interaction between distinct DNA words in a word design, and may also be useful in other applications, such as in design of DNA or RNA probes that bind with high specificity to a DNA or RNA target. We are currently completing our analysis of the thermodynamically based DNA word design software.

Our second contribution is a new algorithm for designing DNA or RNA strands that fold to a given secondary structure. Such algorithms are useful for design of strands for self-assembly of nano-structures. Our RNA designer algorithm, also based on stochastic search, substantially outperforms the previous best known algorithm for this problem, namely the RNA inverse routine from the Vienna RNA package.[46] A web-based user interface has been added, enabling users to run the software. The web page, www.rnasoft.ca, contains both PairFold and RNA Designer, as well as a third tool CombFold, which takes as input a combinatorial set of RNA molecules and finds the molecule in the set with the minimum free energy secondary structure.

In the area of word design, our first goals were (a) to improve generation of DNA word sets by ensuring that hybridizations of word complements at junctions of pairs of words is not predicted to occur. Towards this end, we first measured the likelihood of unwanted hybridizations in our currently designed sets. Then, we developed a new algorithm for arranging words so that unwanted hybridizations are reduced. In the area of DNA and RNA secondary structure prediction, we have developed a new, linear time algorithm for calculating the free energy of a pseudoknotted structure.

Specific hybridization of DNA complements was the backbone of our attachment strategies. Even those that outwardly appeared to depend on enzymatic reactions (e.g. ligation) still relied heavily on hybridization. One critical issue was finding sets of oligonucleotides that were essentially non-interacting for their perfect match. Over the years we have made tremendous progress in designing such highly-discriminating sequences. One of the key improvements to our algorithm was incorporation of a slide match finder. Slide matches occurred when oligos shifted with respect to one another. For example, the two 12 base sequences (A) displayed only three pairing bases (marked in red and underlined) when compared in the traditional manner. However, by shifting the lower sequence one base to the right (B), a situation is revealed where eleven bases are paired. Such unwanted secondary reactions were eliminated to maintain high template specificity in the attachment reactions.

A.) AGCCATTGAGCT
CGGTAACTCGTA

B.) GCCATTGAGCT
CGGTAACTCGTA

In a complex mixture of oligonucleotides, binding between constituents can occur whenever and wherever conditions and energies of formation are favorable. Unintended or non-specific hybridization often occurs because sub-sequences of two oligos are complementary. Elevation of the temperature can eliminate this mis-hybridization so long

as the temperature is low enough for all of the proper hybridizations to occur. To use hybridization between oligonucleotides to create intricate nanoparticle assemblies, then the pairing oligonucleotides should be chosen so that hybridization will occur only between exact matches under the specified set of conditions. Ideally, all of the oligos involved in one step of the assembly process would anneal at nearly the same temperature and non-specific hybridizations would be eliminated through proper design. Choosing a set of oligos for such an operation requires careful attention to all the possible interactions an oligo might have that would hinder correct hybridization. These interactions include mis-hybridization to other set members or their complements as well as the possibility that the oligo might form a hairpin. We developed software which designs sets of specifically interacting oligonucleotides by beginning with a large set of oligos that have similar melting temperatures and slowly whittling the list down as each individual oligo is scanned for mis-hybridizations with other set members. Using 12mers as an example, each member of a generated set will NOT hybridize to any other member or any other members' complement at more than 8 out of the possible 12 positions.

Furthermore, all members of the set will anneal to their perfect complement within a very narrow temperature window. In contrast to our previous work where the G/C content of oligos was fixed to produce a set of similarly melting oligos, we now calculate the melting temperature of each oligo individually using the thermodynamic nearest neighbor melting parameters of Santalucia. The Tm distribution for 12mer oligos with 50% C (at most 2 consecutive Cs and no Gs) is 8.0ºC centered at 42.1ºC and has 1216 elements. Withdrawing the criterion for 50% C and keeping only 2 consecutive Cs and using the same number of elements (1216) reduces the Tm distribution to 0.4ºC (a factor of 20), centered at 39.7ºC. Using the maximum mismatch criterion (8 out of 12 possible matches with a maximum of seven consecutive matches) gives final sets of 27+/-2 elements for the 50% C case and increases to 61+/-4 elements for the unconstrained set. This analysis can be pursued in an alternate fashion. If, instead of using the same number of elements from the unconstrained set we use the same temperature window then we find that there are 10,850 elements from which to pick a set. Using the maximum mismatch criterion (8

out of 12 possible matches with a maximum of seven consecutive matches) gives final set of 91+/-9 elements for this last case.

The utility of this work was extended into the area of DNA computing to create large combinatorial sets of oligonucleotides. There, large combinatorial sets of oligonucleotides are required. For instance, by concatenating one member from each of 6 groups of 16 different oligonucleotides, one can create a combinatorial set of 16.8 million different long oligos. The same hybridization performance described above is required but in addition, no hairpin formation, which could prevent proper hybridization, can be tolerated. To accomplish this, our software scans every junction between concatenated members for possible sources of mis-hybridization. Any offending partners are eliminated from the primary set. All pairings are scanned before the final set is generated. As a last stage, we use software developed in Anne Condon's group to analyze every member of the concatenated combinatorial library for secondary structure. If any of the 16.8 million members has secondary structure, then the entire set is discarded. We previously described a new software package that we created whose purpose is to generate sequences for minimally interacting single-stranded DNA oligomers. These oligomers form the basis for one method of constructing nanoparticle assemblies. By "minimally interacting" we mean there is a large gap in free energy between binding of perfect complements and the most stable partial match. In the design of combinatorial libraries of concatenated words, special attention was given to junctions between concatenated words. Since there is no feature which could distinguish a junction from any other region in the long DNA sequence, it becomes an alternate site for complement binding. By design, any hybridization across a junction would contain a minimum number of matched bases (e.g. 9 out of 12). A subtle feature of that criterion is the number of consecutive matches that are permitted. In addition to hybridization between mismatched sequences, a long concatenated DNA sequence can fold back upon itself and anneal across junction points. This secondary structure has potential to interfere with perfectly matched complements. To investigate this we are currently investigating ways to alter the junctions between words. There are many commercial phosphoramidites which could serve in the specified manner. However, for our intended purpose, sequences

containing these junction breaks will be expected to function normally as templates for polymerase. One candidate is the commercial abasic phosphoramidite called dSpacer. This special molecule is not susceptible to beta-scission as are natural abasic sites and are therefore much more stable. Furthermore, it has been shown that oligos with such abasic sites will work as templates for polymerase provided that the polymerase does not have exonuclease activity.

There is an added benefit to using artificial junction breaks. Our current design criteria don't allow sequences with more than two consecutive Cs. To accomplish this, we have eliminated all component words that either begin or end with two consecutive Cs because if one of these words were selected for use, we wouldn't be able to concatenate it to any other word that begins in C. Using a break or spacer will allow us to reintroduce all those sequences back into the selection pool. This small change will increase the selection pool by nearly 20%. In addition to facilitating the design of sequences with fewer allowed consecutive matches, we should also be able to reduce the range of temperatures from which the set words are chosen. Having component words with similar melting temperatures has many experimental advantages over widely spread sets.

5. CONCLUSIONS

This project has achieved many major accomplishments towards developing DNA based nanostructures and biosensors. We have successfully established protocols for the synthesis and characterization of dendrimer-DNA conjugates using dendrimers based on melamine. Dendrimer chemistries for the preparation of the next generation of bioconjugates have been successful. A significant enhancement of SPR signal when using DNA microarray can be achieved by the use of DNA-amine-terminated dendrimer, DNA-carboxylic-terminated dendrimer adducts and DNA-dendron conjugates. This work can in principle be used as a basis for signal amplification with programmable nanoscale DNA biosensors.

We have also successfully performed the first experiments preparing and characterizing covalently-linked adducts of SWNTs with DNA and with biotin. Our results show that the biologically-modified adducts have many desirable properties and are attractive candidates for biologically-directed assembly of nanostructured materials. In addition, we have found that good algorithm design, particularly stochastic search methods, have lead to an improved method for design of DNA words and also DNA and RNA strands that fold to given secondary structures. Preliminary results indicate that even better results can be obtained by incorporating thermodynamic constraints directly into the design process. The development of enzymatically amplified SPR imaging using RNA and DNA microarrays can be powerfully used in the application of direct detection of genomic DNA and viral RNA.

We have demonstrated a novel surface enzymatic amplification process that utilizes RNase H and RNA microarrays to sufficiently enhance the sensitivity of SPR imaging for the detection of DNA oligonucleotides down to a concentration of 1 fM, corresponding to a remarkable 10^6 enhancement in sensitivity. The utility of this method was further demonstrated by the direct detection of the TSPY gene in human genomic DNA samples. In addition to SPR imaging, this novel method of enzymatic signal amplification can in principle be used with other techniques (e.g., fluorescence quenching, nanoparticle

labeling) and with other surfaces. The ability to detect genomic DNA with the label free technique of SPR imaging should greatly accelerate its application in the areas of genetic testing, bacterial and viral recognition, and gene expression analysis. In addition, this methodology represents just the first of many possible surface enzymatic-processing reactions that can enhance the sensitivity, selectivity and applicability of SPR imaging to nucleic acid identification, manipulation and detection. This technique may be applied to DNA computing as a way to read out the results in replacement of PCR amplification or rolling circle amplification. We would also like to use this technique to study viral RNA, using a combination of reverse transcriptase and RNase H (RT-RNase H). This method would have the advantage over RT-PCR, in that not specialized equipment would be needed.

We successfully demonstrated template directed enzymatic ligation of large DNA molecules, fluorescent antibodies/antigens and fluorescent nanoparticles to surfaces. The ligation of material was performed in an addressed format using the highly unique word sequences designed using our newly generated word design software. The software is a significant improvement over other DNA word design software packages because it considers melting temperature and the arrangement of mismatches.

6. RECOMMENDATIONS

We would like to strongly recommend the continued development of DNA based nanomaterials and enzymatically engineered DNA biosensors, as they show a great promise for many future applications. One objective for our future research is the development of a novel method for the sensitive detection of DNA hybridization using dendrimer-encapsulated Pd nanoparticles (Pd DENs) that contain photoactive, DNA-intercalating psoralen groups on the dendrimer periphery. Psoralens are unique in their ability to detect hybridized DNA: planar psoralen molecules intercalate into a double-stranded DNA, and covalent addition of the psoralen molecules to DNA is achieved by irradiation with long-wave length UV light. To achieve amplified, optical DNA detection, we will choose a hybridization signaling reaction based on one-electron reduction of viologen, which is catalyzed by Pd particles in the presence of hydrogen gas and leads to the formation of intensively colored viologen radical cations. In this approach, the use of Pd DENs provides a means not only to detect double-stranded DNA via the intercalating ability of psoralen groups but also to amplify the detection signals via the catalytic reaction of Pd nanoparticles.

In the research area of DNA computing, we plan to apply our word design software to the design of DNA word sets for nano-scale computation and self-assemble of nano-particle structures. We look forward to learning how the computationally designed strands perform in vitro, and expect that we can improve the design criteria further based on such insights.

In the DNA/RNA biosensor areas, we would like to continue to develop more sensitive detection methodologies engineered by many different types of enzymatic reactions at surfaces. One proposed approach is the further extension of our RNase H work. This method will involve a serial amplification step that will be developed to improve in both rate of reaction and ultimate detection level. For example, the serial RNase H amplification scheme can give lower detection limit (< 0.1 fM) and shorter measurement time for the direct detection of DNA samples. This can be powerfully employed in the

areas of clinical diagnostics, gene expression analysis and bacterial and viral recognition without any PCR amplification steps. Another approach is to study 3' modifications to the RNA probes on the surface since the efficiency in RNase H recruitment and cleavage can be enhanced. This technique may find a wide variety of uses due to the fact that it is applicable to many other detection methods such as fluorescence quenching and nanoparticle labeling. This technique may be applied to DNA computing as a way to read out the results in replacement of PCR amplification or rolling circle amplification.

We would also like to use this technique to study viral RNA, using a combination of reverse transcriptase and RNase H (RT-RNase H). This method would have the advantage over RT-PCR, in that specialized equipment would not be needed. Including, not only DNA detection, this enzymatic technique as a means for detecting viral RNA without the need for PCR amplification can be a promising research area. This enzymatic process may also be combined with other enzymes, such as reverse transcriptases and polymerases, as a way to manipulate nucleic acid sequences on surfaces to aid in the applicability of SPR imaging to other areas of genetic testing and gene expression analysis.

The kinetics of several S peptide variants with individual amino acid residues will be studied. These individual amino acid residues play key roles in the binding of S proteins to S peptides. The enzymatic activity will be determined using multi-component peptide arrays, each of which will be immobilized with RNA probes on individual spots. We will also observe the effect of changing the molar ratio of RNA to peptides during immobilization on the surface cleavage of surface confined RNase S. Since RNase S would not digest RNA duplexes, complementary DNA or RNA sequences will be introduced to anneal RNA probes to see if they are protected from cleavage by regenerated RNase S on surfaces. Our continued application of peptide arrays will be useful to the characterization of other proteins, such as calmodulin (CaM). CaM is a Ca^{2+} dependent protein that regulates a variety of structurally and functionally different enzymes, including the myosin light chain kinase (MLCK). CaM binds with high affinity to MLCK resulting in a conformational change that induces phosphorylation activity.

Specifically, we are interested in studying the differential binding of CaM to peptides based on the MLCK binding site. Arrays based on this interaction will be applied as a calcium sensor, since CaM-MLCK binding is extremely sensitive to calcium concentration.

Additionally, our future efforts in the area of proteomics can be directed to the study of the kinetics of protein-ligand interactions using NTA capture agents as well as other surface chemistries. These measurements will allow the real-time measurement of protein-peptide interactions including affinity association, proteolytic cleavage, and phosphorylation. These methods can also be used to characterize the sugar binding specificities of lectins and antibodies, identifying glycomimetics, and in carrying out high throughput assays for the discovery of compounds that enhance or disrupt lectin-carbohydrate interactions.

7. REFERENCES

(1) Yan, H.; Zhang, X. P.; Shen, X. Y.; Seeman, N. C., *Nature*, **415** 62-65 (2002).

(2) Frutos, A. G.; Smith, L. M.; Corn, R. M., *J. Am. Chem. Soc.*, **120** 10277-10282 (1998).

(3) Francis, M. B.; Goh, S. L.; Prasad, D.; Frechet, J. M., *J. Polym. Mater. Sci. Eng.*, **84** 12-13 (2001).

(4) Capaldi, S.; Getts, R. C.; Jayasena, S. D., *Nucl. Acid. Res.*, **28** e21(2000).

(5) Smith, E. A.; Wanat, M. J.; Cheng, Y. F.; Barreira, S. V. P.; Frutos, A. G.; Corn, R. M., *Langmuir*, **17** 2502-2507 (2001).

(6) Watson, K. J.; Park, S.-J.; Im, J.-H.; Nguyen, S. T.; Mirkin, C. A., *J. Am. Chem. Soc.*, **123** 5592-5593 (2001).

(7) Niemeyer, C. M., *Angew. Chem. Int.*, **Ed. 40** 4128-4158 (2001).

(8) Elghanian, R.; Storhoff, J. J.; Mucic, R. C.; Letsinger, R. L.; Mirkin, C. A., *Science*, **277** 1078-1080 (1997).

(9) Soto, C. M.; Srinivasan, A.; Ratna, B. R., *J. Am. Chem. Soc.*, **124** 8508-8509 (2002).

(10) Shim, M.; Kam, N. W. S.; Chen, R. J.; Li., Y.; Dai, H., *Nano Lett.,* **2** 285-288 (2002).

(11) Shchepinov, M. S.; Case-Green, S. C.; Southern, E. M., *Nucleic Acids Res.*, **25** 1155-1161 (1997).

(12) Lee, P. H.; Sawan, S. P.; Modrusan, Z.; Arnold, L. J.; Reynolds, M. A., *Bioconjugate Chem.,* **13** 97-103 (2002).

(13) Cai, W.; Lin, Z.; Strother, T.; Smith, L. M.; Hamers, R. J., *J. Phys. Chem. B,* **106** 2656-2664 (2002).

(14) Tang, L.; Tsai, C.; Gerberich, W. W.; Kruckeberg, L.; Kania, D. R., *Biomaterials,* **16** 483-488 (1995).

(15) Corrigan, T. D.; Krauss, A. R.; Gruen, D. M.; Auciello, O.; Chang, R. P. H., *Mater. Res. Soc. Symp. Proc.*, **593** 233 (2000).

(16) Milosevic, M.; Sting, D.; Rein, A., *Spectroscopy,* **10** 44-49 (1995).

(17) Haymond, S.; Babcock, G. T.; Swain, G. M., *J. Am. Chem. Soc.*, **124** 10634-10635 (2002).

(18) Brenner, S.; Johnson, M.; Bridgham, J.; Golda, G.; Lloyd, D. H.; Johnson, D.; Luo, S.; McCurdy, S.; Foy, M.; Ewan, M.; Roth, R.; George, D.; Eletr, S.; Albrecht, G.; Vermaas, E.; Williams, S. R.; Moon, K.; Burcham, T.; Pallas, M.; DuBridge, R. B.; Kirchner, J.; Fearon, K.; Mao, J.; Corcoran, K., *Nature Biotech.,* **18** 630-634 (2000).

(19) Faulhammer, D.; Cukras, A. R.; Lipton, R. J.; Landweber, L. F., *Proc. Natl. Acad. Sci.,* **97** 1385-1389 (2000).

(20) Sakamoto, K.; Gouzu, H.; Komiya, K.; Kiga, D.; Yokoyama, S.; Yokomori, T.; Hagiya, M., *Science,* **288** 1223-1226 (2000).

(21) Wang, D.; Coscoy, L.; Zylberberg, M.; Avila, P. C.; Boushey, H. A.; Ganem, D.; DeRisi, J. L., *PNAS*, **99** 15687-15692 (2002).

(22) Volokhov, D.; Chizhikov, V.; Chumakov, K.; Rasooly, A., *J. Clin. Microbiol.*, **41** 4071-4080 (2003).

(23) Schena, M.; Shalon, D.; Davis, R. W.; Brown, P. O., *Science*, **270** 467-470 (1995).

(24) Duggan, D. J.; Bittner, M.; Chen, Y.; Meltzer, P.; Trent, J. M., *Nat. Genet.,* **21** 10-14 (1999).

(25) Lockhart, D. J.; Winzeler, E., *Nature*, **405** 827-836 (2000).

(26) Brockman, J. M.; Frutos, A. G.; Corn, R. M., *J. Am. Chem. Soc.,* **121** 8044-8051 (1999).

(27) Nelson, B. P.; Grimsrud, T. E.; Liles, M. R.; Goodman, R. M.; Corn, R. M., *Anal. Chem.*, **73** 1-7 (2001).

(28) Wegner, G. J.; Lee, H. J.; Marriott, G.; Corn, R. M., *Anal. Chem.*, **75** 4740-4746 (2003).

(29) Syvanen, A.; Soderlund, H., *Nat. Biotech.,* **20** 349-350 (2002).

(30) He, L.; Musick, M. D.; Nicewarner, S. R.; Salinas, F. G.; Benkovic, S. J.; Natan, M. J.; Keating, C. D.. *J. Am. Chem. Soc.*, **122** 9071-9077 (2000).

(31) Steemers, F. J.; Ferguson, J. A.; Walt, D. R., *Nat. Biotech.*, **18** 91-94 (2000).

(32) Nicewarner-Pena, S. R.; Freeman, R. G.; Reiss, B. D.; He, L.; Pena, D. J.; Walton, I. D.; Cromer, R.; Keating, C. D.; Natan, M. J., *Science,* **294** 137-141 (2001).

(33) Nam, J.; Thaxton, C. S.; Mirkin, C. A., *Science*, **301** 1884-1891 (2003).

(34) Song, F.; Zhou, F.; Wang, J.; Nongjian, T.; Jianiao, L.; Vellanoweth, R. L.; Morquecho, Y.; Wheeler-Laidman, J., *Nucleic Acids Res.*, **30** e72 (2002).

(35) Dillon, A. C.; Gennett, T.; Jones, K. M.; Alleman, J. L.; Parilla, P. A.; Hebert, M., *J. Adv. Mater.,* **11** 1354-1358 (1999).

(36) Liu, H. M.; Dandy, D. S., *Diam. Relat. Mater.*, **4** 1173–1188 (1995).

(37) Gruen, D. M., *Ann. Rev. Mater. Sci.*, **29** 211–259 (1999).

(38) Thoms, B. D.; Owens, M. S.; Butler, J. E.; Spiro, C., *Appl. Phys. Let.*, **65** 2957–2959 (1994).

(39) Strother, T., *Langmuir,* **18** 968–971 (2002).

(40) Pease, A. C.; Solas, D.; Sullivan, E. J.; Cronin, M. T.; Holmes, C. P.; Fodor, S. P. A., *Proc. Nat. Acad. Sci. U. S. A.*, **91** 5022-5026 (1994).

(41) Reineke, U.; Volkmer-Engert, R.; Schneider-Mergener, *J. Curr. Opi. in Biotech.*, **12** 59-64 (2001).

(42) Brockman, J. M.; Frutos, A. G.; Corn, R. M., *J. Am. Chem. Soc.,* **121** 8044-8051 (1999).

(43) Nelson, B. P.; Grimsrud, T. E.; Liles, M. R.; Goodman, R. M.; Corn, R. M., *Anal. Chem.*, **73** 1-7 (2001).

(44) Lee, H. J.; Goodrich, T. T.; Corn, R. M., *Anal. Chem.,***73** 5525-5531 (2001).

(45) Tulpan, D. C.; Hoos, H. H., *Canadian Conference,* **Al** 418-433 (2003).

(46) Andronescu, M.; Fejes, A. P.; Hutter, F.; Hoos, H. H.; A., C., *J. of Mol. Biol.*, **336** 607-624 (2004).

APPENDIX A: LIST OF JOURNAL PUBLICATIONS/PATENT APPLICATIONS

1. Megan E. McLean, Stephen A. Bell, Shane E. Tichy, Sang-Keun Oh, Eric E. Simanek, Robert M. Corn and Richard M. Crooks, "Dendrimer-DNA Constructs Increase the Sensitivity of SPR Imaging" (in preparation).

2. Yuan Li, Hye Jin Lee, and R. M. Corn, "Creation of High Fidelity Double-stranded DNA arrays on Chemically Modified Gold Surfaces by Enzymatic Processing for the Study of DNA-Protein Interactions," (in preparation).

3. Greta. J. Wegner, Alastair W. Wark, Hye Jin Lee, Eric Codner, Tomo Saeki, Shiping Fang and R. M. Corn, "Real Time SPR Imaging Measurements for the Multiplexed Determination of Protein Adsorption/Desorption Kinetics and Surface Enzymatic Reactions on Peptide Microarrays," submitted for publication to *Anal. Chem.,* (2004).

4. Terry T. Goodrich, Hye Jin Lee and R. M. Corn, "Direct Detection of DNA by Enzymatically Amplified SPR Imaging Measurements of RNA Microarrays," *J. Am. Chem. Soc.,* **126** 4086-4087 (2004).

5. Mirela Andronescu, Anthony P. Fejes, Frank Hutter, Holger H. Hoos and Anne Condon, " A new algorithm for RNA secondary structure design," *J. Molecular Biology*, **336(3**) 607-624 (2004).

6. Greta J. Wegner, Hye Jin Lee, and Robert. M. Corn, "Fabrication of Histidine-Tagged Fusion Protein Arrays for Surface Plasmon Resonance Imaging Studies of Protein-Protein and Protein-DNA Interactions," *Anal. Chem*., **75** 4740-4746 (2003).

7. Anne Condon, "Problems on RNA secondary structure prediction and design," *Proceedings of the 30th Annual International Colloquium on Automata,*

Languages and Programming (ICALP), Jos C.M. Baeten, Jan Karel Lenstra, Joachim Parrow, Herhard J. Woeginger (Eds.), Lecture Notes in *Computer Science,* Springer-Verlag, **2719** 22-32 (July 2003).

8. Mirela Andronescu, Rosalia Aguirre-Hernandez, Anne E. Condon, and Holger H. Hoos, "RNAsoft: a suite of RNA secondary structure prediction and design software tools," *Nucleic Acids Research*, **31** 3416-3422 (2003).

9. Sarah E. Baker, Tami L. Lasseter, Lloyd M. Smith, and Robert J. Hamers, "Covalently-linked Adducts of Single-walled Nanotubes with Biomolecules: Synthesis, Hybridization, and Biologically-Directed Surface Assembly", *Mat. Res. Soc. Sym. Proc*., **737**, F4.6.1 (2003).

10. Emily A. Smith, William D. Thomas, Laura L. Kiessling, and Robert M. Corn, "Surface Plasmon Resonance Imaging Studies of Protein-Carbohydrate Interactions," *J. Am. Chem. Soc*., **125** 6140-6148 (2003).

11. Tanya Knickerbocker, Todd Strother, Michael P. Schwartz, John N. Russell Jr., James Butler, Lloyd M. Smith, and Robert J. Hamers, "DNA-Modified Diamond Surfaces," *Langmuir*, **19** 1938-1942 (2003).

12. Stephen A. Bell, Megan E. McLean, Sang-Keun Oh, Shane E. Tichy, Wen Zhang, Robert M. Corn, Richard M. Crooks, and Eric E. Simanek, "Covalently Linked Single-Stranded DNA Oligonucleotide-Dendron Assemblies: Synthesis and Characterization," *Bioconjugate Chem.*, **14** 488-493 (2003).

13. Christine E. Heitsch, Anne E. Condon, and Holger H. Hoos, "From RNA Secondary Structure to Coding Theory: A Combinatorial Approach," Lecture Notes in *Computer Science*, Springer, **2586** 2215-2228 (2003).

14. Wensha Yang, Orlando Auciello, James E. Butler, Wei Cai, John A. Carlisle, Jennifer E. Gerbi, Dieter M. Gruen, Tanya Knickerbocker, Tami L. Lasseter, John N. Russell, Jr., Lloyd M. Smith, and Robert J. Hamers, "Preparation and Electrochemical Characterization of DNA-modified Nanocrystalline Diamond Films," *Mat. Res. Soc. Symp. Proc.*, **737** F4.4.1 (2003).

15. Dan C. Tulpan, Holger Hoos, Anne Condon, "Stochastic Local Search Algorithms for DNA Word Design," Proc. 9th Annual Workshop on DNA Based Computing, Lecture Notes in *Computer Science*, Springer, **2568** 182-195 (2003).

16. G. J. Wegner, H. J. Lee, and R. M. Corn, "Characterization and Optimization of Peptide Arrays for the Study of Epitope-Antibody Interactions Using Surface Plasmon Resonance Imaging," *Anal. Chem.,* **74** 5161-5168 (2002).

17. Wensha Yang, James E. Butler, Wei Cai, John Carlisle, Dieter Gruen, Tanya Knickerbocker, John N. Russell, Jr., Lloyd M. Smith, and Robert J. Hamers, "DNA-modified nanocrystalline diamond films as stable, biologically active substrates," *Nature Materials*, **1** 253-257 (2002).

18. Sarah Baker, Wei Cai, Tami Lasseter, Kevin Weidkamp, and Robert J. Hamers, "Covalently-bonded adducts of DNA with single-walled carbon nanotubes: Synthesis and hybridization," *Nano Letters*, **2** 1413-1417 (2002).

19. "Horizontally Configured Surface Plasmon Resonance System (Horizontal SPR)" by E. Codner and R.M. Corn. Invention disclosure to Wisconsin Alumni Research Foundation.

20. "Biologically-Directed Assembly of Nanotubes and other Nanostructured Objects" by R.J. Hamers, T.L. Lasseter, and S. Baker. Invention disclosure to Wisconsin Alumni Research Foundation.

21. “Handheld SPR Imaging System” by E. Codner and R.M. Corn. Invention disclosure to Wisconsin Alumni Research Foundation.

APPENDIX B: LIST OF CONFERENCE PRESENTATIONS

1. R. M. Crooks, "Dendrimer-Encapsulated Metal Nanoparticles: Synthesis, Characterization, and Catalysis," University of Delaware, Newark, DE, Dec 2003.

2. R. M. Crooks, "Electrochemical Detection and Photonic Reporting in Microfluidic-Based Chemical Sensors" Purdue University, West Lafayette, IN, Dec 2003.

3. E. E. Simanek, "Dendrimers Based on Melamine," 7th US-Japan Polymer Drug Delivery Symposium, Maui, HI, Dec 2003.

4. G. J. Wegner, H. J. Lee and R. M. Corn, "SPR Imaging Measurements of Bioaffinity Interactions Using Peptide, Protein and DNA Arrays Fabricated on Gold Thin Films," MRS fall meeting, Boston, MA, Dec 2003.

5. R. M. Corn, "Monitor Bioaffinity Interactions with Surface Plasmon Resonance Imaging Measurements of DNA, Peptide, Protein and Carbohydrate Microarrays," University of Massachusetts, Amherst, MA, Dec 2003.

6. E. E. Simanek, "Dendrimers Based on Melamine," ACS Regional Meeting, Oklahoma City, OK, Oct 2003.

7. E. E. Simanek, "Dendrimers Based on Melamine," Virginia Military Institute, Lexington, VA, Oct 2003.

8. E. E. Simanek, "Dendrimers Based on Melamine," University of Maryland, Baltimore, MD, Oct 2003.

9. E. E. Simanek, “Dendrimers Based on Melamine,” James Madison University, Harrisonburg, VA, Oct 2003.

10. H. J. Lee, G. J. Wegner, and R. M. Corn, “Protein and Peptide Microarrays for SPR Imaging Measurements of Bioaffinity Interactions,” FACSS 2003 conference, Fort Lauderdale, FL, Oct 2003.

11. R. M. Corn, "SPR Imaging Measurements of DNA, Peptide, Carbohydrate and Protein Arrays," Columbia University, New York, NY, Sept 2003.

12. R. M. Corn, "SPR Imaging Measurements of Biomolecular Arrays," University of Michigan, Ann Arbor, MI, Sept 2003.

13. H. J. Lee, G. J. Wegner, G. Marriot and R. M. Corn, “Fabrication of Oriented Protein Arrays Using Micro-Fluidic Networks from PDMS for Optical Imaging measurements,” SmallTalk 2003 The Microfluidics, Microarrays and BioMEMS Conference, San Jose, CA, July 2003.

14. A. Condon, “Problems on RNA secondary structure prediction and design”, International Colloquium on Automata, Languages and Programming (ICALP), July 2003.

15. Dan C. Tulpan and Holger H. Hoos, “Hybrid Randomized Neighborhoods Improve Stochastic Local Search for DNA Code Design. Proc. of the Sixteenth Canadian Conference on Artificial Intelligence,” (AI'2003), July 2003.

16. R. M. Corn, "Monitoring protein adsorption onto peptide, carbohydrate and DNA microarrays with SPR imaging measurements," Gordon Research Conference on Analytical Chemistry 2003, Connecticut College, New London, CT, June 2003.

17. H. J. Lee, Y. Li and R. M. Corn, "Optimization of DNA Hybridization Adsorption and Surface Enzymatic Reactions for SPR imaging Measurements of DNA Microarrays," Gordon Research Conference on Analytical Chemistry 2003, Connecticut College, New London, CT, June 2003.

18. Y. Li, H. J. Lee and R. M. Corn, "Controlling Hybridization Efficiency in DNA Microarrays on Gold Surfaces with SPR Imaging for DNA-Based Nanoscale Biosensors," DNA9 Ninth International Meeting on DNA Based Computers, Madison, WI, June 2003.

19. M. Li, H. J. Lee, Y. Chen, L. Smith and R. M. Corn, "Attomole Detection of DNA in an Array Format with SPR Imaging using Rolling Circle Amplification for the Programmable Nanoscale DNA Biosensors," DNA9 Ninth International Meeting on DNA Based Computers, Madison, WI, June 2003.

20. S. Fang, H. J. Lee, M. Li, R. M. Crooks and R. M. Corn, "Multilayer Amplification Methodology for Attomole Detection of DNA Microarray with SPR Imaging in the Application of DNA-Based Nanostructure," DNA9 Ninth International Meeting on DNA Based Computers, Madison, WI, June 2003.

21. R. J. Hamers, Workshop on Nanostructured Carbon Materials, Argonne National Lab, Argonne, IL, Apr 2003.

22. R. J. Hamers, National Meeting of the American Chemical Society, New Orleans, LA, Mar 2003.

23. H. J. Lee, G. J. Wegner and R. M. Corn, "Spectroscopic and Electrochemical Characterization of Biopolymer Arrays at Gold Surfaces for Biosensor Applications," ACS 2003 spring meeting, New Orleans, LA, Mar 2003.

24. R. M. Corn, H. J. Lee, G. J. Wegner, E. A. Smith, T. T. Goodrich and E. Codner, "SPR Imaging Measurements for the Rapid Microarray Detection of Nucleic Acids and Proteins," ACS 2003 spring meeting, New Orleans, LA, Mar 2003.

25. R. M. Corn, H. J. Lee, G. J. Wegner, T. T. Goodrich and E. A. Smith, "SPR Imaging Measurements of DNA, Peptide and Protein Microarrays," ACS 2003 spring meeting, New Orleans, LA, Mar 2003.

26. H. J. Lee, G. J. Wegner, E. Smith, T. Goodrich and R. M. Corn, "SPR Imaging Measurements of DNA, Peptide and Protein Microarrays," Pittcon 2003 conference, Orlando, FL, Mar 2003.

27. R. J. Hamers, National Meeting of the American Physical Society, Austin, TX. (Unable to deliver talk because of weather-related flight cancellations), Mar 2003.

28. Anne Condon, "Computational approaches to RNA secondary structure prediction", Vancouver Bioinformatics Users Group in Vancouver, Canada, Feb 2003.

29. R. J. Hamers, Gordon Conference on Chemical Reactions at Surfaces, Ventura, CA, Feb 2003.

30. R.J. Hamers, National meeting of the Materials Research Society, Boston, MA, Dec 2002.

APPENDIX C: ABREVIATIONS AND DEFINITIONS

1-D	One dimensional
2-D	Two dimensional
A	Adenine
AC	Alternating current
Ar	Argon
B	Boron
BLAST	**B**asic **L**ocal **A**lignment **S**earch **T**ool
C	Carbon
C	Cytosine
C60	A molecule that consists of 60 carbon atoms, arranged as 12 pentagons and 20 hexagons
CaM	Calmodulin
Carbon nanotubes	nanotubes based on carbon or other elements. These systems consist of graphitic layers seamlessly wrapped to cylinders
CCD	Charge coupled device
CH_4	Methane
DEN	Dendrimer-encapsulated nanoparticle
Dendrimer	Highly branched monomers leading to a monodisperse, tree-like or generational structure
DIPEA	N,N-Diisopropylethylamine
DNA	Deoxyribonucleic acid
DNTP	Deoxynculeotide mix
DsDNA	Double-stranded DNA
DTT	Dithiothreitol
fM	Femtomolar
Fmoc	9-fluorenylmethoxycarbonyl
G	Guanine
GHz	Gigahertz
H	Hydrogen
hr	Hour
HPLC	High pressure liquid chromatography
KY	Kentucky
M	Molar
M^+	Metal ion
MA	Massachusetts

MALDI	Matrix-assisted laser desorption/ionization
MHz	Megahertz
mL	Milliliter
MLCK	Myosin light chain kinase
mRNA	Messenger RNA
MS	Mass Spectrometry
MUAM	11-mercapto-undecylamine
N	Nitrogen
NCD	Nanocrystalline diamond
ng	Nanogram
NHS	*N*-hydroxysuccinimide
NHSS	*N*-hydroxysulfosuccinimide
Ni	Nickel
nm	Nanometer
nmer	n-bases in an oligomer
NRL	Naval Research Laboratory
O	Oxygen
Oligomers	Short, single stranded DNA fragments
PCR	Polymerase chain reaction
Pd	Palladium
PDMS	Polydimethylsiloxane
PEG	Polyethylene glycol
RCA	Rolling circle amplification
RNA	Ribonucleic acids
S	Sulfur
SAM	Self assembled monlayer
SATP	N-Succinimidyl S-acetylthiopropionate
Si	Silicon
SMCC	Succinimidyl-4-(*N*-maleimidomethyl)cyclohexane-1-carboxylate
SPR	Surface Plasmon Resonance
SSMCC	Sulfosuccinimidyl 4-(*N*-maleimidomethyl) cyclohexane-1-carboxylate
SSB	Single-stranded-binding
ssDNA	Single stranded deoxyribonucleic acids
SWNT	Single-wall carbon nanotube
T	Thymine
TCEP	Tri(2-carboxyethyl)phosphine
TFAAD	Trifluoroacetamide-protected 10-aminodec-1-ene

THF	Phentydrone (1,2,3,4-Tetrahydro-9-fluorenone)
TLC	Thin Layer Chromatography
TOF	Time-of-flight
TSPY	Testis specific protein, Y-linked
UF	Ultra Filter
UNCD	Ultra-nanocrystalline diamond
UV	Ultraviolet
Wt %	Weight percent